EXPERIMENTAL INVESTIGATION INTO THE PHYSICO-CHEMICAL PROPERTIES CHANGES OF PALM BIODIESEL UNDER COMMON RAIL DIESEL ENGINE OPERATION FOR THE ELUCIDATION OF METAL CORROSION AND ELASTOMER DEGRADATION IN FUEL DELIVERY SYSTEM

DAVANNENDRAN CHANDRAN, BEng.

Thesis submitted to the University of Nottingham for the Degree of Doctor of Philosophy

JULY 2016

ABSTRACT

Compatibility of fuel delivery materials (FDM) with biodiesel fuel in the fuel delivery system (FDS) under real-life common rail diesel engine (CRDE) operation poses a challenge to researchers and engine manufacturers alike. Although standard methods such as ASTM G31 and ASTM D471 for metals and elastomers, respectively, are deemed suitable for evaluating the effects of water content, total acid number (TAN) and oxidation products in biodiesel on FDM degradation, they do not resemble the actual engine operation conditions such as varying fuel pressure/temperature as well as the presence of a wide range of materials in the FDS of a diesel engine. Hence, the current allowable maximum 20 vol% of biodiesel with 80 vol% of diesel (B20) for use in diesel engines to date is debatable. Additionally, biodiesel utilization beyond B20 is essential to combat declining air quality and to reduce the dependence on fuel imports. This thesis aims to elucidate the actual compatibility present between FDM and biodiesel in the FDS under real-life CRDE operation. This was achieved through multi-faceted experimentations which commenced with analyses on the deteriorated palm biodiesel samples collected during and after CRDE operation. Next, the fuel properties which should be emphasized based on the deteriorated fuel were determined. This was then followed by ascertaining the effects of the emphasized fuel properties towards FDM degradation. Ultimately, the actual compatibility of FDM with biodiesel under engine operation through modified immersion investigations was determined. FDM degradation acceleration factors such as oxidized biodiesel, TAN and water content were eliminated since these factors were not affected based on the analysed fuel samples collected after engine operation. No oxidation products such as aldehydes, ketones and carboxylic acids were detected while the TAN and water content were

within 0.446% and 0.625% of their initial values, respectively. Instead, the biodiesel's dissolved oxygen (DO) concentration and conductivity value were not only found to have changed during and after engine operation by -93% and 293%, respectively, but were also found to have influenced biodiesel deterioration under engine operation. These two properties were subsequently discovered to have adversely affected FDM degradation independently. The copper corrosion rate and nitrile rubber (NBR) volume change increased by 9% and 13%, respectively, due to 22% increase in the conductivity value. In contrast, the copper corrosion rate and NBR volume swelling reduced by 91% and 27%, respectively, due to 96% reduction in the DO concentration. Ultimately, copper corrosion and NBR degradation were determined to be lowered by up to 92% and 73%, respectively, under modified immersion as compared to typical immersion condition. These outcomes distinctly show that acceptable to good compatibility is present between FDM and biodiesel under CRDE operation. The good compatibility is strongly supported since only a maximum lifespan reduction of 1.5 years is predicted for metal exposed to biodiesel as compared to diesel for a typical component lifespan of 15 years. For the elastomers, acceptable compatibility is found present between elastomer and biodiesel based on the determined 11% volume change which conforms to the tolerance level of elastomer degradation as stated by the elastomer manufacturers. These are especially true for the evaluated metals and elastomers investigated under the modified laboratory immersion which replicates similar conditions to a real-life CRDE. Overall, this work has contributed to the advancement of knowledge and application of biodiesel use in diesel engines.

LIST OF JOURNAL PUBLICATIONS

D. Chandran, H.K. Ng, L.L.N. Harrison, S. Gan, Y.M. Choo, S. Jahis, Compatibility of biodiesel fuel with metals and elastomers in the fuel delivery system of a diesel engine, Journal of Oil Palm Research. 28 (2016) 64-73.

D. Chandran, H.K. Ng, L.L.N. Harrison, S. Gan, Y.M. Choo, Deterioration of palm biodiesel fuel under common rail diesel engine operation, Energy. (Under review)

D. Chandran, H.K. Ng, L.L.N. Harrison, S. Gan, Y.M. Choo, Investigation of the effects of palm biodiesel dissolved oxygen and conductivity on metal corrosion and elastomer degradation under novel immersion method, Applied Thermal Engineering. 104 (2016) 294-308.

LIST OF CONFERENCES

D. Chandran, H.K. Ng, L.L.N. Harrison, S. Gan, Y.M. Choo, Compatibility of fuel delivery materials with palm biodiesel fuel under diesel engine operation: Book of abstracts of the IPN-IWNEST 2015 Bandung Conferences: International Conference on Renewable Energy and Green Technology, Bandung, Indonesia, 04-05 Dec 2015, p.41. ***'Awarded Best Presenter'***

D. Chandran, H.K. Ng, L.L.N. Harrison, S. Gan, Y.M. Choo, Physico-chemical properties changes of palm biodiesel fuel under diesel engine operation, International Journal of Mining, Metallurgy & Mechanical Engineering, 3 (2015) p.151.

D. Chandran, H.K. Ng, L.L.N. Harrison, S. Gan, Y.M. Choo, Experimental investigation into the deterioration of palm biodiesel fuel under engine operation for the elucidation of fuel delivery materials degradation: Book of abstracts of the MPOB International Palm Oil Congress (PIPOC 2015): Chemistry, Processing Technology & Bio-energy, Kuala Lumpur, Malaysia, 06-08 Oct 2015, p.70.

D. Chandran, H.K. Ng, L.L.N. Harrison, S. Gan, Y.M. Choo, Effects of biodiesel deterioration on existing fuel system materials as a result of common rail diesel engine operation in: Book of abstracts of the MPOB International Palm Oil Congress (PIPOC 2013): Chemistry, Processing Technology & Bio-energy, Kuala Lumpur, Malaysia; 19-21 Nov 2013, p.91-92.

DEDICATION

This thesis is dedicated to my parents Mr Chandran and Madam Nalini for their endless love, support and encouragement.

ACKNOWLEDGEMENTS

I would like to acknowledge the constructive guidance and consistent support provided by my supervisors, Prof Ng Hoon Kiat and Prof Gan Suyin from The University of Nottingham Malaysia Campus, as well as Dr Harrison Lau Lik Nang and Datuk Dr Choo Yuen May from The Malaysian Palm Oil Board.

I would like to express my gratitude for the financial and facilities assistance provided by The Malaysian Palm Oil Board through the MPOB's Graduate Student Assistantship Scheme, as well as the scholarship awarded by The Faculty of Engineering of The University of Nottingham Malaysia Campus.

I deeply appreciate the unconditional love and unending support shown by my family members Mr Chandran, Madam Nalini, Madam Priyatharshini, Mr Rayndran and last but not least my future wife Miss Revathi Raviadaran, towards me achieving my goals.

I would also like to acknowledge the support and assistance to all of those who supported me in any respect throughout my research. There is no doubt in my mind that without all these support and counsel, I could not have completed this process successfully.

Above all, I thank GOD for blessing and choosing me to accomplish this task.

TABLE OF CONTENTS

ABSTRACT i

LIST OF JOURNAL PUBLICATIONS iii

LIST OF CONFERENCES iv

DEDICATION v

ACKNOWLEDGEMENTS vi

TABLE OF CONTENTS vii

LIST OF ABBREVIATIONS x

LIST OF FIGURES xiii

LIST OF TABLES xv

CHAPTER 1-INTRODUCTION 1

CHAPTER 2-LITERATURE REVIEW 24

2.1 Compatibility of biodiesel with FDM 24

2.1.1 Metal corrosion due to the exposure of biodiesel 24

2.1.2 Elastomer degradation due to the exposure of biodiesel 31

2.2 Assess the compatibility of biodiesel with FDM under a physical diesel engine 37

2.2.1 Standard methods used in existing compatibility studies 37

2.2.2 Evaluated materials in existing compatibility studies 42

2.3 Summary 45

CHAPTER 3-DETERIORATION OF PALM BIODIESEL FUEL UNDER COMMON RAIL DIESEL ENGINE OPERATION 48

3.1 Background 48

3.2 Material and methods 53

3.2.1 Experimental set-up of the engine test-bed facility 53

3.2.2 Test fuels 57

3.2.3 Speed-load test cycle and engine operation duration 58

3.2.4 Fuel sampling and analytical tests 62

3.2.5 Experimental procedure for the third-stage investigations 68

3.3 Results and discussion 70

3.3.1 First stage-deterioration of biodiesel under to CRDE operation 70

3.3.1.1 Biodiesel oxidation....70
3.3.1.1.1 Overall discussion on biodiesel oxidation....81
3.3.1.2 Total acid number value....85
3.3.1.3 Water content....86
3.3.2 Second stage....88
3.3.2.1 First comparison....88
3.3.2.2 Second comparison....92
3.3.2.3 Third comparison....98
3.3.2.4 Fourth comparison....102
3.3.3 Third stage-characterization of biodiesel's conductivity value....105
3.4 Summary....109
CHAPTER 4-COMPATIBILITY OF FUEL DELIVERY METAL AND ELASTOMER IN PALM BIODIESEL....110
4.1 Background....110
4.2 Material and methods....114
4.2.1 Evaluated metal specimens....114
4.2.2 Evaluated elastomer specimens....114
4.2.3 Test fuel....117
4.2.4 First-stage investigation....118
4.2.5 Second-stage investigations....120
4.2.6 Metal corrosion investigation procedure and analysis....122
4.2.7 Elastomer degradation investigation procedure and analysis....122
4.2.8 Surface morphology and elemental compositions material analysis....123
4.2.9 Analytical test....123
4.3 Results & discussion....126
4.3.1 First stage-effects of biodiesel's DO and conductivity value on FDM degradation....126
4.3.2 Second stage-compatibility of FDM with biodiesel under modified immersion....132
4.3.2.1 First phase-influence of modified and typical immersion on the compatibility of FDM with biodiesel....132
4.3.2.1.1 Deterioration of biodiesel under modified and typical immersion investigation....133
4.3.2.1.2 Compatibility of FDM with biodiesel under engine operation condition....136

4.3.2.2 Second phase-influence of temperature on the compatibility of FDM with biodiesel under modified immersion....142

4.3.2.2.1 Effects of immersion temperature on FDM degradation upon biodiesel exposure....143

4.3.2.3 Third phase-influence of immersion duration on the compatibility of FDM with biodiesel under modified immersion....149

4.3.2.3.1 Effects of immersion duration on FDM degradation upon biodiesel exposure....150

4.3.2.4 Fourth phase-influence of biodiesel concentration in biodiesel-diesel fuel blends on the compatibility of FDM with biodiesel under modified immersion....154

4.3.2.4.1 Effects of biodiesel concentration in biodiesel-diesel fuel blends on FDM degradation....155

4.3.2.5 Fifth phase-degradation of different FDM due to biodiesel exposure under modified immersion....159

4.3.2.5.1 Compatibility of different FDM with biodiesel....160

4.3.3 Recommendations for mitigating the effects of biodiesel exposure on FDM degradation....165

4.4 Summary....167

CHAPTER 5-CONCLUSIONS AND RECOMMENDATIONS FOR FURTHER WORK....168

5.1 Conclusions....168

5.2 Recommendations for further work....175

REFERENCES....177

APPENDICES....209

APPENDIX A-EXPERIMENTAL SETUP....209

APPENDIX B-ENGINE OPERATION PROTOCOL....212

APPENDIX C-EXAMPLE CALCULATION OF METAL CORROSION RATE....215

APPENDIX D- EXAMPLE CALCULATION OF ELASTOMER VOLUME CHANGE....216

APPENDIX E-EXAMPLE CALCULATION OF ELASTOMER TENSILE STENGTH CHANGE....217

APPENDIX F-EXAMPLE CALCULATION OF ELASTOMER HARDNESS CHANGE....218

APPENDIX G- EXAMPLE CALCULATION OF PROPAGATION ERROR USING STANDARD DEVIATIONS....219

LIST OF ABBREVIATIONS

Al	aluminium
ASTM	American Society Testing and Materials
ASTM D130	Standard Test Method for Corrosiveness to Copper from Petroleum Products by Copper Strip Test
ASTM D412	Standard Test Method for Vulcanized Rubber and Thermoplastic Elastomers-Tension
ASTM D471	Standard Test Method for Rubber Property-Effect of Liquids
ASTM D664	Standard Test Method for Acid Number of Petroleum Products by Potentiometric Titration
ASTM D2240	Standard Test Method for Rubber Property-Durometer Hardness
ASTM D6751	Standard Specification for Biodiesel Fuel Blend Stock (B100) for Middle Distillate Fuels
ASTM D7467	Standard Specification for Diesel Oil, Biodiesel Blend (B6 to B20)
ASTM G1	Standard Practice for Preparing, Cleaning, and Evaluating Corrosion Test Specimens
ASTM G31	Standard Practice for Laboratory Immersion Corrosion Testing of Metals
ASTM G59	Standard Test Method for Conducting Potentiodynamic Polarization Resistance Measurement
ASTM G184	Standard Practice For Evaluating and Quantifying Oil Field and Refinery Corrosion Inhibitors Using Rotating Cage
B100	100% biodiesel/neat biodiesel
B20	20% biodiesel and 80% diesel
Biodiesel	100% biodiesel
Br	brass
cc	cubic centimetre
CEC F-98-08	Direct Injection-Common Rail Diesel Engine Nozzle Coking Test

CI	cast iron
Cr	chromium
CRDE	common rail diesel engine
CS	carbon steel
Cu	copper
DO	dissolved oxygen
FDM	fuel delivery material/materials
FDS	fuel delivery system
Fe	iron
FKM	fluoroelastomer
FTIR	Fourier transform infrared spectroscopy
g	gram
GS	galvanized steel
h	hour/hours
HC	unburned hydrocarbon
ISO 2160	Petroleum products-Corrosiveness to copper-Copper strip test
kW	kilowatt
l	litre
LPR	linear polar resistance
meq	milliequivalent
mgKOH/g	milligrams of potassium hydroxide per gram
min	minute/minutes
ml	milliliter
MS	mild steel
NBR	nitrile rubber
OS	oxidation stability

ppm	parts per million
rev/min	revolution per minute
SEM	scanning electron microscope
SLTC	speed-load test cycle
SR	silicone rubber
SS	stainless steel
TAN	total acid number
vol	volume
WHSC	World Harmonized Stationary Cycle
wt	weightage
Zn	zinc

LIST OF FIGURES

Fig. 1.1 Changes in biodiesel production and consumption in selected countries/regions 4

Fig. 1.2 Fuel delivery and storage system in a typical diesel engine 11

Fig. 1.3 Fundamental framework of the research 17

Fig. 1.4 Stages of work of the research programme 19

Fig. 3.1 Overview of investigations in Chapter 3 49

Fig. 3.2 Schematic representation of engine test-bed facility 56

Fig. 3.3 Flowchart of test sequence 63

Fig. 3.4 Deterioration of biodiesel fuel's oxidation stability under CRDE operation 71

Fig. 3.5 Changes of biodiesel fuel's fatty acid composition under CRDE operation 72

Fig. 3.6 Changes of biodiesel fuel's hydrogen ion concentration under CRDE operation 73

Fig. 3.7 Changes of biodiesel fuel's peroxide value under CRDE operation 74

Fig. 3.8 Initial and final FTIR spectrums for WHSC, CEC F-98-08 and in-house developed 75

Fig. 3.9 Changes of biodiesel fuel's dissolved oxygen concentration under CRDE operation 76

Fig. 3.10 Changes of biodiesel fuel's dissolved oxygen concentration corresponding to fuel temperature changes 77

Fig. 3.11 Changes of biodiesel fuel's viscosity value under CRDE operation 78

Fig. 3.12 Changes of biodiesel fuel's conductivity value under CRDE operation 79

Fig. 3.13 Changes of dissolved (a) aluminium, (b) iron, (c) copper and (d) zinc under CRDE operation duration 80

Fig. 3.14 Changes of biodiesel fuel's total acid number value under CRDE operation 85

Fig. 3.15 Changes of biodiesel fuel's water content under CRDE operation 87

Fig. 3.16 FTIR spectrums of Vance Bioenergy and Carotech biodiesel fuel after CRDE operation under CEC F-98-08 SLTC 97

Fig. 3.17 FTIR spectrums of 1 full tank operation and 5 consecutive days of CRDE operation 100

Fig. 3.18 Changes of conductivity value with respect to (a) fuel temperature, (b) dissolved copper, (c) oxidized biodiesel and (d) fuel heating duration 106

Fig. 4.1 Overview of investigations in Chapter 4 111

Fig. 4.2 Dimensions of nylon dog-bone specimen 116

Fig. 4.3 Laboratory setup to manipulate and measure biodiesel fuel's dissolved oxygen concentration 119

Fig. 4.4 SEM micrographs of copper after under typical and modified immersion investigations 139

Fig. 4.5 SEM micrographs of NBR after under typical and modified immersion investigations 140

Fig. 4.6 Initial and final biodiesel fuel's FTIR spectrum under typical and modified immersion investigations 141

Fig. 4.7 SEM micrographs of copper after under modified immersion at 25 and 100 °C 146

Fig. 4.8 Elemental composition of (a) copper and (b) NBR after under modified immersion at 25 and 100 °C 147

Fig. 4.9 SEM micrographs of NBR after under modified immersion at 25 and 100 °C 148

Fig. 4.10 Changes of (a) copper's corrosion rate, (b) NBR's volume change and (c) NBR's tensile strength change corresponding to the modified immersion investigations' duration 151

Fig. 4.11 SEM micrographs of copper corresponding to the modified immersion investigations' duration 152

Fig. 4.12 SEM micrographs of NBR corresponding to the modified immersion investigations' duration 153

Fig. 4.13 Changes of (a) copper's corrosion rate, (b) NBR's volume change and (c) NBR's tensile strength change corresponding to the concentrations of biodiesel-diesel fuel blends under modified immersion investigations 156

Fig. 4.14 SEM micrographs of copper after exposed to B0, B10, B20, B50 and B100 under modified immersion investigations 157

Fig. 4.15 SEM micrographs of NBR after exposed to B0, B10, B20, B50 and B100 under modified immersion investigations 158

Fig. 4.16 (a) Corrosion rate of metals, (b) volume change of elastomers and (c) tensile strength change of elastomers after under modified immersion investigations 162

Fig. 4.17 SEM micrographs of metals after under modified immersion 163

Fig. 4.18 SEM micrographs of elastomers after under modified immersion 164

Fig. 4.19 Changes of biodiesel fuel's conductivity value and dissolved oxygen concentration corresponding to fuel temperature 166

LIST OF TABLES

Table 1.1 Pollutants emitted from the petroleum refineries 2

Table 1.2 Advantages and disadvantages in terms of economic, environment, emission and diesel engine operation perspectives with the adoption of biodiesel 5

Table 1.3 The amount of biodiesel utilization in selected countries/regions 6

Table 1.4 Comparison of properties between diesel and biodiesel 7

Table 1.5 Comparison between diesel and biodiesel's production method and chemical composition 8

Table 1.6 Materials used in the fabrication of fuel storage and delivery components 11

Table 1.7 Diesel engine exhaust emissions operated with rapeseed-based biodiesel as compared to diesel 14

Table 2.1 Bibliographic studies on the compatibility of metals in biodiesel 29

Table 2.2 Bibliographic studies on the compatibility of elastomers in biodiesel 35

Table 2.3 Results of biodiesel's corrosiveness from ASTM D130 and ISO 2160 standard methods.....38

Table 2.4 Working principles of the standard methods and the corresponding reference studies 40

Table 2.5 Evaluated fuel delivery metals and elastomers with the corresponding studies in literature ...44

Table 3.1 Second-stage investigations in detail 52

Table 3.2 Specifications of engine test-bed facility 55

Table 3.3 Palm biodiesel fuels specifications 57

Table 3.4 Details of WHSC test cycle 60

Table 3.5 Details of CEC F-98-08 test cycle 61

Table 3.6 Details of in-house developed test cycle 61

Table 3.7 Details of sample collection for each speed-load test cycle 64

Table 3.8 Specifications of the equipment for analytical tests 65

Table 3.9 Analytical tests conducted on biodiesel samples 66

Table 3.10 Test samples for determining the influence of oxidized biodiesel on conductivity value 69

Table 3.11 Comparisons of the dissolved metals concentration under CRDE operation 79

Table 3.12 Research specifications of the present study and the study from literature 90

Table 3.13 Comparison of biodiesel deterioration from stage 1 with the study from literature 91

Table 3.14 Comparison of biodiesel deterioration with different initial physical properties.....95

Table 3.15 Comparison on the rate of change for biodiesel properties under CRDE operation.....96

Table 3.16 Comparison of palm biodiesel deterioration under 1 full tank operation to under 5 full tanks of operation 99

Table 3.17 Research specifications of the immersion study from literature.....102

Table 3.18 Comparison of fuel deterioration under CRDE operation and immersion investigation 104

Table 4.1 Elemental composition of metal specimens 115

Table 4.2 Dimensions of elastomer specimens.....116

Table 4.3 Palm biodiesel fuel specifications 117

Table 4.4 Fuel quantity for each specimen.....117

Table 4.5 Comparison of biodiesel fuels' initial physical properties 119

Table 4.6 Details of second-stage investigations.....121

Table 4.7 Analytical tests conducted on biodiesel samples.....124

Table 4.8 Specifications of equipment for analytical and materials tests.....125

Table 4.9 Comparisons of untreated and treated biodiesel fuels on copper and NBR degradation 128

Table 4.10 Comparisons of modified and typical immersion investigations on copper and NBR degradation.....138

Table 4.11 Comparisons of biodiesel fuel deterioration under typical and modified immersion investigations for copper and NBR degradation.....138

Table 4.12 Comparisons of fuel temperature effects on copper and NBR degradation under modified immersion investigations.....145

CHAPTER 1-INTRODUCTION

To date, emissions from the consumption of fossil fuel in the transportation sector which accounts for 20% of the global energy supply is observed as among the major factors for the decline in air quality [1, 2]. Despite more stringent emission regulations, the increase in vehicle purchases globally offsets the net reductions achieved. Apart from fossil fuel consumption, the refining process of fossil fuel itself as summarized in Table 1.1 also heavily contributes towards the air quality declination [3]. As such, based on the current dependence on fossil fuel, as well as the demand for energy supply which is bound to further increase in future due to the rapid growth of population and industrialization, the air quality is expected to further worsen.

The foreseen adverse effect based on the situation described above has initiated the interest to identify suitable renewable energy to break the dependence placed on fossil fuel. Besides the declining air quality, several other factors such as the diminishing energy reserves, the classification of diesel exhaust emission as carcinogenic to human-Group 1 [4] as well as the poor accessibility of fossil fuel in rural and upland areas have also driven this interest. Based on the continuous research conducted throughout the years globally, oil seed crops have been indicated as among the most exploitable renewable energy capable of displacing refined fossil fuel products [5].

Table 1.1 Pollutants emitted from the petroleum refineries [3].

Pollutants	**Species**	**2005 National Emissions Inventory Emissions (tons per year)**	**Health effects**
Criteria air pollutants	Sulphur oxides, nitrogen oxides, carbon monoxide and particulate matter.	423,757	Respiratory effects, airway inflammation, reduction of oxygen delivery to organs and tissues.
Volatile organic compounds	Photo chemically reactive organic compounds.	114,852	Reduced lung function. Symptoms include chest pain, coughing, nausea and pulmonary congestion.
Carcinogenic hazardous air pollutants	Benzene, naphthalene, 1,3-butadiene and polycyclic aromatic hydrocarbons.	14,000	Neurological effects, irritation to eye, skin and respiratory tract, leukaemia, cancer, damage to liver and cardiovascular.
Other pollutants	Greenhouse gases.	220 million metric tons of carbon dioxide	Increased average temperatures, higher levels of ground-level ozone, harm to water resources, ecosystems and wildlife.

Today, biodiesel fuel commonly produced from vegetable or animal oil through the trans-esterification process has emerged as the most suitable renewable energy to power diesel engines. Its physico-chemical properties which is suitable to be used without general engine and infrastructure alteration is the major reason for its acceptance as a diesel fuel alternative. Furthermore, its production flexibility using geographical feedstock, a century of history to prove its suitability as well as its advantages over diesel as exhibited in Table 1.2 also heavily influenced this acceptance. The use of biodiesel to power diesel engine was commenced in blended form with diesel and has reached a typical maximum of 20 vol% of biodiesel with 80 vol% of diesel (B20) to date as shown in Table 1.3. The B100 and B20 fuels are typically expected to meet the specifications as per stipulated in the ASTM D6751-15c [6] and the ASTM D7467-15c [7] standards, respectively. The significant growth of biodiesel today can also be observed from its changes in production and consumption in selected nations/regions as per shown in Fig. 1.1 for the past six years (2008-2014).

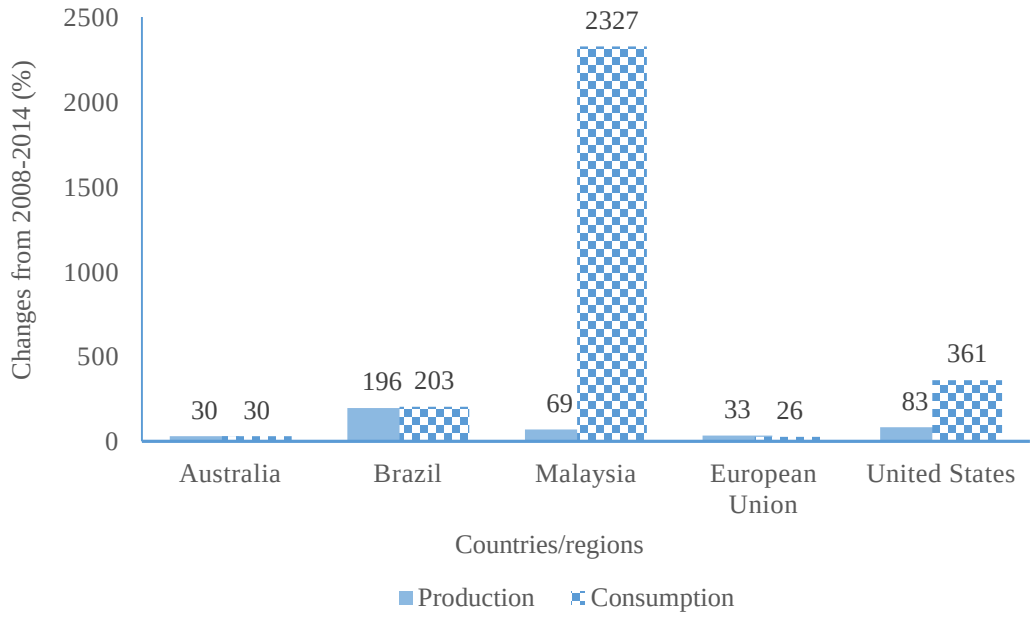

Fig. 1.1 Changes in biodiesel production and consumption in selected countries/regions [8-15].

Table 1.2 Advantages and disadvantages in terms of economic, environment, emission and diesel engine operation perspectives with the adoption of biodiesel [16-25].

Advantages	Disadvantages
1. Reduce dependence on foreign crude oil. 2. Contribution to rural economy. 3. Low sulphur content. 4. Zero aromatic. 5. Reduction of net CO_2 emission from life-cycle basis. 6. Nontoxic and biodegradable. 7. Reduction in PM, HC and CO. 8. High cetane and flash point. 9. Better lubricity. 10. High oxygen content promotes a more complete combustion due to improved homogeneity in the fuel air mixture. 11. The biodiesel fuel air mixture is able to achieve stoichiometric conditions which support complete combustion almost 15% quicker than fossil fuel mixtures.	1. High production cost. 2. Food versus fuel. 3. Increase in NO_X emission. 4. Deforestation and wildlife threat. 5. Fuel delivery material incompatibility. 6. Injector fouling. 7. Formation of sludge and sediments. 8. Reduced fuel filter service life. 9. Cold weather flow degradation. 10. Higher oxidation tendency due to lower oxidation stability. 11. Increased engine oil dilution leading to premature oil change. 12. Reduced power and torque. 13. Microbial growth in old or weathered fuel.

Table 1.3 The amount of biodiesel utilization in selected countries/regions.

Nations	Current utilization	Future target
Australia	B5-B20 [26]	B20-B100 [27]
Brazil	B7 [28]	B10 [28]
Ecuador	B5 [28]	B10 [28]
Indonesia	B5 [28]	B10 [28]
Peru	B2 [28]	B5 [28]
United States	B5-B20 [28, 29]	No available information
Uruguay	B2 [28]	B5 [28]
European Union	B5.75 [28]	B10 [28]
Malaysia	B7 [30]	B10 [31]

The use of biodiesel to power diesel engine is however limited beyond B20 to date. This is majorly due to the difference in the oxidation stability (OS) value between biodiesel and diesel as exhibited in Table 1.4. Corresponding to this, the root cause for the differences of OS value between diesel and biodiesel is briefly discussed here. As exhibited in Table 1.5, it is observed that diesel undergoes 3 distinct processes such as separation, upgrading and conversion to produce a high quality product from fossil fuel. On the other hand, biodiesel only undergoes a single trans-esterification process majorly to reduce the high viscosity vegetable oil to be in line with the diesel engine operation. The explicit differences in the processes aim above as well as the higher number of processes involved in the

production of diesel in comparison to biodiesel are the major reasons behind the much higher OS of diesel as compared to biodiesel.

Table 1.4 Comparison of properties between diesel and biodiesel [73].

Property		**Diesel**	**Palm biodiesel**
Oxidation stability	(h)	>40	~10
Flash point	(°C)	60	130
Cetane number		44	55
Sulphur	(ppm)	<15	<15
Relative density @ 15°C	(kg/m^3)	0.85	0.88
Kinematic viscosity @ 40°C	(mm^2/s)	2.6	6
Heating value	(kJ/kg)	42.7	40.6

Table 1.5 Comparison between diesel and biodiesel's production method and chemical composition [73-75].

	Diesel		**Biodiesel**			
Feedstock	Petroleum		Vegetable oil, animal oil, waste cooking oil			
Chemical process	Refining-3 distinct stages 1. Separation: distillation 2. Upgrading: hydro treating 3. Conversion: catalytic cracking/hydrocracking		Transesterification			
Specific reason for the process	Separation-separation of components based on the boiling point. Upgrading-removal of undesirable compounds such as sulphur. Conversion-cracking of large molecules into small ones.		Reduce oil's viscosity. Typically reduce 40 mm^2/s to 5 mm^2/s.			
Final product	Majorly carbon and hydrogen		Majorly carbon, hydrogen and oxygen			
Major component (wt%)	Quantity	EN 590	Fatty acid	Palm	Rapeseed	Soy
	Paraffin	29.0	Palmitic C16:0	44.0	4.0	11.0
	Naphthenic	52.0	Stearic C18:0	4.0	2.0	4.0
	Total aromatics	18.9	Oleic C18:1	39.0	62.0	23.0
	Others	0.1	Linoleic C18:2	11.1	22.0	53.0
			Linolenic C18:3	0.0	10.0	8.0
			Others	1.9	0.0	1.0
Chain saturation (wt%)		EN 590		Palm	Rapeseed	Soy
	Saturated	81.0	Saturated	46.7	5.8	15.5
	Unsaturated	18.9	Unsaturated	51.1	89.4	83.5

Fuel in general is typically required to have a minimum OS value to prevent rapid deterioration under engine operating conditions. For example, in a diesel engine equipped with common rail type fuel injection system, the fuel would normally be pressurized up to 1350 bar which leads to a significantly high fuel temperature in excess of 100 °C [32]. High fuel temperature coupled with the presence of various materials such as copper and nitrile rubber (NBR) in the fuel delivery system (FDS) can catalyse the oxidation process which causes the fuel quality to deteriorate [33-35].

The fuel return system as shown in Fig. 1.2 allows the deteriorated fuel to be recirculated back into the storage, contaminating the fuel in the reservoir [36]. Taking into account the biodiesel's lower OS than fossil diesel, this problem is aggravated when biodiesel is used. In order to arrest this, antioxidants are routinely added to improve biodiesel's OS with success [37-67]. The major drawback to this approach is the need for exact quantification of antioxidant concentration. For example, lower concentration than required might delay the oxidation process, but not completely prevent it [68]. On the other hand, a higher concentration than necessary could cause the antioxidant free radicals to react with oxygen which accelerates the oxidation process instead [68].

The unresolved biodiesel's low OS value coupled with the engine operating conditions which favour fuel deterioration as described above have led to fuel delivery materials (FDM) incompatibility problem. As demonstrated in Fig. 1.2, fuel tank, fuel lines, fuel filter, fuel pump, fuel rail and fuel injectors are among the components present in a typical diesel engine's fuel delivery and storage system. These components were fabricated with chosen materials as listed in Table 1.6 based on the appropriateness of the component's functionality as well as due to its good compatibility with diesel. These components were nevertheless designed to last for a foreseen lifespan of 10-15 years depending on their functions.

However, use of deteriorated fuel as a result of engine operation could significantly reduce the lifespan of these components due to accelerated metal corrosion and elastomer degradation. This is mainly because the formed oxidized products such as aldehydes, ketones and short-chain acids from biodiesel deterioration have been proven to accelerate the FDM degradation process [18, 35, 69-72]. These adverse effects on the components are evident in the form of hose rupture, seal breakage and line leakage peaking at fuel leakage and loss of compression.

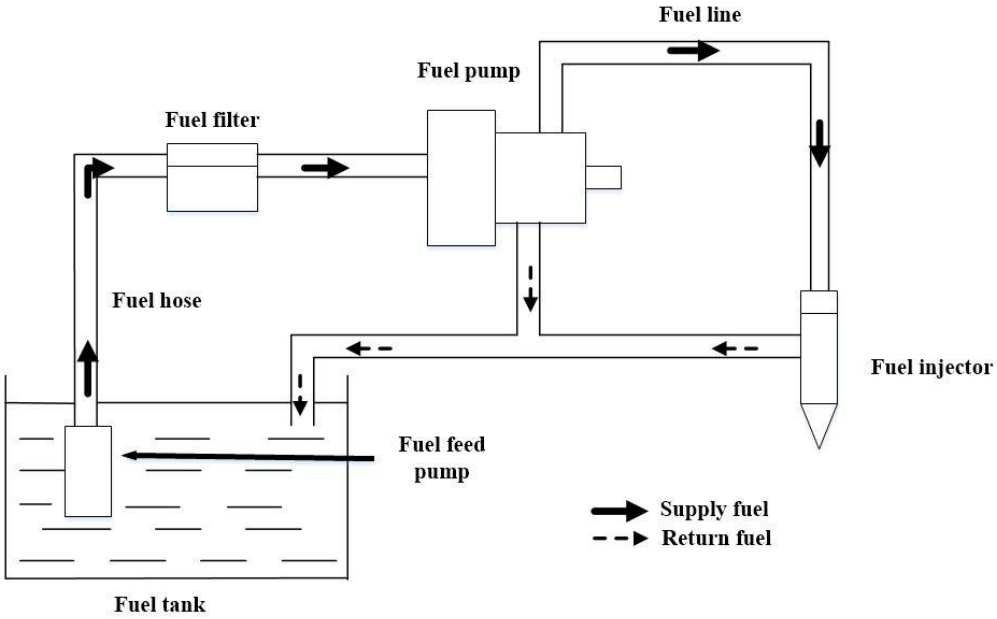

Fig. 1.2 Fuel delivery and storage system in a typical diesel engine.

Table 1.6 Materials used in the fabrication of fuel storage and delivery components [18, 76-79].

Parts	**Materials**
Fuel tank	Steel, plastic
Fuel feed pump	Aluminium alloy, iron-based alloy, copper-based alloy
Fuel lines	Steel, plastic, rubber
Fuel filter	Aluminium, plastic, paper, resin impregnated paper
Fuel pump	Aluminium alloy, iron-based alloy, copper-based alloy
Fuel injector	Stainless steel
Nozzles	Steel
Gasket	Elastomer, paper, cork, copper

With regard to the aforementioned implications above, extensive studies have been conducted in determining the compatibility of biodiesel with fuel delivery metals and elastomers. Here, greater metal corrosion with the use of biodiesel than diesel has been reported [80-82]. For example, the addition of even a small amount of biodiesel in diesel blend such as 2 vol% in terne cups at 80 °C for 1000 hours (h), increased the leaching of lead by 22,900% when compared with diesel [83]. Furthermore, the corrosion rate is also reported to increase with increasing biodiesel concentration in diesel [35]. The rise in the copper corrosion rate in biodiesel when compared to diesel is typically within the range of 68% to 148% [35, 84, 85]. Copper has a significant incompatibility with biodiesel in comparison to other metals such as aluminium and steel. The utilization of corrosion inhibitors in controlling metal corrosion is unsuitable despite being effective [86-89] since it adversely affects elastomers by inducing further crosslinks [90]. In addition, leached metal ions due to corrosion could adversely affect biodiesel's stability by acting as catalyst in promoting biodiesel oxidation leading to the formation of undesirable oxidized products such as aldehydes and ketones [18, 33, 91-96]. Oxidized biodiesel is also found to be more corrosive than unoxidized biodiesel since rise in corrosion rate of copper by 59% was reported when immersed in oxidized palm biodiesel at 80 °C for 840 h than in un-oxidized biodiesel [35].

In addition to the adverse effects of biodiesel towards metals as described above, most elastomers which showed good compatibility with diesel underwent significant degradation when tested with biodiesel [97-99]. For instance, 250% higher degradation in the form of mass change was reported for NBR immersed in *Jatropha curcas* biodiesel at 26 °C for 672 h than in diesel [100]. In a different study, the degradation of poly-tetrafluoroethylene in the form of volume change was reported to be 3 times higher when immersed in palm biodiesel at 26 °C for 1000 h than in diesel [101]. It is essential to highlight that the degradation of elastomers in general is not as direct as metal degradation which is apparent in the course of mass loss [101]. This is mainly because elastomers composed of high molecular weight monomers are dependent on its chemical structure in ensuring its functionality. Fuel permeation/attack on elastomers adversely affect its properties. Hence, the degradation is quantified in the form of volume, mass, dimensions, hardness and tensile strength changes [102, 103]. Hardness and tensile strength changes in general come hand in hand with volume change [70, 104]. Elastomer manufacturers have stated that the tolerance level of elastomer degradation in the form of volume change observed as swelling is 30% and 10-15% for static and dynamic applications, respectively [70].

Since the majority of the studies agreed that the FDM degradation exceeded the acceptable level with the use beyond B20, these findings influenced the policy makers in not recommending biodiesel use beyond B20 to power diesel engines. However, to meet the energy demand worldwide without further increase in the

fossil fuel consumption, it is crucial to use biodiesel beyond B20 even though the cost of biodiesel is still higher than diesel. The present higher cost of biodiesel is due to the biodiesel's higher priced feedstock and higher production technology cost. It is anticipated that this cost will reduce in time to come with the utilization of cheap feedstock and more cost-efficient production technology. Additionally, as shown by the comparisons displayed in Table 1.7, significant reductions in the exhaust emissions of unburned hydrocarbon, carbon monoxide and nitrogen oxide could be attained with the utilization of biodiesel beyond B20. With regard to the increase in particulates, the use of an improved diesel particulate filter could curb this problem.

Table 1.7 Diesel engine exhaust emissions operated with rapeseed-based biodiesel as compared to diesel [105].

Emission		**B20**	**B100**
HC change	(%)	-19.0	-52.4
CO change	(%)	-26.1	-47.6
NO_x change	(%)	-3.7	-10.0
CO_2 change	(%)	0.7	0.9
Particulates change	(%)	-2.8	9.9

Corresponding to the necessity of utilizing beyond B20, the common practice involved in determining the compatibility present between biodiesel and FDM were evaluated. Here, it was observed that the existing studies so far were mostly carried out under immersion investigations instead of a physical diesel engine's operating condition. The immersion investigations referred here are primarily the employment of standard methods such as the ASTM G31 and ASTM D471 for metal and elastomer, respectively. In general, the metal's mass loss is determined to calculate the metal corrosion rate while the elastomer's volume, mass, tensile strength and hardness changes are determined to evaluate the elastomer degradation level. The obtained findings from these studies were nevertheless used as guidelines by the policy makers in recommending the permissible biodiesel-diesel fuel blend for use in diesel engine [18, 102, 106]. Taking into account that this judgment was made based on immersion investigation instead of the engine operating condition, the adequacy of the findings from the existing studies in evaluating the actual compatibility between FDM and biodiesel in a physical diesel engine was subsequently appraised.

The existing studies in this subject area were found insufficient to appraise the compatibility of FDM with biodiesel in the FDS of a physical diesel engine. This is chiefly due to two main reasons. Firstly, the standard methods used in determining the compatibility of biodiesel with FDM do not represent the actual conditions in the FDS of a typical diesel engine. This is especially true in terms of the varying fuel pressure/temperature and the presence of a variety of materials in

the FDS. Secondly, there is a lack of available studies which investigated the exact materials compatibility with biodiesel, especially for the elastomers. This is essential because the elastomers' resistance towards biodiesel attack is very dependent on its elemental compositions.

Based on the discussion above, the aim of the present study is to elucidate the actual compatibility present between biodiesel and FDM in the FDS of a physical diesel engine as displayed in Fig. 1.3. The specific objectives of this research programme are:

- Determination of palm biodiesel deterioration under common rail diesel engine (CRDE) operation by analysing the fuel samples collected during and after engine operation.
- Identification of the biodiesel property which should be given emphasis based on its influence towards biodiesel deterioration under CRDE operation.
- Determination of palm biodiesel's dissolved oxygen (DO) concentration and conductivity value impact towards the FDM degradation.
- Elucidation of the actual compatibility of FDM with biodiesel in the FDS of a real-life CRDE.

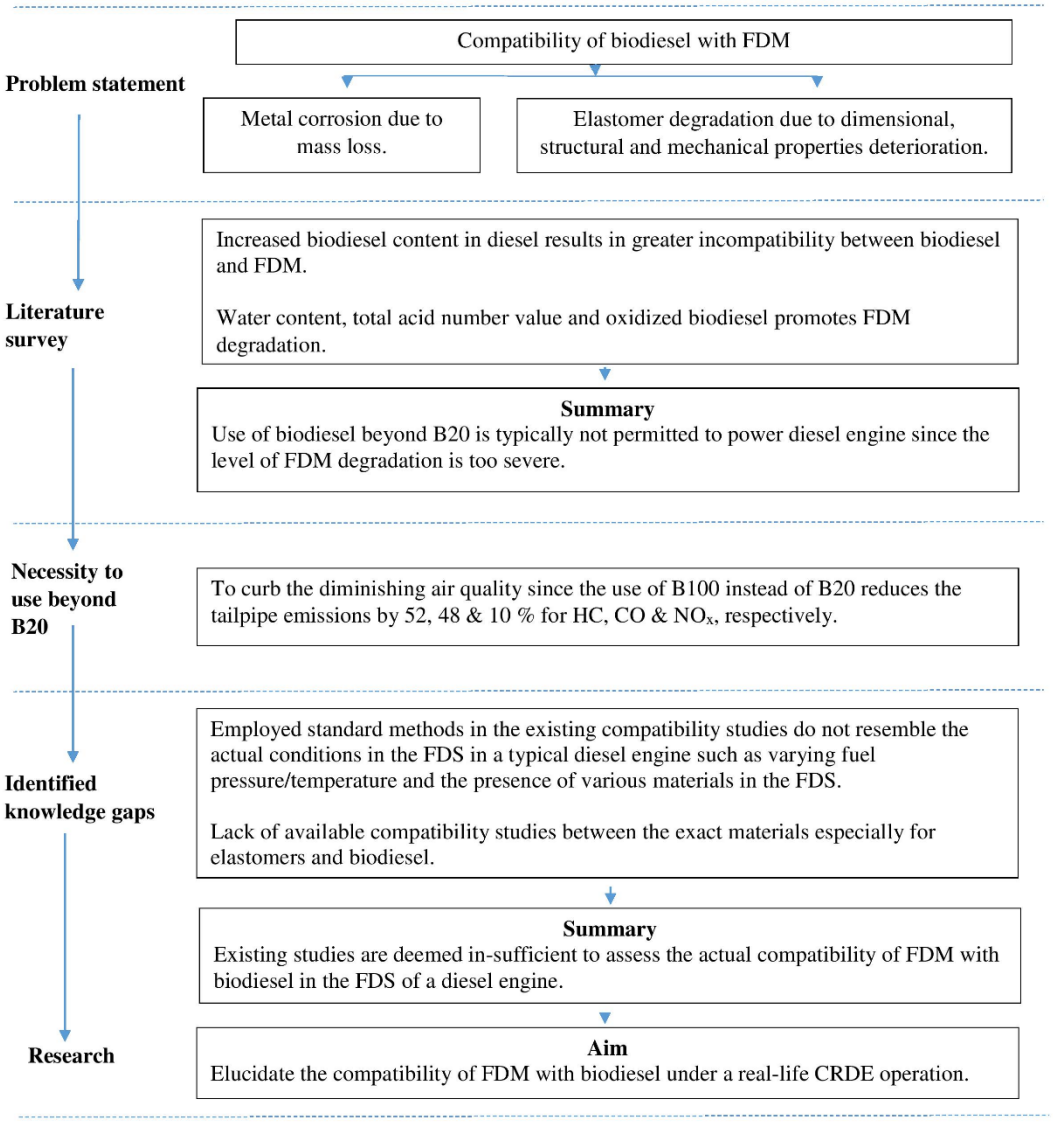

Fig. 1.3 Fundamental framework of the research.

To accomplish the aim of the present study to a considerable depth within the stipulated duration of 36 months, the scope of the present study was set beforehand. Palm-based biodiesel is the feedstock of interest here due to the vast availability of palm oil supply in Malaysia. A diesel engine equipped with a common rail fuel-injection system, precisely the first-generation Toyota 1KD-FTV 3.0 litre (l) CRDE was utilized for ascertaining the deterioration of biodiesel under engine operation. This type of diesel engine's fuel-injection system was specifically chosen here due to its popularity as the current mainstream fuel delivery setup. Distinguished standard methods from widely accepted organisations such as American Society Testing and Materials (ASTM), Society of Automotive Engineers (SAE) and International Organisation for Standardisation (ISO) were utilized here for analytical and material analyses based on the suitability of testing and available facilities.

The experimental work here commenced with the investigation into the deterioration of palm biodiesel under real-life CRDE operation as illustrated in Fig. 1.4. Fuel samples during and after engine operation were analysed for determining the deterioration in terms of biodiesel oxidation, total acid number (TAN) and water content under CRDE operation. Next, the fuel properties which should be given emphasis corresponding to the biodiesel deterioration under CRDE operation were determined. This was then followed by the investigation into the influence of the emphasized fuel properties towards FDM degradation. Ultimately, the compatibility of FDM with biodiesel under a modified laboratory

immersion was investigated. The above investigations were all important in clarifying the actual compatibility of FDM with biodiesel in the FDS of a physical CRDE.

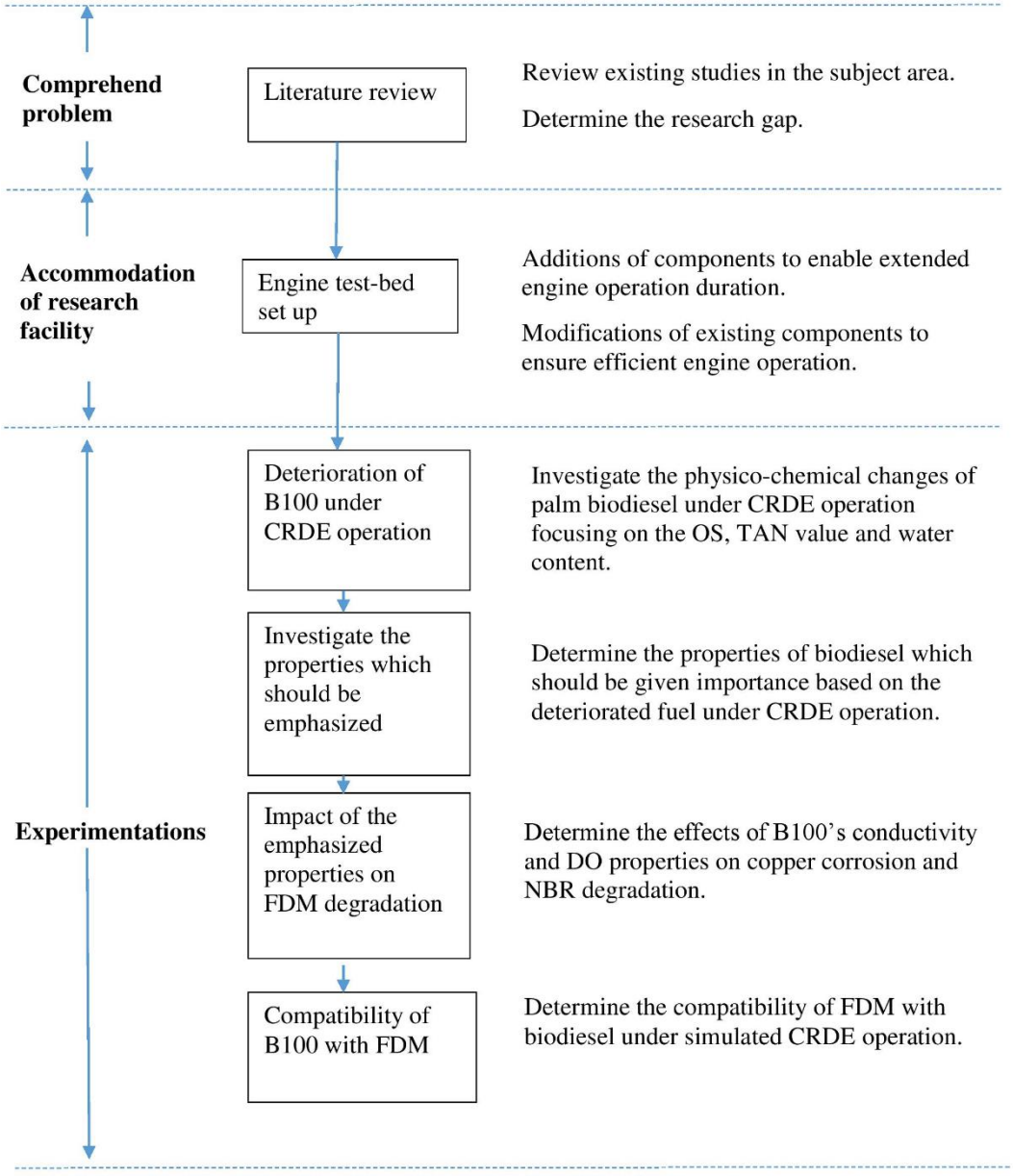

Fig. 1.4 Stages of work of the research programme.

The major significance of the present study is the elucidation of the actual compatibility present between FDM and biodiesel in the FDS of a real-life CRDE operation. Through the experimental investigations carried out, the actual compatibility of FDM exposed to biodiesel was found acceptable to good contradicting to the findings from the existing studies so far. This outcome nevertheless suggests re-assessment towards the prohibition placed on the use of higher concentration biodiesel-diesel fuel blend especially beyond B20 to power diesel engines. The specific original contributions to knowledge from the present study are:

- Elucidation of biodiesel deterioration under CRDE operation by analysing fuel samples collected during and after engine operation.

- Elimination of the concerned FDM degradation promoting factors such as water content, TAN and biodiesel oxidation products since these factors were absent in the analysed biodiesel collected after CRDE operation.

- Emphasis was placed on biodiesel's conductivity and DO properties since these two properties were not only observed to have changed after and during CRDE operation, respectively, but also influenced the fuel deterioration under CRDE operation heavily.

- The biodiesel's conductivity and DO were observed to influence metal corrosion and elastomer degradation.

- The actual degradation of FDM with biodiesel exposure in the FDS of a real-life CRDE operation was determined through simulated experimental investigations through the incorporation of fuel renewal for ASTM G31 and ASTM D471 immersion standard methods for metals and elastomers, respectively.

Based on the aim and the scope of the present study as discussed above, the thesis structure is as described below.

Chapter 1 presents the background of the conducted work and highlights the novelty/contribution of the present study. This is then followed by a summary of the thesis structure.

Chapter 2 presents the conducted literature survey in two stages of evaluation. In the first stage, a summary of the available compatibility studies between biodiesel and FDM is presented. This is then accompanied by an evaluation on the adequacy of the findings from the existing studies so far in assessing the actual compatibility present between biodiesel and FDM in the FDS of a real-life diesel engine.

Chapter 3 presents the experimental determination on the deterioration of palm biodiesel under CRDE operation in three stages of investigation. In the first stage, the collected biodiesel samples at respective engine operation intervals were analysed for ascertaining the effects of CRDE operation on biodiesel oxidation, TAN and water content. In the second stage, four comparisons were conducted between the findings obtained from the first-stage investigation precisely under the CEC F-98-08 SLTC with: firstly, to an existing study from literature; secondly, to the deterioration of biodiesel with different initial physical

properties; thirdly, to the deterioration of biodiesel under much longer engine operation duration, and finally, to the deterioration of biodiesel under metal immersion study. In the third stage, the characteristics of biodiesel's conductivity value as a result of instantaneous change of fuel temperature, the presence of dissolved copper, the presence of biodiesel oxidation products as well as heating are presented.

Chapter 4 presents the experimentations carried out to evaluate the compatibility of FDM with palm biodiesel in two stages of investigation. In the first stage, the impact of biodiesel's conductivity value and the concentration of DO on FDM degradation is presented independently. This is then followed with the FDM degradation evaluation under a modified laboratory immersion which incorporated fuel renewal at specific intervals. This modification made here was chiefly to replicate similar fuel deterioration under laboratory immersion as per under CRDE operation.

Chapter 5 presents the conclusions drawn from this research. This is then followed by the recommendations for further work. Supplementary details pertaining the present study are presented in the Appendices.

CHAPTER 2-LITERATURE REVIEW

The literature review covers two major aspects in the form of the compatibility of biodiesel with the FDM, as well as the evaluation of the existing studies in appraising the compatibility of FDM with biodiesel under a physical diesel engine operation. Based on the knowledge gaps identified from the conducted literature survey, the direction of this programme of study was determined.

2.1 Compatibility of biodiesel with FDM

The effects of biodiesel exposure on metal corrosion and elastomer degradation are critically reviewed in this section.

2.1.1 Metal corrosion due to the exposure of biodiesel

Extensive studies have reported on the compatibility of biodiesel with a wide range of metals such as copper, brass, steel, aluminium and cast iron as summarized in Table 2.1. Based on it, a number of factors such as the concentration of biodiesel in diesel, the presence of biodiesel oxidation products, water content, TAN, as well as the fuel flow condition, have been vastly reported to increase the corrosion rate [35, 83, 107-109]. For instance, the corrosion rate of copper immersed at 80 °C for 600 h was reported to increase with increasing concentration of rapeseed-based biodiesel in diesel [107]. A similar trend was also reported when copper and bronze were evaluated in palm-based biodiesel at 25-30 °C for 2640 h [35].

Bearing on the effects of oxidized biodiesel on metal corrosion, Haseeb et al. [35] reported 59% increase in the corrosion rate for copper when compared between oxidized and unoxidized palm biodiesel at 60 °C for 840 h. The higher corrosion rate of metals in oxidized biodiesel is nevertheless suggested due to the presence of oxidation products such as aldehydes, ketones and lactones which are acidic in nature, in comparison to the unoxidized fuel [71]. These oxidation products have also been attributed to the increase in TAN which is again another fuel property reported to adversely affect metal corrosion. Close attention is required for these two factors considering the biodiesel's high oxidation tendency coupled with high operating fuel temperature in a real-life diesel engine which favours the oxidation process.

As for the adverse effect of water towards the increase in corrosion rate, the condensation of water on metal surface is nevertheless suggested for this [84]. On top of that, the hygroscopic nature [35, 110], as well as the biodiesel's capability to hold 40 times more dissolved water than diesel [111], have also been suggested to promote the water condensation process. Furthermore, the failure of water separator in removing free water due to the high miscibility present between biodiesel and water molecules, further favours the influence of water present in biodiesel on corrosion.

Contradicting to the above, Meenakshi et al. [112, 113] reported otherwise by suggesting that the presence of water in the FDS does not inevitably lead to corrosion by employing wettability method. Here, the authors measured the contact angle between the biodiesel-water and metal to determine the influence of water present in biodiesel towards corrosion. According to the utilization of this method, Meenakshi et al. [112, 113] reported the formation of obtuse angle between the biodiesel-water and mild steel (127 °), aluminium (118 °) and copper (139 °). As such, the authors thus suggested that oil preferably wets the metal surface and this phenomena nevertheless isolates the metal from the corrosive effect of water. Similar findings were also reported for the wettability of carbon steel, aluminium, copper and brass in *Jatropha*-based biodiesel by Anisha et al. [114].

Nonetheless, although the corrosive effect of water present in biodiesel could probably be ruled out based on the above discourses, it is essential to note that the presence of water in biodiesel has also been associated with the conversion of esters back to fatty acid [111, 115, 116]. This conversion nevertheless results in the increase of biodiesel's corrosivity [69, 83]. Therefore, it is essential to ensure that the fuel storage and transportation tanks are cleaned and dried prior to the filling process to prevent the adverse effects of water in biodiesel.

Concerning the different metals for instance aluminium, brass, cast iron and copper, as well as the different biodiesel feedstock such as *Jatropha curcas*, *Karanja*, *Madhuca indica* and *Salvadora oleoides*, differences in the resulted corrosion rate under similar investigation conditions were observed [80, 85]. Here, the majority of the studies agreed that copper is the worst affected metal [71, 81, 99, 109] while, aluminium and stainless steel are the least [98, 99]. As for the influence of immersion duration on corrosion rate, the continuous rise in the copper corrosion rate in palm biodiesel until 1200 h before it eventually reduced, was nevertheless suggested due to the formation of passive layer on the metal surface which prevented further corrosion [117].

As for the influence of fuel temperature on corrosion rate, increased corrosion rate with increasing fuel temperature was reported by Fazal et al. [72] who evaluated the corrosion rate of mild steel in palm-based biodiesel at 26, 50 and 80 °C for 1200 h. Here, the authors also reported the percentage of oxygen on the immersed metal surface were found increased with increasing fuel temperature. Similarly, Haseeb et al. [35] reported higher corrosion rate at 60 °C than at room temperature (~ 25 °C) for copper and leaded bronze immersed in palm-based biodiesel. Here, the authors suggested that this outcome could nevertheless be attributed due to the condensation or dissolution of more oxygen into the biodiesel at a higher temperature than at room temperature.

However, contradicting findings on the influence of fuel temperature on corrosion rate was reported by Aquino et al. [118] who investigated the corrosion rate of copper in biodiesel at 26 and 55 °C for 120 h. Here, the authors reported reduced corrosion rate with increasing fuel temperature and suggested that this outcome is majorly influenced due to the reduced DO at a higher temperature. Nevertheless, the influence of DO on metal corrosion has also been suggested in many other studies so far but, no study to date has typically investigated in this subject area in specific [102, 117].

Concerning the effects of biodiesel's conductivity on corrosion rate, the addition of 1% sodium chloride in biodiesel by the study of Anisha et al. [114] resulted in contradicting corrosion rate for carbon steel and copper. Here, the authors reported increased corrosion rate for carbon steel while, reduced corrosion rate for copper. It is essential to highlight here that, the addition of sodium chloride in biodiesel could have nevertheless possibly altered the biodiesel's properties. On top of that, the reported initial biodiesel's conductivity prior to the study for both the carbon steel and copper are not similar. Corresponding to this, the influence of biodiesel's conductivity on corrosion rate could possibly be misjudged from the method employed in the present study. A more appropriate approach of manipulating the biodiesel's conductivity value without altering the fuel's physical properties is needed.

Table 2.1 Bibliographic studies on the compatibility of metals in biodiesel.

Ref	Method	Condition	Fuel	Specimen	CR (mm/y)		Comments
[107]	Immersion	80 °C for 600 h	B0 (diesel), B50, B75, B100 (rapeseed)	Cu	B0 B50 B75 B100	0.00889 0.01575 0.02032 0.02337	Increase in CR with increasing biodiesel concentration in diesel.
[72]	Immersion	26, 50 & 80 °C for 1200 h	B100 (palm)	MS	26 °C 50 °C 80 °C	0.00135 0.00144 0.00149	Increase in CR with increasing fuel temperature.
[118]	Immersion	26 & 55 °C for 120 h	B100	Cu	26 °C 55 °C	0.00440 0.00050	Decrease in CR with increasing fuel temperature.
[35]	Immersion	60 °C for 840 h	B100 (palm), Oxidized B100 (palm)	Cu	B100 Oxidized B100	0.00135 0.00214	Higher CR in oxidized than unoxidized biodiesel.
[85]	Immersion	26 °C for 2880 h	B100 (palm)	Al, Br, CI, Cu	Al Br CI Cu	0.00440 0.00533 0.00285 0.00998	Different metal results in different CR.
[80]	Immersion	26 °C for 7200 h	B100 (*Jatropha curcas*, *Kranja*, *Madhuca indica*, *Salvadora oleoides*)	Piston metal	*Jatropha curcas* *Kranja* *Madhuca indica* *Salvadora oleoides*	0.00030 0.00015 0.00015 0.00314	Different feedstock results in different CR.
[117]	Immersion	26 °C for 200, 300, 600, 1200 & 2880 h.	B100 (palm)	Cu	200 h 300 h 600 h 1200 h 2880 h	0.00750 0.01120 0.00152 0.00180 0.00145	Increase in CR with increasing immersion duration.
[108]	Immersion	2016 h	B100 (soy), B100 (soy) with 1% water	Low CS	B100 B100 +1% water	0.01429 0.01786	Presence of water increases CR.

26 °C was used for the temperature referred as room; CR: corrosion rate.

Table 2.1 Bibliographic studies on the compatibility of metals in biodiesel. (Continued).

Ref	Method	Condition	Fuel	Specimen	CR (mm/y)	Comments
[83]	Immersion	80 °C for 1000 h. Fuel replaced every 250 h. Fresh air was supplied once per day.	B1, B3, B5	Terne steel (cup)	Intial TAN (mg KOH/g): B1 0.05; B3 0.06; B5 0.07 Final metal concentration (ppm): Pb / Sn — B1 8 / 1 >; B3 40 / 1 >; B5 1800 / 12	Increase in CR with increasing acid value.
[114]	Immersion	100 h	B100 (*Jatropha curcas*), B99 (*Jatropha curcas* + 1% NaCl)	CS, Cu	CS: Intial conductivity (μΩ) / CR (mm/y) — B100 0.120 / 0.01935; B99 0.320 / 0.03402 Cu: Intial conductivity (μΩ) / CR (mm/y) — B100 0.68 / 0.00617; B99 0.68 / 0.00216	Increase in conductivity results in the increase of CR for CS but reduced the CR for Cu.
[109]	Immersion, Rotating cage	100 h, Rotating cage @ 500 rpm	B100 (*Pongamia pinnata*)	Cu	Immersion 0.00556; Rotating cage 0.06868	Fuel flow increases CR.
[119]	Immersion, Linear polar resistance (LPR)	100 h, LPR measured every 24 h	B100 (*Jatropha curcas*)	Br, Cu	Immersion / LPR — Br 0.01238 / 0.00342; Cu 0.02872 / 0.00360	Higher duration averaged CR than instantaneous CR.

TAN: total acid number.

2.1.2 Elastomer degradation due to the exposure of biodiesel

Like the metals, extensive studies have evaluated and reported on the compatibility of biodiesel with a number of elastomers such as NBR, butadiene rubber-poly vinyl chloride (NBR/PVC), hydrogenated nitrile rubber (HNBR) and fluoroelastomer (FKM) as summed up in Table 2.2. Based on it, the concentration of biodiesel in diesel, fuel temperature, immersion duration, the percentage of acrylonitrile content in NBR, the percentage of fluorine content in FKM as well as the presence of water, carboxylic acid and biodiesel oxidation products in biodiesel was reported to influence the elastomer degradation rate [69, 70, 97, 100, 101, 120].

For instance, higher NBR degradation in the form of mass change was found with increasing concentration of *Jatropha curcas* biodiesel in diesel immersed at 26 °C for 672 h [100]. Concerning the effects of temperature on elastomer degradation, higher volume change by 11% was found for NBR immersed at 50 °C in palm biodiesel for 500 h than at 25 °C [97]. Here, the authors indicated that this outcome resulted due to the higher rate of biodiesel diffusion in elastomer under higher fuel temperature. Agreeing to this, high rate of elastomer degradation in the FDS of a diesel engine is expected due to the high engine operational fuel temperature of 80-100 °C. As for the effects of immersion duration on elastomer degradation, higher NBR degradation in the form of volume and weight changes were found for the sample immersed at 26 °C in palm-based biodiesel for 500 h than for 250 h [101]. This outcome nevertheless suggests that the degradation of

elastomers exposed to biodiesel will continue to rise until the component fails in the form of breakage or rupture.

Furthermore, although the presence of water in biodiesel has been commonly ascribed to the increase in elastomer degradation, the addition of 0.05% of water in rapeseed biodiesel did not result in the increase of elastomer degradation in the form of volume change when compared to the sample immersed in reference fuel [69]. Nevertheless, the addition of 30% of carboxylic acid on top of the 0.05% of water in biodiesel in the same study as the above resulted in 10% higher volume change. This outcome nevertheless suggests that the water does not directly influence the elastomer degradation. Instead, the water acts as an initiator for the hydrolysis reaction of esters in biodiesel at which subsequently affects the elastomers adversely consequent to the formed carboxylic acid [115, 121-123]. It is essential to highlight here that carboxylic acid is among the oxidation products of biodiesel [124].

Apart from the influence of water towards the formation of oxidation products, biodiesel's susceptibility towards oxidation proceeds in as little as a few h with the exposure to air depending on the storage conditions and the amount of unsaturation of the fatty acids. Formed oxidation products such as aldehydes, ketones, short-chain acids and carboxylic acids are vastly reported to increase the elastomer degradation rate [16, 69, 121]. As such, precautions should be taken to

preclude the formation of oxidation products in controlling the elastomer degradation rate.

Bearing on the effects of TAN on elastomer degradation, contradicting outcomes were found for FKM and NBR immersed in biodiesel at 26 °C for 672 h with different level of TAN [98]. Here, the authors reported higher volume change for FKM immersed in the biodiesel with the higher TAN while, it was found otherwise for NBR. With regard to this, Hu et al. [100] in a different study suggested that the degradation of elastomer is not directly related to the biodiesel's TAN. Rather, the differences in the chemical polarity between the fuel and the elastomer were suggested as the primary cause for the degradation. As such, the influence of biodiesel's TAN on elastomer degradation could not be judged.

For elastomers in general, the addition of curing agents and accelerators in the formulation of elastomers creates cross-links between the polymer chains [97]. It is this network of cross-links that heavily influences its physical attributes. The addition of carbon black and silica fillers in the formulation nevertheless improves its hardness, abrasion resistance, tensile strength and tear strength. Upon exposure of elastomers with biodiesel, the cross-linking agent and/or filler seems to react with the fuel. This reaction thereby causes deterioration to its physical and mechanical attributes. As such, the deviations in the reaction level for

different elastomers such as NBR, HNBR, NBR/PVC and FKM, as well as with different biodiesel feedstock such as *Jatropha*, palm, cotton seed, soy and rapeseed, resulted in different level of degradation [100, 125].

Here, a majority of the studies agreed that FKM showed acceptable to good compatibility with biodiesel [18, 70, 98, 126] while, NBR showed significant degradation [18, 70, 98, 126]. Higher resistance exhibited by FKM in comparison to other types of elastomers is suggested due to the presence of a CH3-F bond in it which is nevertheless a bond with high bond dissociation energy. It is apparent that this bond dissociation energy is associated with the establishment of thermal stability and ease of abstraction of crosslinks in an elastomer [127]. Therefore, this explains the good resistance of FKM towards biodiesel attack. Furthermore, the increase in fluorine content in FKM is also noted to result in better resistance towards biodiesel permeation [127]. Similarly, greater acrylonitrile content in NBR is also found to result in better resistance towards biodiesel attack. Besides, there are also suggestions that the lower affinity of biodiesel towards higher acrylonitrile content NBR resulted in this outcome [120].

In the next section, the sufficiency of the findings from the existing studies so far in appraising the compatibility of biodiesel with FDM in the FDS of a physical diesel engine is critically reviewed.

Table 2.2 Bibliographic studies on the compatibility of elastomers in biodiesel.

Ref	Condition	Fuel	Specimen	Elastomer degradation			Comments
[100]	26 °C for 672 h	B100 (*Jatropha curcas*), B100 (palm), B100 (cotton seed), B100 (soy), B100 (rapeseed)	NBR		Mass change (%)		Different feedstock results in different elastomer degradation level.
				Jatropha curcas	3.5		
				Palm	4.8		
				Cotton seed	7.5		
				Soy	7.0		
				Rapeseed	6.0		
[100]	26 °C for 672 h	B0, B5, B10, B20, B50, B100 (*Jatropha curcas*)	NBR		Mass change (%)		Increasing elastomer degradation with increasing biodiesel concentration in diesel.
				B0	1.0		
				B5	1.5		
				B10	1.5		
				B20	2.0		
				B50	2.0		
				B100	3.5		
[97]	25 & 50 °C for 500 h	B100 (palm)	NBR		VC (%)	HaC (%)	TSC (%)	Increasing elastomer degradation with increasing temperature.
				25 °C	20.0	-12.8	-3.8	
				50 °C	30.0	-16.4	-16.3	
[101]	26 °C for 250 and 500 h	B100 (palm)	NBR		VC (%)	Weight change (%)		Increasing elastomer degradation with increasing immersion duration.
				250 h	12.0	4.5		
				500 h	18.0	7.0		
[98]	26°C for 672 h	B100 (waste cooking oil 1), B100 (waste cooking oil 2)	FKM, NBR		Initial TAN (mgKOH/g)	FKM mass change (%)	NBR mass change (%)	Increase in acid value increased the degradation of FKM but decreased the degradation of NBR.
				Waste cooking oil 1	12.64	4.5	6.0	
				Waste cooking oil 2	0.26	0.9	7.0	

Immersion standard method was utilized in all the studies; HaC: hardness change; TAN: total acid number; TSC: tensile strength change; VC: volume change.

Table 2.2 Bibliographic studies on the compatibility of elastomers in biodiesel. (Continued).

Ref	Condition	Fuel	Specimen	Elastomer degradation			Comments
[125]	100 °C for 1008 h	B10 (palm)	NBR,		VC (%)	HaC (%)	TSC (%)	Different elastomers result in different elastomer degradation level.
			HNBR,	NBR	0.0	5.5	-23.0	
			NBR/PVC,	HNBR	9.5	-6.5	5.0	
			FKM	NBR/PVC	-1.0	2.0	-4.0	
				FKM	2.4	-3.6	-24.0	
[120]	70 °C for 70 h	B100 (coconut)	NBR	% Acrylonitrile	HaC (%)		TSC (%)	Increase in the % of acrylonitrile in NBR, increased its resistance towards degradation.
			(with	28	-70.0		-90.0	
			different % of	33	-60.0		-75.0	
			acrylonitrile)	45	-18.0		-10.0	
[69]	125 °C for 3024 h	B100 (rapeseed)	FKM (with		% Fluorine		VC (%)	Increase in the % of fluorine in FKM, increased its resistance towards degradation.
			different % of	FKM-GLT-S	64		6.5	
			fluorine)	FKM-A401C	66		5.5	
				FKM-F605C	70		4.0	
[69]	125 °C for 336 h	B100 (rapeseed),	FKM				VC (%)	Presence of water does not increase the degradation level. But, presence of carboxylic acid which is formed due to the presence of water increases degradation level.
		B100 with 0.05% water,		B100			4.0	
		B100 with 0.05% water		B100 + 0.05% water			4.0	
		and 30% carboxylic acid		B100 + 0.05% water + 30% carboxylic acid			14.0	
[70]	60 °C for 1000 h	B20 (soy),	FKM,			FKM		Oxidized biodiesel results in significant increase in elastomer degradation level.
		Oxidized B20 (soy)	NBR		VC (%)	HaC (%)	TSC (%)	
				B20	5.0	-3.9	0.0	
				Oxidized B20	4.4	-5.3	-0.9	
						NBR		
					VC (%)	HaC (%)	TSC (%)	
				B20	12.2	-7.8	-18.6	
				Oxidized B20	30.6	-21.9	-43.6	

2.2 Assess the compatibility of biodiesel with FDM under a physical diesel engine

Based on the outcomes of the existing compatibility studies as reviewed in the previous section, the use of biodiesel to power diesel engines beyond B20 is typically not permitted to date. This judgement was nevertheless made based on the existing studies so far which employed immersion, linear polar resistance and rotating cage standard methods instead of a real-life diesel engine operation. Corresponding to this, it is important to ascertain the accuracy of the findings from these studies in representing the actual compatibility of biodiesel with FDM. Since no review is typically available in this subject area to date, the sufficiency of the findings from the existing studies in appraising the compatibility of biodiesel with FDM in the FDS of a physical diesel engine is critically reviewed here. Among the focused aspects are the standard methods utilized for the compatibility studies and the evaluated FDM.

2.2.1 Standard methods used in existing compatibility studies

To date, there are two analytical tests to determine the fuel's corrosive effect on metals: the ASTM D130 and ASTM D664. ASTM D130 [128] evaluates the effects of an immersed copper strip in fuel, with a standardized reference strip. The results are rated on a scale of slight tarnish 1A, B to heavy tarnish 4A-C. As shown in Table 2.3, 1A result (marginal corrosion) was obtained for all the tested samples irrespective of diesel, biodiesel (from cottonseed, rapeseed and soy) and B20 biodiesel-diesel fuel blend. This demonstrates that this analytical test is

incapable of distinguishing the corrosive effects of diesel fuel, biodiesel, biodiesel-diesel fuel blends, as well as different biodiesel feedstock towards copper corrosion [18]. Nevertheless, this test determines the corrosivity of the fuel based on the quantity of sulphur compound present [128]. Since biodiesel does not contain sulphur, this test is not able to measure its corrosivity.

Table 2.3 Results of biodiesel's corrosiveness from ASTM D130 and ISO 2160 standard methods [18].

Reference	Standard method	Fuel	Results
[129]	ASTM D130	Diesel	1A
		B20 (feedstock not mentioned)	1A
[130]	ASTM D130	B20 (feedstock not mentioned)	1A
		B100 (feedstock not mentioned)	1A
[131]	ASTM D130	B100 (cottonseed)	1A
[70]	ASTM D130	B20 (soy; oxidized)	1A
[37]	ISO 2160	B100 (rapeseed)	1A
[132]	ASTM D130	B100 (soy)	1A

ASTM D664 [133] is the other analytical test utilized to determine the fuel's corrosive effect on metal. This test works by determining the required mass of bases solution (KOH) in neutralizing the acidity of the fuel. The acidity of the fuel could typically be correlated to the fuel's corrosivity. However, there is no general correlation between the acid number and the corrosive tendency of the biodiesel [133]. The varying corrosivity of the oxidation products and the organic

acids which are naturally present in biodiesel are believed to be the key parameters governing this observation. Therefore, this analytical test is also deemed unsuitable to determine the corrosive effect of biodiesel and biodiesel-diesel fuel blends.

Apart from these two analytical tests, a number of standard methods have been utilized in evaluating the compatibility between biodiesel and metals. Among these are the immersion standard method ASTM G31 [134], rotating cage standard method ASTM G184 [135] and the linear polarization resistance standard method ASTM G59 [136]. Typically, metal deterioration is evident from mass loss. Therefore, the analysis which is given the most importance is corrosion rate. The major difference between ASTM G31 and ASTM G184 is the flow condition as shown in Table 2.4. In ASTM G31, the fuel is in a static condition while the fuel is travelling at a specified speed in ASTM G184. Meenakshi et al. [109] compared the corrosion rate of copper in *Pongamia pinnata* oil under ASTM G31 and ASTM G184 standard methods for 100 h at a rotational speed of 500 revolution per minute. The authors reported higher corrosion rate of copper by 1135% under ASTM G184 than ASTM G31. Corresponding to this, higher metal corrosion is anticipated when the fuel travels through the FDS than when stored in the fuel tank. In terms of the ASTM G31 and ASTM G59, the earlier measures the duration averaged corrosion rate, while the latter measures the instantaneous corrosion rate. In a study by Anisha et al. [119], the corrosion rate of copper, brass and carbon steel were compared under ASTM G31 and ASTM

G59 standard methods. Here, higher corrosion rate was reported under ASTM G31 than ASTM G59 for copper, brass and carbon steel by 698%, 262% and 426%, respectively. The higher corrosion rate under ASTM G31 than ASTM G59 nevertheless shows that the corrosion rate of metals in biodiesel increases with duration.

Table 2.4 Working principles of the standard methods and the corresponding reference studies.

Standard method	Working principle	References
ASTM G31	Determines the average corrosion rate by accelerating the metal deterioration by simulating the conditions of interest through immersion study (typically static).	[35, 72, 138]
ASTM G184	Determines the corrosion rate by simulating pipeline flow under laboratory conditions (dynamic).	[109]
ASTM G59	Determines the corrosion rate by monitoring the relationship between the electrochemical potential and current generated between electrically charged electrodes.	[119]
ASTM D471	Determines the effects on elastomers by accelerating the elastomer degradation by simulating the conditions of interest.	[69, 70, 97]

On the other hand, the most commonly utilized standard method in evaluating the compatibility between biodiesel and elastomers is the ASTM D471 [137]. ASTM D471 and ASTM G31 are similar in a way where both the standard methods accelerate the material deterioration process by simulating the conditions of interest in evaluating the effects on the materials. Among the commonly evaluated conditions of interest include the effects of water content, TAN and oxidized products present in biodiesel on FDM degradation. For example, Haseeb et al. [35] utilized ASTM G31 to evaluate the effects of oxidized products present in palm biodiesel on copper corrosion rate immersed at 60 °C for 840 h. In another study, McCormick et al. [70] utilized ASTM D471 to evaluate the effects of oxidized products present in B20 soy biodiesel on NBR's degradation immersed at 60 °C for 1000 h.

All these standard methods are excellent in benchmarking the effects of biodiesel, diesel and biodiesel-diesel fuel blends on FDM degradation. However, the conditions employed in these standard methods do not resemble the actual operating conditions in the FDS of diesel engines. The conditions in the FDS system are dependent on the varying speed-load, which instantaneously alters the fuel pressure and hence directly affects the fuel temperature. The effects of varying fuel temperature, together with the presence of a variety of FDM, could not be simulated by any of these standard methods. As a consequence, the identified factors promoting material degradation such as water content, TAN and oxidized products determined from these standard methods may not inevitably be

present in the actual FDS. Besides, there are also chances that the adverse effects observed on FDM especially using the immersion test could be influenced by secondary effects. The secondary effects here refer to the effects induced by the formed oxidation products such as aldehydes, ketones and short-chain acids. The presence of these products is known to accelerate the FDM deterioration [35].

2.2.2 Evaluated materials in existing compatibility studies

Despite the compatibility of several metals and elastomers with biodiesel, diesel, as well as biodiesel-diesel fuel blends have been evaluated to date as listed in Table 2.5, very few of these studies typically provided the elemental composition of the evaluated materials. This information is nevertheless essential for elastomers especially since its chemical resistance is very dependent on its elemental composition. For instance, higher percentage of acrylonitrile content in NBR is perceived to contribute towards higher resistance against fuel permeation/attack. In a study by Linhares et al. [120], the effects of coconut-based biodiesel on NBR with 28% and 45% acrylonitrile content were evaluated. The authors here reported 80% higher tensile strength reduction was experienced by the NBR with 28% acrylonitrile in comparison to the latter. Similarly, higher fluorine content in FKM is perceived to contribute towards the higher resistance against fuel permeation/attack. To date, the least resistant FKM evaluated in biodiesel has 64% fluorine content by weight [69]. Based on this, biodiesel is said to have sufficient compatibility with FKM only if the existing FKM has a minimum fluorine content of 64 wt%.

Another important point observed from these studies is that, none typically investigated the exact elastomers especially present in the FDS prior to the study. The typical approach of evaluating the common FDM such as those listed in handbooks [76, 77] might not be sufficient as the compatibility of elastomers with fuels are very dependent on their elemental composition as described above.

Based on the above, the compatibility of biodiesel with the exact elastomers present in the FDS of a diesel engine could only be determined through two ways. Firstly, by comparing the elemental composition of the evaluated elastomers so far, with the elemental composition of the exact elastomers. Or secondly, by determining the compatibility of the exact elastomers itself with biodiesel. However here, the in-availability of both the evaluated elastomers' elemental composition so far, as well as the lack of available compatibility studies between the exact elastomers and biodiesel, typically prevents accurate judgement in this subject area.

Table 2.5 Evaluated fuel delivery metals and elastomers with the corresponding studies in literature.

Metals			
Type	**Immersion studies (Ref.)**	**Linear Polar Resitance studies (Ref.)**	**Rotating Cage studies (Ref.)**
Aluminium	[84, 85, 107, 119, 138-140, 142-145]	[119, 140-141]	
Brass	[85, 109, 118, 119, 140]	[119, 140]	[109]
Bronze	[35]		
Carbon steel	[72, 108, 119, 139, 140, 146-147, 149, 151-153]	[108, 119, 140, 147-148, 150]	
Cast iron	[85, 88]		
Copper	[35, 84, 85, 107, 109, 117-119, 139, 140]	[119, 140]	[109]
Galvanized steel	[149]		
Magnesium	[138]		
Monel steel		[148]	
Stainless steel	[84, 139, 154]	[148]	
Steel		[155]	

Elastomers	
Type	**Immersion studies (Ref.)**
Acrylic rubber	[125]
Chloroprene	[101]
Ethylene-propylene-diene monomer	[98, 100, 101, 156-158]
Fluoroelastomer	[69, 70, 97, 98, 100, 122, 125, 158-161]
Fluorosilicone	[122, 160, 162]
Hydrogenated nitrile rubber	[70, 125, 158, 160]
Nitrile rubber	[70, 97, 98, 100-101, 120, 125, 158, 160, 161, 163-171]
Nylon	[172]
Polyamide	[158]
Polychloroprene	[97]
Polyethylene	[173]
Poly-tetrafluoroethylene	[101, 174]
Synthetic rubber	[98]
Silicone rubber	[98, 101]

2.3 Summary

Based on the discussions above, several factors are deemed to produce greater metal corrosion and elastomer degradation. Among it are the increasing concentration of biodiesel in diesel, increasing TAN, as well as the presence of water and biodiesel oxidation products. These were found to be true based on the existing compatibility studies of FDM with biodiesel so far. Nevertheless, considering the fact that these studies were conducted mainly through laboratory investigations, the sufficiency of these studies so far in representing the actual compatibility of biodiesel with the FDM in a real-life diesel engine should be re-evaluated.

In line with the discussions on this subject area, the existing studies are deemed inadequate to comprehensively evaluate the compatibility of FDM in the FDS of a diesel engine with biodiesel. This is primarily because the current standard methods used in evaluating the compatibility present between FDM and biodiesel do not resemble the actual conditions in the FDS of a typical diesel engine. This is especially true in terms of the varying fuel pressure/temperature and the various materials present in the FDS. Corresponding to this, the identified factors promoting material deterioration from these studies may not necessarily be present under the actual operating conditions. Besides, there are also chances for the formed oxidation products to be influencing the findings observed mainly from immersion studies. Secondly, very few studies typically provided the elemental composition of the evaluated materials. On top of that, there is also a

lack of available studies which evaluated the exact materials compatibility with biodiesel. The above is crucial especially for elastomers since its resistance towards biodiesel is heavily influenced by its elemental composition. This nevertheless prevented any attempt to determine the exact elastomers compatibility with biodiesel.

All these nevertheless suggest that a more systematic study is required to appropriately appraise the compatibility present between the FDM and biodiesel in the FDS. Firstly, the deterioration of biodiesel under diesel engine operation should be determined. Here, the deterioration of fuel under a common rail type diesel engine should be given emphasis due to its popularity as the current mainstream fuel delivery setup. The fuel deterioration determination is nevertheless crucial in order to understand if biodiesel actually oxidizes under actual diesel engine operations, as well as to ascertain the presence of common factors promoting FDM degradation such as water content and TAN. From here, the effects of oxidized biodiesel, water content and TAN on FDM degradation could be resolved. Secondly, investigations into the biodiesel property which should be given emphasis based on the fuel deterioration need to be carried out. This shall be accompanied by the determination into the identified properties' corresponding effects towards FDM degradation. Ultimately, the compatibility of FDM with biodiesel under simulated diesel engine operation should be determined. Here, either the exact elastomers should be utilized, or the elemental composition of the evaluated elastomers should be provided. Once all as

described above have been completed, only then the compatibility of FDM with biodiesel in the FDS of a real-life diesel engine can be conclusively determined.

CHAPTER 3-DETERIORATION OF PALM BIODIESEL FUEL UNDER COMMON RAIL DIESEL ENGINE OPERATION

This chapter presents the details of all investigations carried out as outlined in Fig. 3.1. The fuel deterioration refers precisely to the changes in the palm biodiesel's physico-chemical properties in terms of OS, fatty acid composition, hydrogen ion concentration, peroxide value, Fourier transform infrared spectroscopy spectrum, DO concentration, viscosity value, conductivity value and dissolved metal concentration due to engine operation.

3.1 Background

As discussed in the literature review in Chapter 2, the existing studies were deemed insufficient to comprehensively assess the compatibility of FDM with biodiesel in the FDS of a real-life diesel engine. This is primarily because the current standard methods utilized for determining the compatibility between the FDM and biodiesel do not represent the actual conditions in the FDS of a real-life diesel engine. Following this, a three-stage investigation was carried out to determine the deterioration of palm biodiesel under CRDE operation as shown in Fig. 3.1. The experiments conducted were essential in assessing the oxidation condition of biodiesel as well as to establish the presence of FDM promoting factors such as TAN and water content under actual CRDE operation.

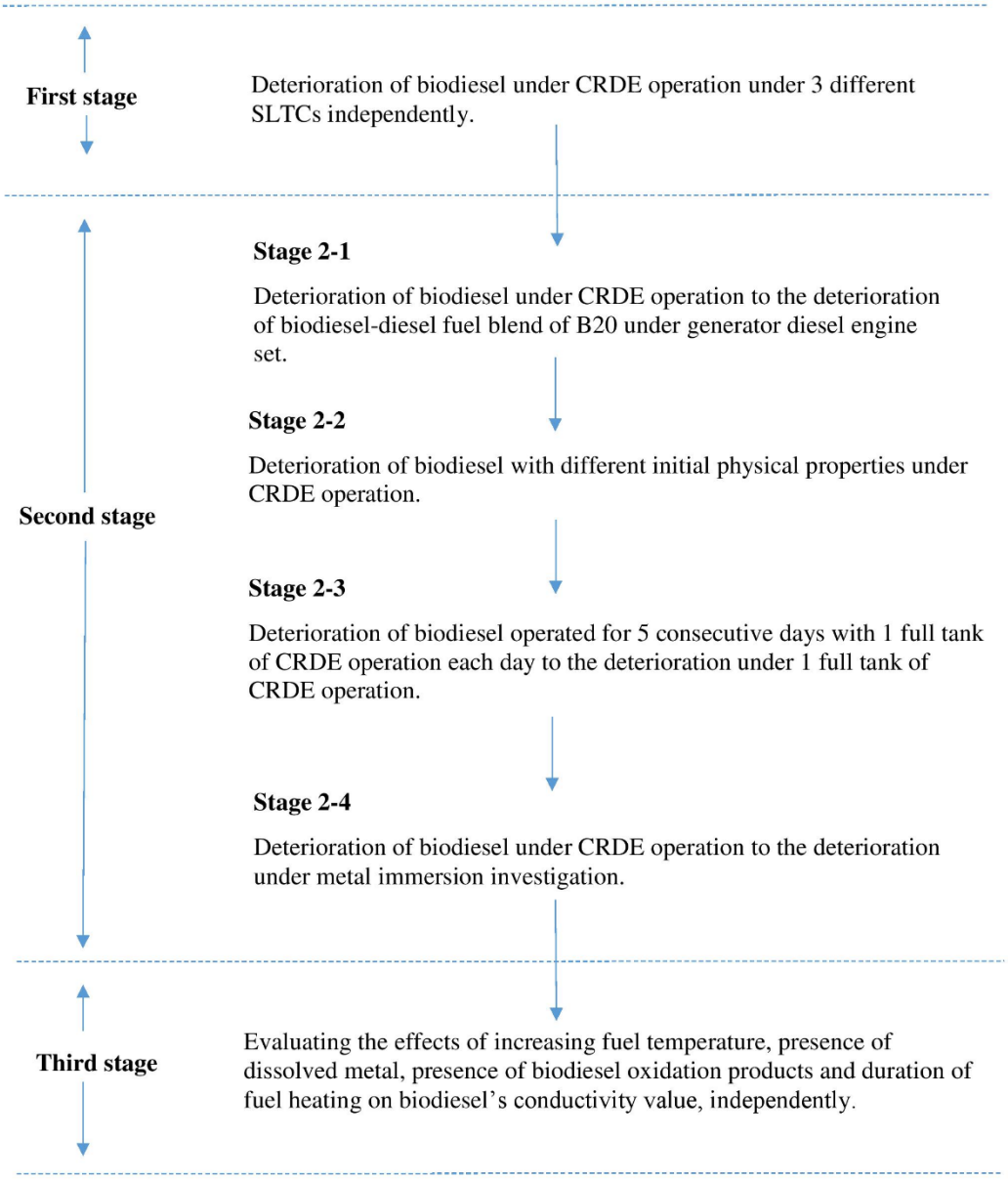

Fig. 3.1 Overview of investigations in Chapter 3.

For the first stage, the deterioration of palm biodiesel with 10.5 h of OS under CRDE operation was determined using an engine test-bed set up with a Toyota 1KD-FTV engine coupled to a SAJ Group's SE-250 model dynamometer. The World Harmonized Stationary Cycle (WHSC), Direct Injection-Common Rail Diesel Engine Nozzle Coking Test (CEC F-98-08) and an in-house developed speed-load test cycles (SLTC) were employed independently to simulate typical driving, severe driving and maximum fuel deterioration conditions, respectively. Analytical tests were then conducted on the collected biodiesel samples from the bottom of the storage prior to the tests, as well as at the end of every 32, 30 and 32 minutes (min) intervals for WHSC, CEC F-98-08 and in-house developed SLTC, respectively. Among the conducted analytical tests to determine the oxidation condition of biodiesel under CRDE operation were OS, Fourier transform infrared spectroscopy (FTIR), peroxide value, fatty acid composition, dissolved metal, DO, viscosity, hydrogen ion concentration and conductivity value. To ascertain the influence of engine operation on biodiesel's TAN and water content, the TAN and water content analyses were also conducted.

For the second-stage, four comparisons were conducted using the findings from the first-stage under the CEC F-98-08 SLTC as summarized in Table 3.1. This SLTC was chosen over the other two SLTCs due to its highest fuel deterioration under CRDE operation as compared to the other two. The experimental conditions such as the utilized fuel quantity and fuel sampling quantity for stage 2-2 and stage 2-3 were the same as that of the first-stage. The CEC F-98-08 SLTC was

utilized for the stage 2-2 and stage 2-3 investigations. Similar analytical tests as described for the first-stage were conducted for the biodiesel samples collected from the stage 2-2 and stage 2-3 investigations.

The third-stage investigations were then conducted based on the results of the first-stage investigation which demonstrated that the deterioration level of biodiesel under engine operation could be gauged using the biodiesel's conductivity value. As such, 4 tests were performed to understand the characteristics of biodiesel's conductivity value. These included the influence of fuel temperature, the presence of dissolved metal, oxidized biodiesel and the effects of heating the biodiesel at 100 °C on biodiesel's conductivity value independently.

Table 3.1 Second-stage investigations in detail.

	Description	Aim	Additional investigation
Stage 2-1	Compare the deterioration of B100 under CRDE operation against the deterioration of B20 under generator diesel engine set.	Examine the similarities and the differences of B100 & B20 deterioration trend under diesel engine operation.	None
Stage 2-2	Compare the deterioration of B100 with different initial physical properties under CRDE operation.	Evaluate the similarities and the differences of B100 deterioration trend with different initial physical properties.	An additional CRDE operation by utilizing palm-based B100 from Carotech with 8 h of OS was conducted.
Stage 2-3	Compare the deterioration of B100 under CRDE operated for 5 consecutive days with 1 full tank each day against the deterioration of B100 under CRDE operated under 1 full tank.	Investigate the similarities and the differences of B100 deterioration trend under different CRDE operation duration. This is essential to investigate if B100 oxidizes under much longer CRDE operation duration.	An additional engine operation was conducted utilizing palm-based B100 from Vance Bioenergy for 5 consecutive days with 1 full tank of CRDE operation each day.
Stage 2-4	Compare the deterioration of B100 under CRDE operation against the deterioration of B100 under metal immersion under the ASTM G31 standard method.	Examine the similarities and differences of B100 deterioration under CRDE operation and under metal immersion investigation. This is essential since the compatibility of B100 with FDM is not only influenced by the initial fuel properties, but also due to the fuel deterioration under investigation condition.	None

3.2 Material and methods

The material and methods involved in the first two stages of investigations which determined the deterioration of biodiesel under CRDE operation are presented from sections 3.2.1 to 3.2.4. Additionally, the experimental procedures involved in the biodiesel's conductivity characterization which comes under the third-stage investigations are described in section 3.2.5.

3.2.1 Experimental set-up of the engine test-bed facility

As shown in Table 3.2, the engine test-bed here consists of a Toyota 1KD-FTV engine which is coupled to a SAJ Group's SE-250 model dynamometer. The engine is a 3.0 l, inline 4-cylinder CRDE with a turbocharger and intercooler, while the dynamometer is a 150 kilowatt eddy current dynamometer. Fig. 3.2 shows the schematic representation of the engine test-bed facility. The engine utilizes Toyota's D-4D common rail fuel injection technology for operation at an ultra-high pressure of up to 1350 bars. This is combined with a 32-bit engine control unit which governs the fuel quantity, valve-timing and boost pressure at different engine parameters.

A cooling system was installed for the turbocharger's intercooler to increase the intake charge density by maximizing the heat rejection of the compressed air (from the turbocharger) at the intercooler in order to obtain maximum power output. This system was designed to draw in external air through a duct to blow at the intercooler using a Toyo 2.2 kilowatt blower.

A heat exchanger with a capacity of 12 l was installed in place of the radiator to improve the engine's cooling system. Another heat exchanger was also installed to further improve heat rejection from the engine oil. The additions of both the heat exchangers with cooling towers were crucial to facilitate high speed-load engine operations at the specified durations which demands for a more efficient cooling system.

Data was monitored and recorded using DSG's DaTAQ PRO data-acquisition system. The input and output data for the fuel flow rate and fuel temperature were recorded here using a flow meter and K-Type thermocouples, respectively. The DaTAQ PRO has a refresh rate of 5 seconds and 100 points were averaged. Among the data of interest were engine speed, engine load, engine power, fuel temperatures (supply and return) and the fuel flow rate for determining fuel consumption.

Table 3.2 Specifications of engine test-bed facility.

Engine test-bed facility specifications			
Engine	Manufacturer		Toyota
	Model		1KD-FTV
	Type		Inline 4-cylinder
	Displaced volume	(cc)	2982
	Bore x stroke	(mm)	96 x 103
	Valves/cylinder		4
	Compression ratio		17.9:1
	Injection system		Common rail
	Maximum pressure	(MPa)	1350
	Turbocharger		Variable nozzle vane
	Maximum power @ engine speed		110 kW @ 3400 rev/min
	Maximum torque @ engine speed		320 Nm @ 1800-3400 rev/min
Dynamometer	Manufacturer		SAJ Group, India
	Model		SE-250
	Type		Eddy current
	Maximum power	(kW)	250
	Maximum torque	(Nm)	1200
	Maximum speed (rev/min)		8000
Data acquisition and control system	Manufacturer		DSG Group, United Kingdom
	System		DaTAQ Pro
	Features		Fully digital PID control system with bumpless switching between automatic and manual control Standard data logging rates from 1 Hz to 1 kHz
Cooling tower	Manufacturer		King Sun
	Model		KST-N-10
	Flow rate	(l/min)	130
	Fan motor	(kW)	0.187
Water pump	Manufacturer		Pentax
	Model		CMT 200
	Flow rate	(l/min)	20-120
	Power	(kW)	1.65
Heat exchanger	Capacity	(l)	12
Blower	Manufacturer		Toyo
	Model		TAFS-NF-24-1-s
	Type		Axial flow fan
	Capacity	(kW)	2.2
	Air volume	(cfm)	11,600
Duct	Material		Steel
Fuel flow meter	Manufacturer		Kubold
	Model		DOB-11FOH
	Range	(l/min)	1-70

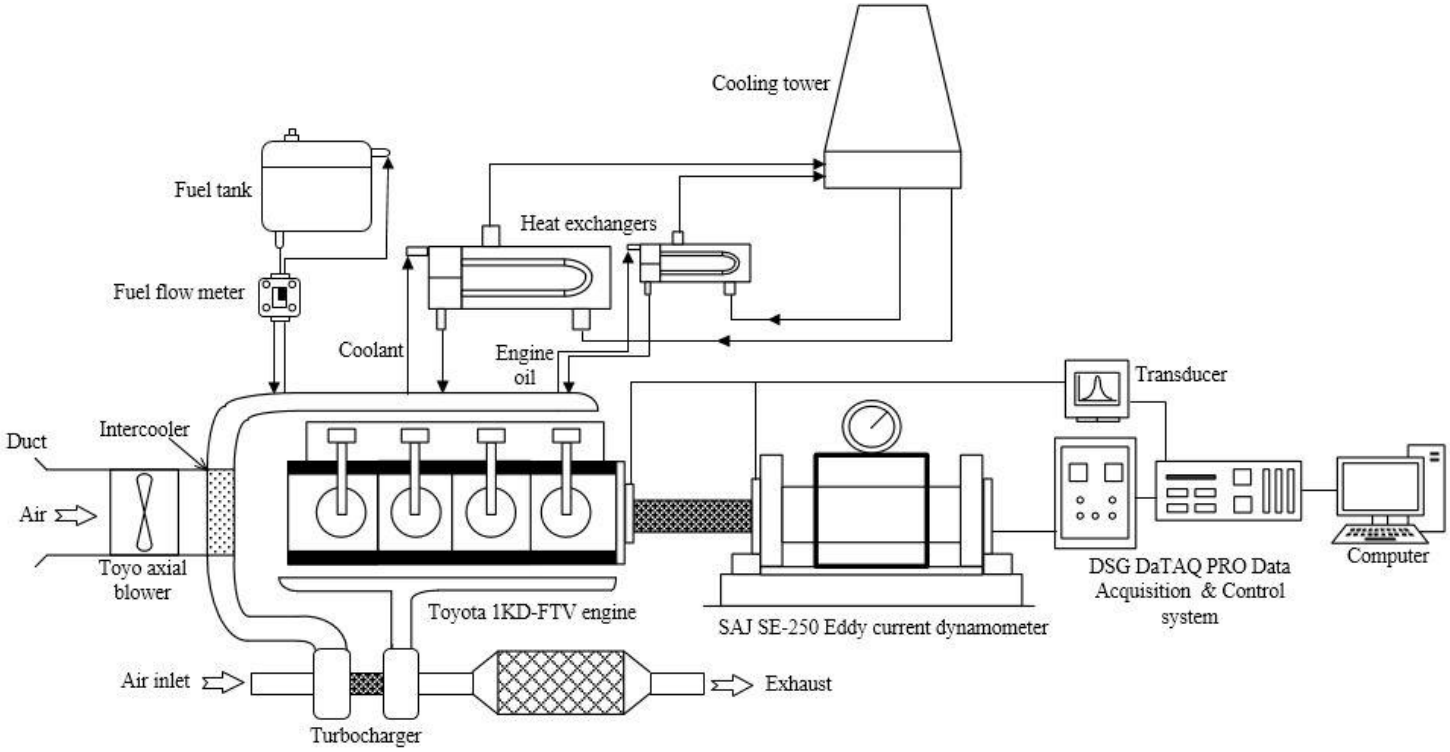

Fig. 3.2 Schematic representation of engine test-bed facility

3.2.2 Test fuels

Two palm biodiesel fuels without additives were utilized throughout this chapter, with the specifications as shown in Table 3.3. Firstly is the palm biodiesel from Vance Bioenergy, Singapore with 10.5 h of OS. This fuel was utilized in all the three stages of this chapter. Secondly is the palm biodiesel from Carotech, Malaysia with 8 h of OS, obtained from the University of Nottingham Malaysia Campus. This fuel was utilized only for the stage 2-2 investigation. To eliminate batch to batch variations, the same batch of fuel was used for all the tests. 76 l of fuel was fixed for all the experiments to match the typical fuel storage of the Toyota Hilux sold in Malaysia, which is equipped with the similar 1KD-FTV, 3.0 l CRDE. Based on the observation of the required fuel quantity to sustain engine operation and for the subsequent analytical tests, minimum levels of 3.0 and 2.4 l of fuel were required, respectively. As such, the engine was operated under the respective SLTCs to consume an approximated 70.6 l of fuel during each test.

Table 3.3 Palm biodiesel fuels specifications.

Tests		Methods	Specification	Vance Bioenergy	Carotech
Ester content	(%)	EN 14103	96.5 minimum	98.30	98.50
Density @ 15 °C	(kg/m^3)	ISO 12185	860-900	874.00	873.00
Kinematic viscosity @ 40 °C	(mm^2/s)	ISO 3104	3.50 - 5.00	4.54	4.56
Water content	(%)	ISO 12937	0.05 maximum	0.02	0.01
Copper strip corrosion, 3 h @ 50 °C	(Rating)	ISO 2160	Class I	1a	1a
Oxidation stability @ 110 °C	(h)	EN 14112	6.0 minimum	10.50	8.00
Total acid number	(mg KOH/g)	EN 14104	0.50 maximum	0.28	0.15

3.2.3 Speed-load test cycle and engine operation duration

Three different SLTCs in the form of the WHSC, CEC F-98-08 and in-house developed test were employed in the present study to determine deterioration of neat palm biodiesel under CRDE operation for typical driving, severe driving and maximum fuel deterioration conditions, respectively. The WHSC is a steady-state engine exhaust emission SLTC defined by the global technical regulation No. 4 [175]. This test procedure represents the typical driving conditions in the European Union, United States of America, Japan and Australia. The standard test utilizes 13 modes for 1 set of cycle as shown in Table 3.4. On the other hand, the CEC F-98-08 is a steady-state injector choking SLTC developed by the CEC TDG-F-98 group [176]. This test represents a step change in severity compared to CEC F-23-01 XUD-9 method, which is based on a much older indirect injection engine. The standard test utilizes 12 modes for 1 set of SLTC as shown in Table 3.5.

Finally, the in-house developed SLTC test was principally designed due to the unavailability of existing tests to date to determine the maximum deterioration of fuel as a result of engine operation. In a CRDE, the maximum fuel deterioration is expected to occur under high fuel temperature, typically in excess of 100 °C as well as with maximum fuel return to storage concurrently. Here, the ‘rated power’ speed-load condition which is achieved by operating at full throttle and concurrently applying load until the engine speed decreases to the specified rated

speed provided by the engine manufacturer is observed to fulfil both the required conditions above [177].

However, since the common rail type diesel engine is designed to produce high pressure fuel at rated power speed-load condition, this would force the fuel pump to work at its maximum capacity. Extended operation duration of fuel pump at its maximum capacity would result in a significant increase in the engine temperature which would lead to the interruption of engine control unit as a precautionary measure against fuel pump failure. The interruption of engine control unit could cause the engine power to reduce automatically until the engine has cool down to the specific temperature set by the manufacturer. Hence, in achieving a continuous engine operation without the interruption of the engine control unit, an additional speed-load condition which could cool down the engine whilst simultaneously consuming the least amount of fuel is required. Here, the 'low idling' which is achieved by operating at no throttle and no load condition concurrently is observed to fulfil both these requirements [177].

Based on engine operation trials conducted utilizing these two speed-loads specifically at several engine operation durations, it was observed that a continuous engine operation without the engine control unit interruption was only possible with 'low idling' speed-load conditions of 1.5 min duration followed by the 'rated power' speed-load conditions of 3 min duration. As such, engine

operation under these two speed-loads as shown in Table 3.6 were counted as 1 cycle which accounted for 4.5 min of engine operation duration. For the present study, each SLTC was run twice and the average values of the measurements are reported throughout here.

Table 3.4 Details of WHSC test cycle [175].

Mode	Engine speed (%)	Load (%)	Mode length (s)
1.	0	0	210
2.	55	100	50
3.	55	25	250
4.	55	70	75
5.	35	100	50
6.	25	25	200
7.	45	70	75
8.	45	25	150
9.	55	50	125
10.	75	100	50
11.	35	50	200
12.	35	25	210
13.	0	0	210

Table 3.5 Details of CEC F-98-08 test cycle [176].

Mode	Engine speed (rev/min)	Load (%)	Mode length (s)
1.	1750	20	120
2.	3000	60	420
3.	1750	20	120
4.	3500	80	420
5.	1750	20	120
6.	4000	100	600
7.	1250	10	120
8.	3000	100	420
9.	1250	10	120
10.	2000	100	600
11.	1250	10	120
12.	4000	100	420

Table 3.6 Details of in-house developed test cycle.

Mode	Description	Engine speed	Load (%)	Mode length (s)
1.	Low idling	0%	0	90
2.	Rated power	3400 rev/min	44	180

3.2.4 Fuel sampling and analytical tests

The fuel storage and line were flushed each time before the start of the test to ensure 100% fresh palm biodiesel was utilized during the engine operation. The flushing was initiated by releasing the remaining fuel in the storage as illustrated in Fig. 3.3. Then, 10 l of fresh palm biodiesel was filled in the tank. This was accompanied by the start of the engine and allowing it to idle for 5 min. The combined re-circulated fuel from pump, injector leak backs and common rail was channelled to a separate storage. This enables the fuel line to be flushed. After 5 min, the engine was stopped and the remaining fuel in the storage was released.

As for fuel sampling, biodiesel samples of 200 ml were collected at specific time intervals during the engine tests as shown in Table 3.7, (in example 32 min, 30 min and 32 min for WHSC, CEC F-98-08 and in-house developed SLTC, respectively). These specific time intervals were determined by measuring the maximum possible number of test cycles that can be obtained by consuming 70.6 l of fuel as explained in section 3.2.2. The results obtained from the samples collected at these intervals were used to detect for any irregularities in the results obtained. An additional sample was also taken at each collection. All the samples were analysed within 72 h of collection and stored in dark room condition (25 °C) prior to testing. The specifications of the utilized equipment for analytical tests are presented in Table 3.8, while the analytical tests performed on the collected biodiesel samples are described in Table 3.9. Each analytical test was conducted twice throughout the present study. For the graphs in the results section, error bars

based on standard errors are shown to provide an estimated precision of the measured parameters. On the other hand, error bars based on standard deviations are presented in the tables to show the dispersion of the measured parameters.

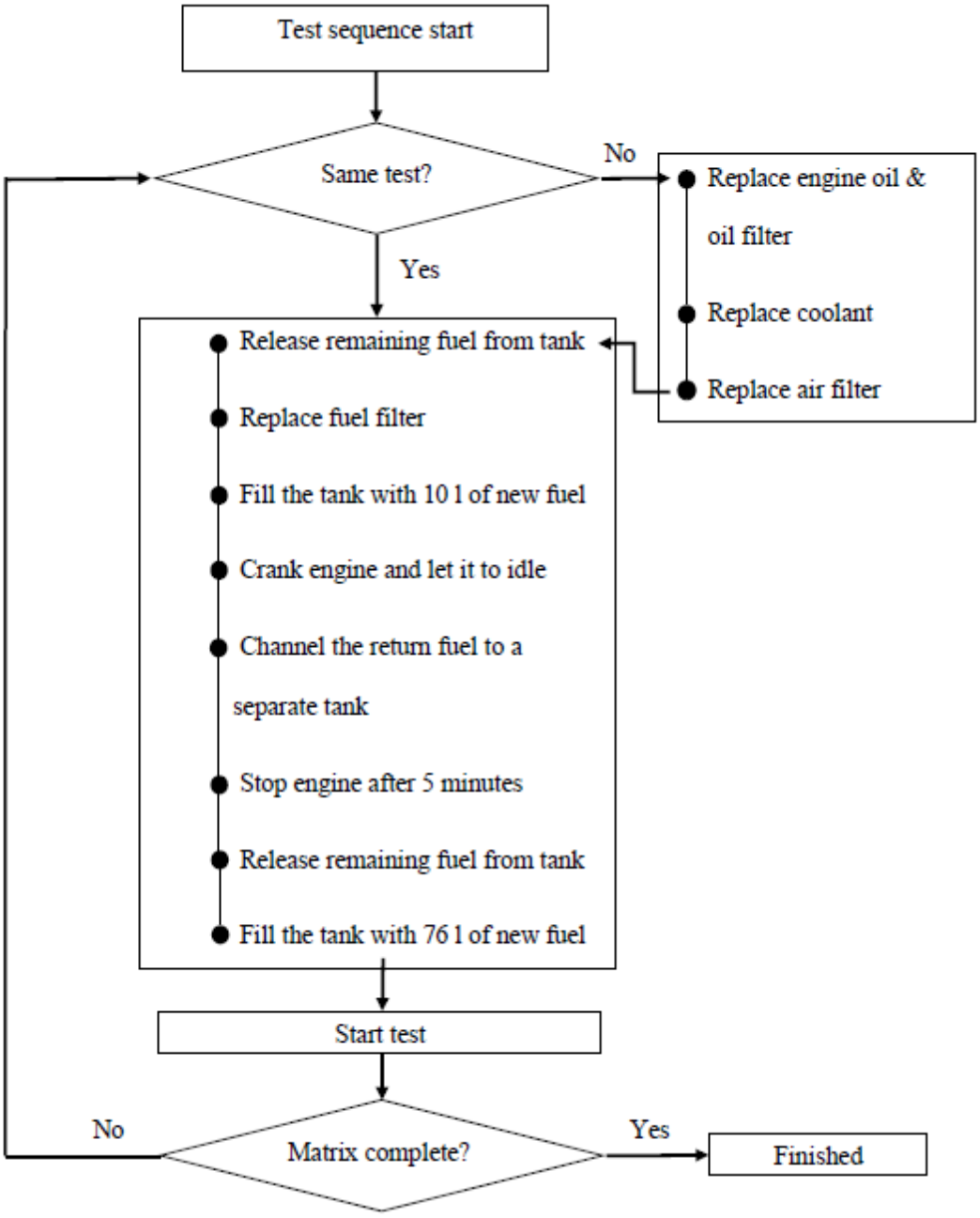

Fig. 3.3 Flowchart of test sequence.

Table 3.7 Details of sample collection for each speed-load test cycle (SLTC).

Investigation	Palm biodiesel	SLTC	First collection	Collection interval (min)	Collection location	Total number of samples
Stage 1	Vance Bioenergy	WHSC	Prior to the start of the test (after flushing)	32	Bottom of the storage tank	6
		CEC F-98-08		30		5
		In-house		32		6
Stage 2-2	Carotech	CEC F-98-08	Prior to the start of the test (after flushing)	End of each day	Bottom of the storage tank	2
Stage 2-3	Vance Bioenergy	CEC F-98-08	Prior to the start of the test (after flushing)	End of the test	Bottom of the storage tank	2

Table 3.8 Specifications of the equipment for analytical tests.

Analytical equipment	Parameter		Details
Rancimat	Manufacturer		Methrohm
	Model		743
	Temperature range	(°C)	50-220
	Conductivity range	(µS/m)	0-400
	Air flow range	(l/h)	7-25
Total acid number titrator	Manufacturer		Metrohm
	Model		809 Titrando (with 800 Dosino and 804 Ti Stand)
	Range	(mg/g)	0.05-250
Gas chromatography	Manufacturer		Perkin Elmer
	Model		Autosystem XL
	Temperature range	(°C)	37-450
	Initial time	(min)	0-999
	Rate	(°C/min)	0.1-45
Fourier transform infrared spectrometer	Manufacturer		Perkin Elmer
	Model		Frontier
	Wavelength range	(nm)	680-4800
	Software		Spectrum
Inductively coupling plasma-optical emission spectrometer	Manufacturer		Perkin Elmer
	Model		7300V
	Power	(W)	1500
	Wavelength range	(nm)	163-782
	Software		WinLab 32
Viscometer	Manufacturer		Herzog (PAC)
	Model		HVM 472
	Range	(mm^2/s)	0.5-5000
Conductivity meter	Manufacturer		Stanhope Seta
	Model		99708-0
	Range	(pS/m)	0-2000
Dissolved oxygen meter	Manufacturer		Fisher Scientific
	Model		Traceable DO meter pen
	Range	(mg/l)	0-20
	Resolution	(mg/l)	0.1
pH meter	Manufacturer		Oakton
	Model		pHTestr 2
	Range	(pH)	-1.0-15.0
	Resolution	(pH)	0.1
Karl Fischer titrator	Manufacturer		Metrohm
	Model		831 KF Coulometer
	Range		10 µg-200mg
	Precision		± 3 µg

Table 3.9 Analytical tests conducted on biodiesel samples.

Analytical test	Standards	Equipment	Conditions
Oxidation stability	EN 14112:2003 [178]	Metrohm 743 Rancimat instrument	Samples of 7.5 g were analysed at a heating block temperature of 110 °C and a constant air flow of 10 l/h. The volatile compounds formed were collected in the conductivity cell with 60 ml of distilled water. The inflection point of the derivative curve of conductivity as a function of time was reported as the OS.
Fatty acid composition	EN 14103: 2003 [179]	Perkin Elmer's Autosystem XL Gas Chromatograph	The gas chromatograph has a column length of 60 meters, internal diameter of 0.25 mm and coating of 0.25 µm. The column was held at 120 °C for 1 min, then ramped to 240 °C at 20 °C/min, and finally held at 240 °C for 13 min. The transfer line of gas chromatograph was kept at 240 °C. Helium was used as the carrier gas at a flow rate of 1.5 ml/min. Other gases which were also used are hydrogen and purified air.
Hydrogen ion	No information	Oaktron's pHTesr 2 pH meter	50 ml of distilled water was added to 50 ml of sample and treated with ultrasonic waves for 30 min [180]. Then, the exponent of samples' pH value was measured to determine the hydrogen ion concentration.
Peroxide value	AATM-516: 01 [181]	No information	Manual titration which required 5 g of sample and 0.1 N of sodium thiosulfate solution was utilized.
Fourier transform infrared spectroscopy	No information	Perkin Elmer's Frontier model FTIR spectrometer	The functional groups in the FTIR spectrum were utilized for identifying the presence of secondary oxidation products here. Among the functional groups of concern here are aldehydes (C=O stretch at 1750-1625 cm^{-1}, C-H stretch off C=O at 2850 cm^{-1}, C-H stretch off C=O at 2750-2700 cm^{-1}), ketones (C=O stretch at 1750-1625 cm^{-1}) and carboxylic acid (C=O stretch at 1730-1650 cm^{-1}, hydrogen bonded O-H stretch at 3400-2400 cm^{-1}).

Table 3.9 Analytical tests conducted on biodiesel samples. (Continued).

Analytical test	Standards	Equipment	Conditions
Dissolved oxygen	No information	Fisher Scientific's Traceable DO meter pen	This analysis was conducted at room temperature (~ 25°C).
Viscosity	ISO 3104:1994 [182]	Herzog's HVM 472 viscometer	40 ml of sample was used.
Conductivity	No information	Stanhope Seta's 997808-0 conductivity meter	Fuel sample of 30 ml in quantity was utilized.
Dissolved metal	ASTM D5185: 2013 [183]	Perkin Elmer's Optima 7300V Inductively Coupling Plasma-Optical Emission Spectrometer	The sample introduction system consists of low-flow Gemcone nebulizer, a 4 mm baffled cyclonic spray chamber and a 1.2 mm injector. Calibration standards were made using Conostan S-21 and sulphur-free kerosene. Cobalt was utilized as the internal standard. Here, the metals of concern are aluminium, iron, copper and zinc. The wavelengths for these metals are 228.613, 394.408, 259.940, 324.757 and 213.854 nm for cobalt, aluminium, iron, copper and zinc respectively.
Total acid number	ASTM D664: 2011 [133]	Metrohm's 809 Titrando	Biodiesel samples of 10.0 g and standard titrant 0.01 M alcoholic KOH were used.
Water content	ISO 12937:2000 [184]	Metrohm's 831 KF Coulometer	2.0 g of samples was utilized.

3.2.5 Experimental procedure for the third-stage investigations

The experimental procedures for characterizing the biodiesel's conductivity value by evaluating the influence of fuel temperature, dissolved metal, oxidized biodiesel, as well as duration of fuel heating on the biodiesel's conductivity value are presented here.

For the first test, the influence of fuel temperature on the conductivity value was determined by heating the fuel sample from 25 to 100 °C while measuring the corresponding conductivity value. For the second test, the influence of dissolved metal on the conductivity value was determined by adding copper powder obtained through the collection of copper dust from the polishing process of copper coupons with 99.9% purity using 800 grit sandpaper. For this test, 5 samples of 500 ml palm biodiesel each were prepared with the different copper ion concentrations. The tested copper ion concentrations were 0.2, 0.4, 0.6, 0.8 and 1.0 parts per million (ppm).

For the third test, the influence of oxidized biodiesel on conductivity value was established. For this test, biodiesel samples collected after rancimat operation as explained in Table 3.9 according to EN 14112 was utilized as oxidized biodiesel. Here, the samples were divided into 5 bottles as shown in Table 3.10. In the final test, the conductivity value of the biodiesel samples due to heating duration for 2, 4, 6, 8 and 10 h at 100 °C in a closed and dark condition were determined. Here,

the samples were allowed to cool to room temperature prior to measuring the conductivity value. Additionally, hydrogen ion analysis was conducted on the fifth sample of the third and final tests in order to determine the concentration of hydrogen ions in the samples. This test was necessary for identifying the effects of oxidized biodiesel and heated biodiesel on hydrogen ion concentration. Here, additional sample was also analysed under each condition as described above.

Table 3.10 Test samples for determining the influence of oxidized biodiesel on conductivity value.

	Oxidized biodiesel by vol%	**Biodiesel by vol%**
First bottle	20	80
Second bottle	40	60
Third bottle	60	40
Fourth bottle	80	20
Fifth bottle	100	0

3.3 Results and discussion

The influence of CRDE operation towards the deterioration of palm biodiesel can be ascertained by evaluating the biodiesel samples collected during and after engine operation. Through this, essential information especially on the presence of FDM degradation promoting factors such as the biodiesel oxidation products, TAN and water content can be conclusively determined. The results obtained under all the 3 stages of investigations are presented here.

3.3.1 First stage-deterioration of biodiesel under CRDE operation

The deterioration of biodiesel under CRDE operation based on the WHSC, CEC F-98-08 and in-house developed SLTCs are collectively presented in terms of biodiesel oxidation, TAN and water content.

3.3.1.1 Biodiesel oxidation

Among the results that would be individually presented and then collectively discussed under this category are the OS, fatty acid composition, hydrogen ion concentration, peroxide value, FTIR spectrum, DO concentration, viscosity value, conductivity value and dissolved metal concentration.

As shown in Fig. 3.4, the OS was found to reduce linearly with increasing engine operation duration under all the three utilized SLTCs. The highest OS change at the

end of the test was experienced under the CEC F-98-08 SLTC with 11% reduction, followed with the in-house developed SLTC at 10% reduction, and finally a 6% reduction was measured under the WHSC SLTC. This difference in OS deterioration is caused by the greater severity of engine operating conditions under the CEC F-98-08 SLTC as explained in section 3.2.3. Additionally, higher OS reduction by 1% was measured under the CEC F-98-08 SLTC than in the in-house developed SLTC. It is crucial to highlight here that although the in-house developed SLTC was chiefly designed to create maximum fuel deterioration biodiesel CRDE operation, yet higher OS reduction occurred under the CEC F-98-08 SLTC. Despite the difference in the OS reduction of 1% was measured between the CEC F-98-08 and in-house developed SLTC is considered minimal, the CEC F-98-08 SLTC in specific was utilized for the further investigations as it created the highest OS reduction under CRDE operation.

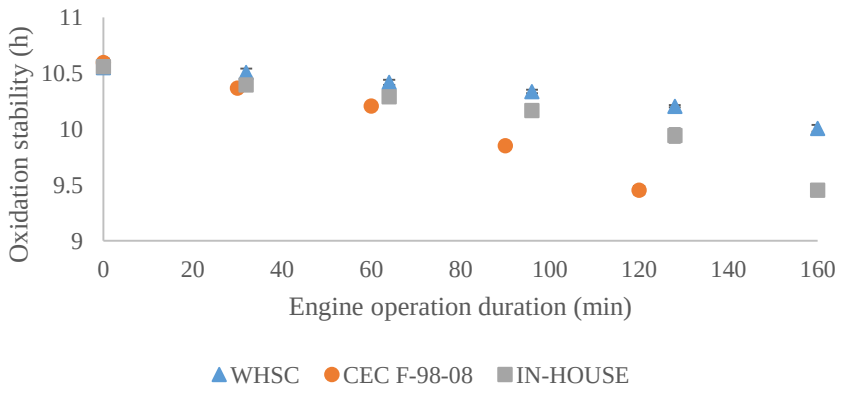

Fig. 3.4 Deterioration of biodiesel fuel's oxidation stability under CRDE operation.

As shown in Fig. 3.5, the compositional values of the C12:0, C14:0, C16:0, C18:0, C18:1, and C18:2 fatty acids after the tests remained close to the initial values measured prior to the engine operation under all the three utilized SLTCs. Here, a maximum difference of 0.625%, 0.230%, 0.010%, 0.437%, 0.073% and 0.206% under all the three utilized SLTCs were measured between prior and after engine operation for C12:0, C14:0, C16:0, C18:0, C18:1, and C18:2 fatty acids, respectively. On the other hand, the compositional value of the C18:3 fatty acid reduced under engine operation under all the three utilized SLTCs. Here, a maximum difference of 9% in the compositional value was measured between before and after engine operation under all the three SLTCs. This observed change in C18:3 is mainly due to its greater vulnerability in forming radicals than the other fatty acids [185, 186].

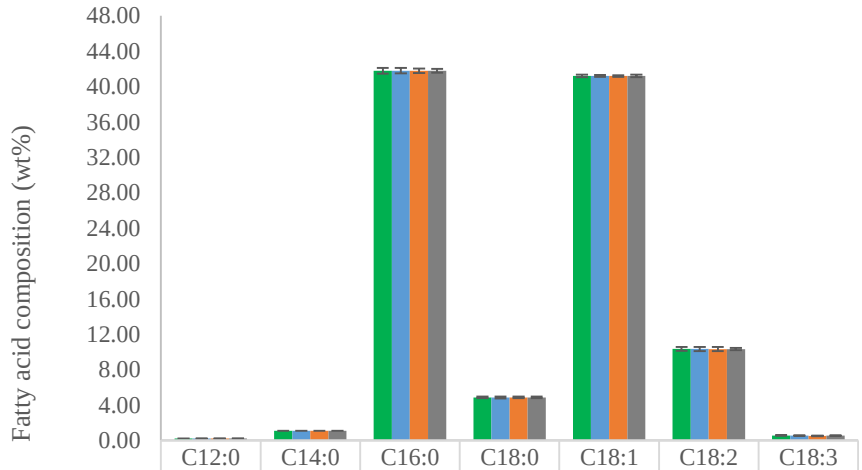

	C12:0	C14:0	C16:0	C18:0	C18:1	C18:2	C18:3
Initial	0.20	1.09	41.78	4.86	41.21	10.34	0.55
WHSC	0.20	1.08	41.78	4.84	41.20	10.33	0.54
CEC F-98-08	0.20	1.08	41.77	4.85	41.18	10.32	0.51
IN-HOUSE	0.20	1.08	41.78	4.86	41.19	10.32	0.53

Fig. 3.5 Changes of biodiesel fuel's fatty acid composition under CRDE operation.

As shown in Fig. 3.6, the concentrations of hydrogen ion were found to increase linearly with increasing duration of engine operation under all the three utilized SLTCs. The highest hydrogen ion concentration change at the end of the test was measured under the CEC F-98-08 SLTC with 117% increase, followed with the in-house developed SLTC at 111% increase and finally a 110% increase was determined under the WHSC SLTC. This is mainly due to the more severe engine operating conditions of the CEC F-98-08 SLTC. However, these resulted differences in the change of hydrogen ion concentration between the 3 different SLTCs' are considered minimal and hence insignificant.

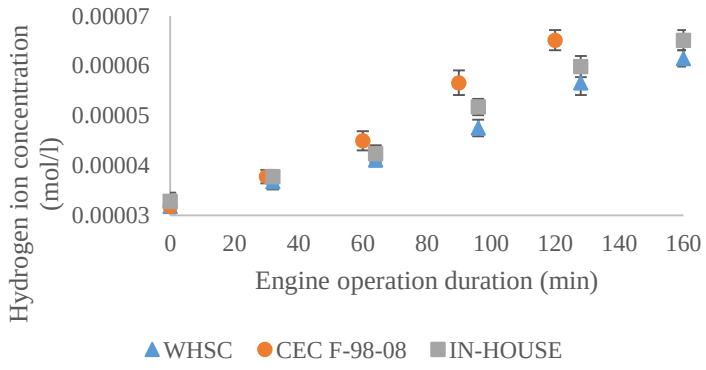

Fig. 3.6 Changes of biodiesel fuel's hydrogen ion concentration under CRDE operation.

As shown in Fig. 3.7, the peroxide value throughout the test under all the three SLTCs were noted to remain close to the initial value of 15.9 milliequivalent (meq) measured prior to the engine operation. The maximum difference in the peroxide value throughout the test here for all the three SLTCs is within 0.05% of

the initial value. As such, the unchanged biodiesel's peroxide value here indicates that no primary oxidation products were formed under CRDE operation.

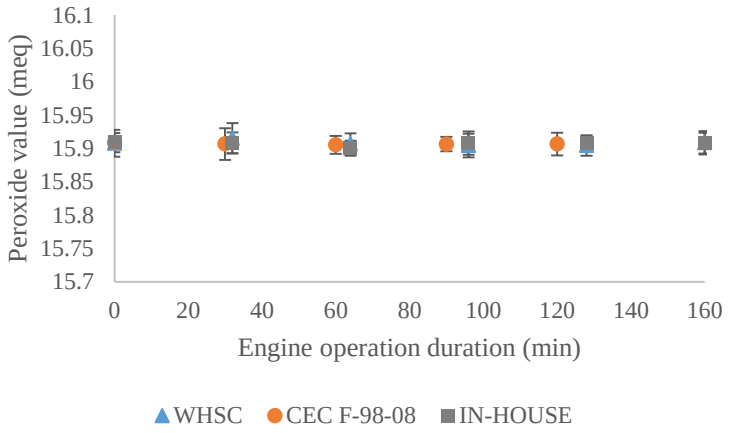

Fig. 3.7 Changes of biodiesel fuel's peroxide value under CRDE operation.

As shown in Fig. 3.8, the final FTIR spectrum under all the three SLTCs remained close to the initial spectrum obtained prior to the tests. This shows that the biodiesel's FTIR spectrum did not undergo changes under CRDE operation. On top of that, by further analysing the final FTIR spectrum, the absence of the concerned functional groups such as aldehydes, ketones and carboxylic acid implies that no secondary oxidation products were formed under CRDE operation.

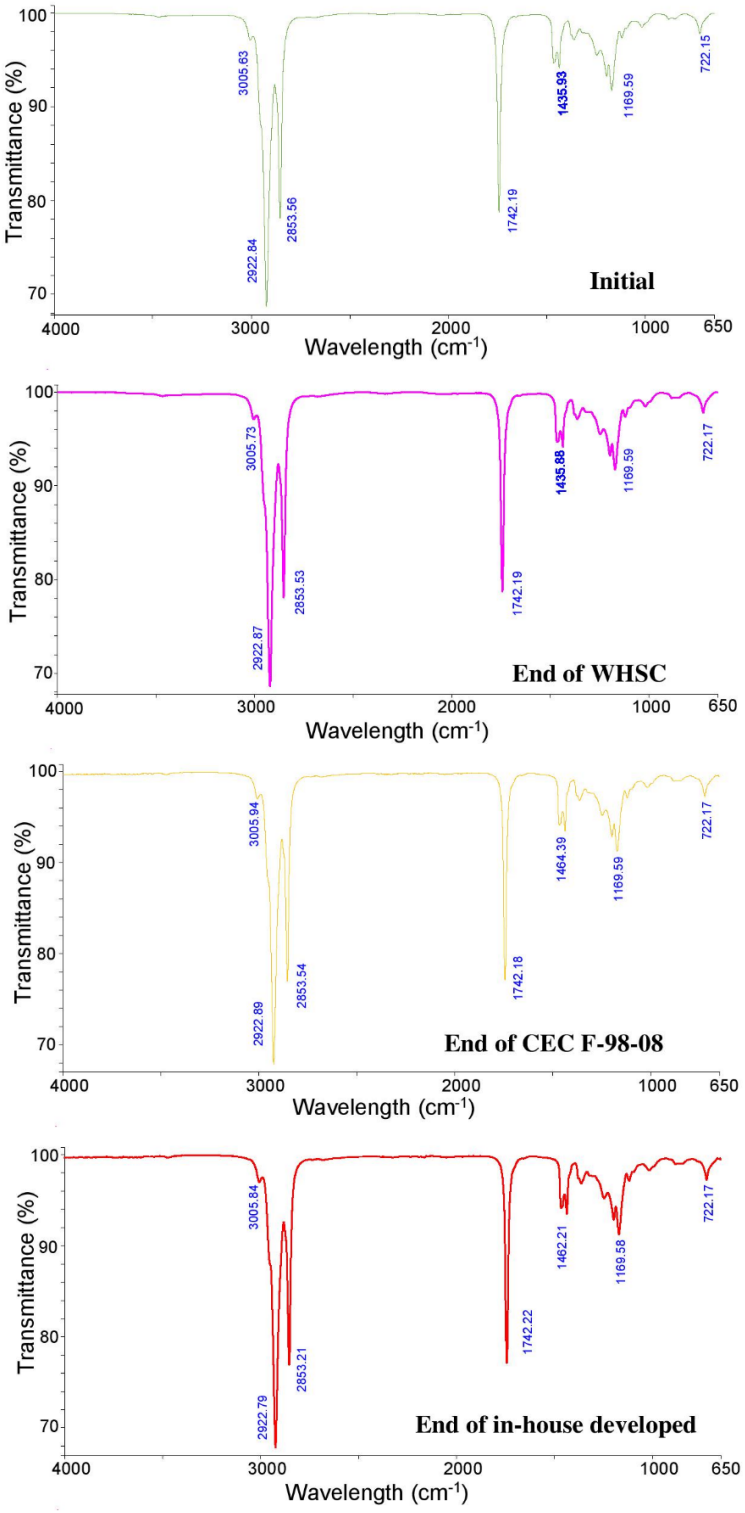

Fig. 3.8 Initial and final FTIR spectrums for WHSC, CEC F-98-08 and in-house developed test.

As shown in Fig. 3.9, the DO concentration throughout the test under all the three SLTCs remained close to the initial value of 7.950 ppm measured prior to the tests. The maximum difference in the DO concentrations throughout the tests for all the three SLTCs was within 0.315% of the initial value. This shows that the biodiesel's DO concentration did not undergo changes under CRDE operation.

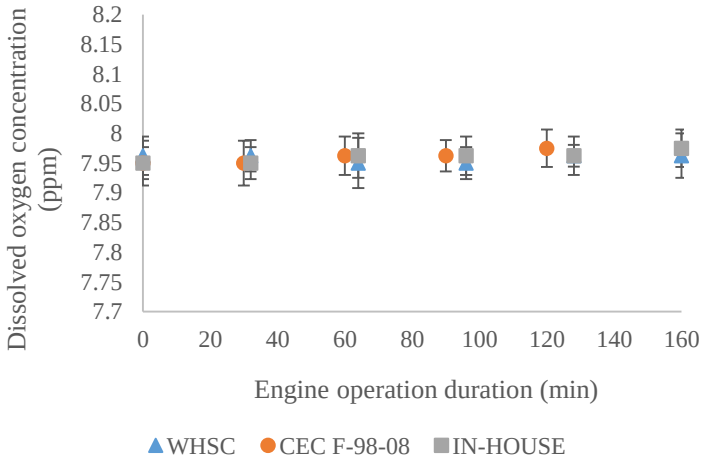

Fig. 3.9 Changes of biodiesel fuel's dissolved oxygen concentration under CRDE operation.

However, since it is known that the concentration of dissolved substance such as water in biodiesel could be influenced by the fuel temperature [116] and by considering the high fuel temperature during CRDE operation of 80-110 °C logged in the present study, the effect of fuel temperature on the concentration of DO in biodiesel was measured. From Fig. 3.10, it is observed that the concentration of DO in biodiesel reduces with increasing biodiesel temperature. Here, the effect of biodiesel temperature on the concentration of DO in biodiesel

is shown up to the instrument limit of 80 °C. There is a clear strong negative linear relationship present between the biodiesel's temperature and the concentration of DO. The maximum reduction in the DO concentration measured between 25 and 80 °C is 93%. Based on this decreasing trend, the concentration of DO is expected to further decline beyond 80 °C. As such, it is clear from the interpreted results above that the DO concentration in biodiesel across the temperature range of 80-110 °C examined in the present study during engine operation would be lower than 1 ppm.

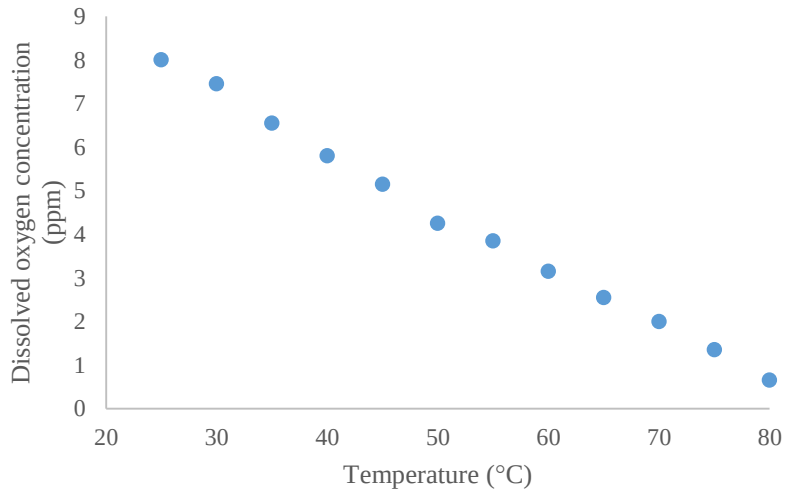

Fig. 3.10 Changes of biodiesel fuel's dissoved oxygen concentration corresponding to fuel temperature changes.

As shown in Fig. 3.11, the viscosity values throughout the test under all the three SLTCs remained close to the initial value of 4.538 mm^2/s measured prior to the engine operation. The maximum difference in the viscosity values throughout the test for all the three SLTCs was within 0.221% of the initial values. As such, the

biodiesel's viscosity value did not undergo significant changes under the CRDE operation.

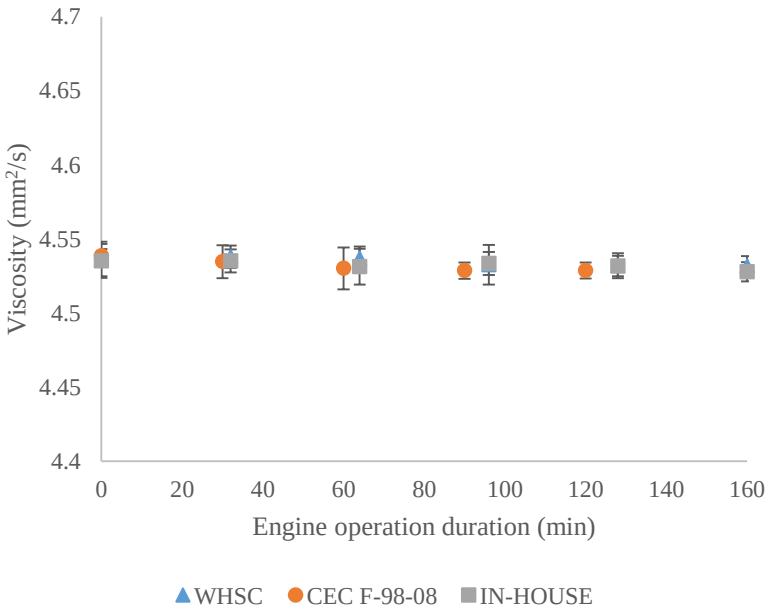

Fig. 3.11 Changes of biodiesel fuel's viscosity value under CRDE operation.

As shown in Fig. 3.12, the conductivity values were found to increase linearly with increasing duration of engine operation for all the three utilized SLTCs. The highest conductivity value change at the end of the test here was measured under the CEC F-98-08 with 293% increase, followed with the in-house developed at 278% increase and finally a 218% increase was measured under the WHSC. The higher conductivity value change measured under the CEC F-98-08 SLTC is mainly due to the greater severity of the engine test conditions imposed.

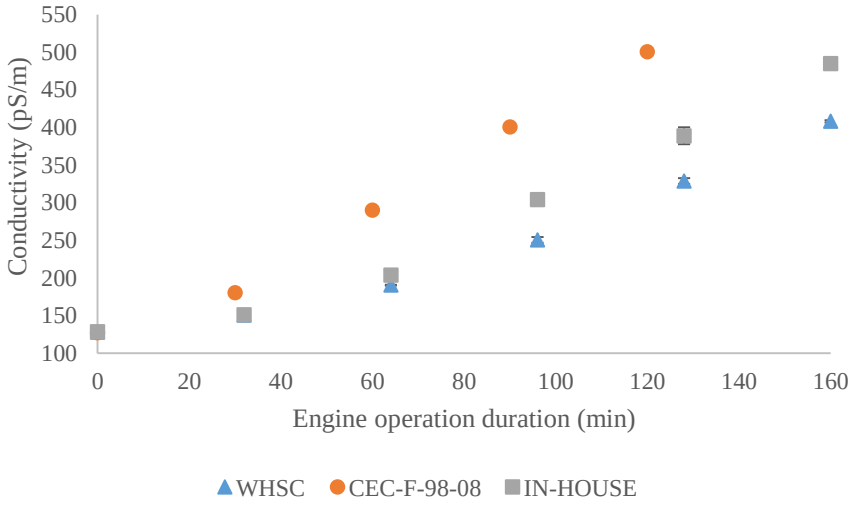

Fig. 3.12 Changes of biodiesel fuel's conductivity value under CRDE operation.

As shown in Fig. 3.13-a, Fig. 13-b, Fig. 13-c and Fig. 13-d, the concentration of aluminium, iron, zinc and copper, respectively, were found to increase continuously with increasing length of engine operation under all the three SLTCs. As shown in Table 3.11, a higher change in dissolved metals concentration was measured under the CEC F-98-08 due to the more severe operating conditions in comparison to the in-house developed and WHSC SLTC.

Table 3.11 Comparisons of the dissolved metals concentration under CRDE operation.

Dissolved metals	**Differences of final to initial concentration (number of times)**		
	CEC F-98-08	**In-house developed**	**WHSC**
Aluminium	1258	1098	1022
Iron	428	394	295
Zinc	192	165	152
Copper	680	533	524

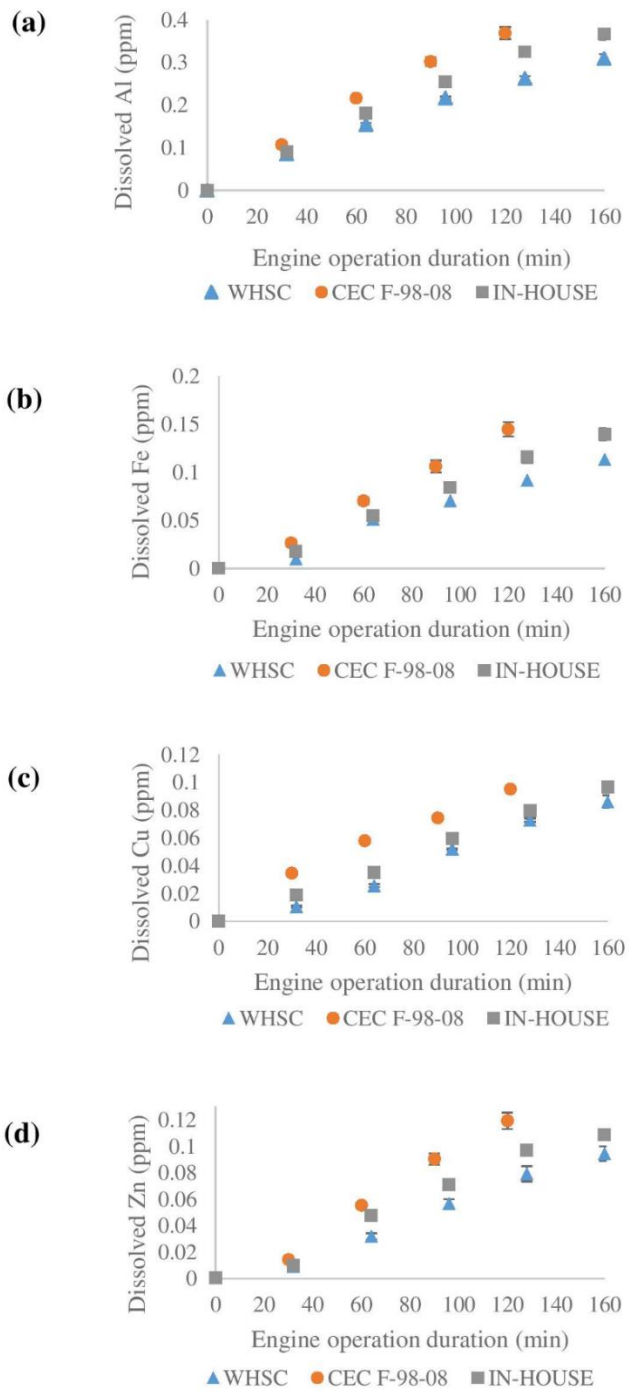

Fig. 3.13 Changes of dissolved (a) aluminium, (b) iron, (c) copper and (d) zinc under CRDE operation duration.

3.3.1.1.1 Overall discussion on biodiesel oxidation

Based on the results above especially from the peroxide value and FTIR analyses which showed the absence of primary and secondary oxidation products, respectively, the biodiesel samples collected in the present study were found to have not undergone oxidization under CRDE operation. This is typically unexpected considering the biodiesel's high oxidation tendency coupled with favourable oxidation conditions in the FDS such as high fuel temperature and the presence of various FDM which can catalyse the oxidation process. Nevertheless, changes were observed for the C18:3 fatty acid based on the biodiesel's fatty acid compositional value. The changes indicate that the initiation stage of the biodiesel's oxidation process have occurred during engine operation. This is further substantiated by the hydrogen ion analysis which clearly demonstrated a continuous increase in the concentration of hydrogen ion with respect to the engine operation duration. The hydrogen ions are typically expected to be present in the fuel due to the released hydrogen radicals in excited state from the unsaturated chain in the biodiesel [187]. Although this finding suggests the occurrence of the initiation stage of the biodiesel's oxidation process, the biodiesel was found to remain unoxidized as described above which implies that the conditions inside the FDS must have arrested the progress of the oxidation process.

For the oxidation process of the biodiesel which comprises initiation, propagation and termination stages [188], the presence of DO in the fuel is essential in order

for the initiation stage to progress to the propagation stage. Corresponding to the concentration of measured DO of lower than 1 ppm over the temperature range of 80-110 °C during engine operation in the present study, the progression of biodiesel oxidation process from initiation to propagation stage was hindered [189]. Most importantly, the prevention of a complete fuel oxidation could result in the radical-radical recombination process which is a type of termination process among the initiated radicals [189]. The occurrence of this process could lead to higher fuel viscosity especially due to the formation of alkane polymer. Since the viscosity value of biodiesel remained closed to its initial value under engine operation, this implies that the termination process under engine operation is too minimal to be reflected on the biodiesel's viscosity value. As such, the biodiesel's viscosity value is expected to be unaffected under engine operation.

Similarly, the findings from the OS analysis which showed a minimum final OS value of 89% of its initial value under all the three SLTCs indicate that the biodiesel remained unoxidized. Here, the increase in the dissolved metals concentration under engine operation is believed to have caused the reduction in OS value measured. To date, the catalytic effects of dissolved metal in biodiesel on OS have been extensively reported. For example, Sarin et al. [33] found that the presence of metals such as iron, nickel, manganese, cobalt and copper in biodiesel reduces the OS. Furthermore, the authors also reported an OS reduction by 87% due to the presence of 3 ppm of copper in biodiesel. In a separate study, Shiotani et al. [190] investigated the influence of metal in biodiesel on OS and

reported that the presence of metal indeed reduces the OS. Here, the authors also reported that copper has the greatest adverse effect on the OS value followed by tin, iron, zinc and magnesium. Similarly, several other studies have also reported on reduced biodiesel's OS due to metal contamination [92, 191-197]. The continuous increase of the dissolved metals concentration in biodiesel under engine operation reported in the present study has indeed resulted in the declining OS value.

Apart from the reduction in the OS value, the increase in the dissolved metals concentration under engine operation is also suggested to have influenced the increase in conductivity value of the fuel. This is mainly attributed to the conductivity's working principle which is established according to the number of ions present in the solution. By considering the working principle of conductivity and also the increase in hydrogen and metal ions due to the deterioration effects of biodiesel under engine operation, the fuel's conductivity is found here as a more suitable property to indicate the biodiesel deterioration level under actual engine operation.

The biodiesel's initial (prior to engine operation) conductivity value is also proposed to have influenced the increase in dissolved metals concentration under engine operation. In a study by Meenakshi et al. [109] which investigated the effects of manipulating the biodiesel's initial conductivity value towards copper

corrosion rate under rotating cage investigation method (ASTM G184), the authors reported higher metal leaching with higher biodiesel's initial conductivity value. From the discussions above, further investigations were carried out to understand the characteristics of biodiesel's conductivity value in determining the deterioration level of biodiesel under engine operation. The outcomes of this investigation are presented in section 3.3.3.

3.3.1.2 Total acid number value

As shown in Fig. 3.14, the TAN throughout the test under all the three SLTCs remained close to the initial value of 0.28 mg KOH/g measured prior to the start of the engine operation. The maximum difference in the TAN throughout the test for all the three SLTCs was within 0.446% of the initial value. The biodiesel's TAN is seen not to undergo changes during the CRDE operation. Several studies so far have conclusively determined that the increase in TAN promotes metal corrosion and elastomer degradation [83, 98]. These studies examined the effects of biodiesel's TAN on FDM degradation by utilizing the ASTM G31 and ASTM D471 immersion standard methods for metal corrosion and elastomer degradation, respectively. Corresponding to these findings, specific focus is placed on the rise in TAN due to diesel engine operation.

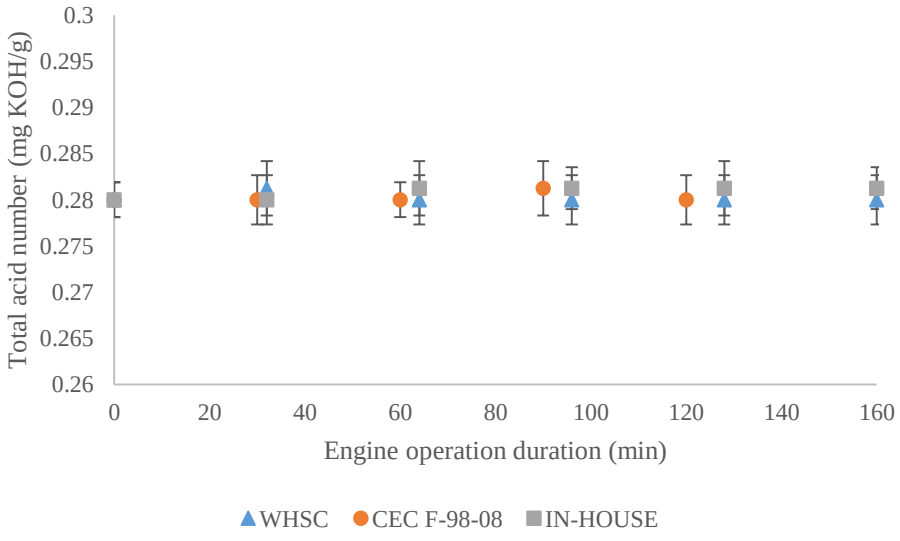

Fig. 3.14 Changes of biodiesel fuel's total acid number value under CRDE operation.

Generally, the biodiesel's TAN is attributed to the acidity of the organic acids such as the fatty acids and the oxidation products present in the fuel. Based on the results obtained from the TAN analysis which clearly demonstrated that the TAN were not affected under CRDE operation, this implies that the organics acids present in the fuel were not altered during engine operation. The organic acids here are the formed oxidized products such as aldehydes, ketones, carboxylic acid and short-chain acids which can be detected from the FTIR spectrum. Since these organic acids were not detected as shown in Fig. 3.8, this explains the unchanged TAN throughout the engine operation. Based on these findings, the concern regarding the acceleration of FDM degradation due to the increase in TAN under engine operation can be alleviated.

3.3.1.3 Water content

As shown in Fig. 3.15, the water content under all the three SLTCs remained close to the initial value of 0.020% measured prior to the start of the tests. The maximum difference in the water content throughout the test for all the three SLTCs was within 0.625% of the initial value. This implies that the biodiesel's water content did not undergo changes during CRDE operation.

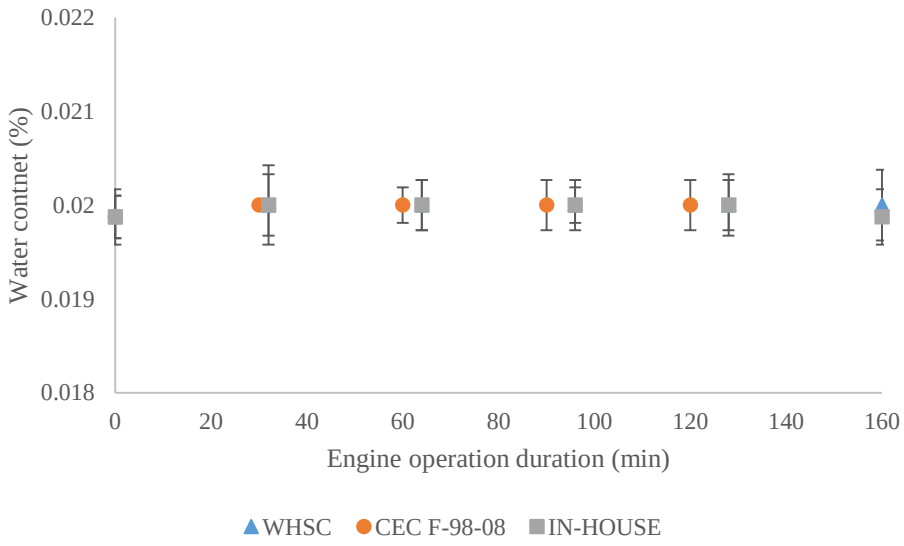

Fig. 3.15 Changes of biodiesel fuel's water content under CRDE operation.

Several studies to date have investigated the effects of water content in biodiesel on FDM degradation utilizing similar methods as those in determining the TAN and noted that the increase of water content in biodiesel promotes metal corrosion and elastomer degradation [69, 108]. For this reason, any increase in the biodiesel's water content under diesel engine operation should be an issue. However, the concern regarding the acceleration of FDM degradation due to the increase in biodiesel water content under engine operation can be ruled out too since water content was found to be unchanged in the present study.

3.3.2 Second stage

Four comparisons were conducted here by utilizing the findings obtained from the first-stage investigation as described ealier in Table 3.1 of section 3.1

3.3.2.1 Stage 2-1

The deterioration of biodiesel under CRDE operation was firstly compared to the deterioration of B20 under generator diesel engine set [36]. This comparison was conducted to evaluate the trend of fuel deterioration under diesel engine operation. The differences in experimental parameters between these two studies differences in the form of utilized biodiesel concentration, fuel quantity, test duration as well as the type of diesel engine fuel injection system used are shown in Table 3.12.

In Table 3.13, higher than 5% difference between the initial and final value of each property is considered changed whereas anything below that is considered unchanged. By focusing on the trend of physico-chemical properties changes, 89% of the properties underwent similar trends in changes. This includes the biodiesel's OS, C12:0 fatty acid, C14:0 fatty acid, C16:0 fatty acid, C18:0 fatty acid, C18:1 fatty acid, dissolved aluminium, iron, zinc and copper concentration. Conversely, the C18:2 fatty acid was observed not to follow the same trend of changes. The C18:2 fatty acid from the study in literature [36] experienced 12% change at the end of the test when compared to its initial value while the fatty acid

remained close to its initial value at the end of the test from the first-stage investigation.

It is essential to highlight that for the B20 fuel used in the study from literature, the most vulnerable unsaturated fatty acid to undergo biodiesel oxidation process is the C18:2 fatty acid. In contrast, the most vulnerable unsaturated fatty acid to undergo biodiesel oxidation process for the B100 from the present study is the C18:3 fatty acid. Taking into account the most vulnerable unsaturated fatty acid to undergo biodiesel oxidation process aspect, both the fatty acids from the respective studies independently underwent changes. This finding therefore reveals that the trend of changes in both the studies are actually 100% similar.

Based on the comparison above, it is indeed conclusively determined that the trend of fuel deterioration changes irrespective of neat or blended form under diesel engine operation in general could be expected. The findings obtained from the first-stage investigation could be used as a reference for neat or blended form biodiesel deterioration under diesel engine operation in general.

Table 3.12 Research specifications of the present study and the study from literature.

	Research specifications	
	First stage	**Study from literature** [36]
Fuel	B100	B20 (20 vol%. biodiesel in winter grade diesel)
Biodiesel feedstock	Palm	Not reported
Fuel quantity (l)	76	1514
Additive	None	Cold Flo 6200RK & BHA (concentration not reported)
Engine manufacturer	Toyota	John Deere
Model	1KD-FTV	5030TF270
Fuel injection type	Common rail direct injection	Unit pump
Engine description	In-line 4 cylinder, 3000 cc	In-line 5 cylinder, 3050 cc
Engine maximum power	110 kW @ 3400 rev/min	60 kW @ 1800 rev/min
Speed-load test cycle	CEC F-98-08	Steady load of 30 kW
Test duration (min)	153	7680

Table 3.13 Comparison of biodiesel deterioration from stage 1 with the study from literature.

		This research						Research from literature				
		Initial		Final		Difference (%)	Change	Initial	Final	Difference (%)	Change	Similarity
		Mean	SD	Mean	SD							
Oxidation stability (h)		10.60	0.10	9.45	0.11	10.78	C	16.30	8.28	49.20	C	Yes
FAC (%)	C12:0	0.20	0.01	0.20	0.01	0.01	U	Not reported				
	C14:0	1.09	0.02	1.09	0.03	0.05	U	1.82	1.80	1.10	U	Yes
	C16:0	41.78	0.87	41.77	0.73	0.02	U	24.10	24.10	0.00	U	Yes
	C16:1	Not applicable						0.18	0.18	0.00	U	
	C18:0	4.86	0.26	4.85	0.25	0.21	U	14.74	14.74	0.00	U	Yes
	C18:1	41.21	0.27	41.18	0.30	0.07	U	42.77	42.77	0.00	U	Yes
	C18:2	10.34	0.84	10.32	0.65	0.19	U	16.39	14.45	11.84	C	No
	C18:3	0.55	0.08	0.51	0.09	7.27	C	Not reported				
DM (ppm)	Al	2.93E-04	2.25E-05	0.37	0.01	1.26E+05	C	0.10	0.32	220.00	C	Yes
	Fe	3.38E-04	9.19E-06	0.15	7.40E-03	4.27E+04	C	0.02	0.13	550.00	C	Yes
	Zn	6.20E-04	4.20E-06	0.12	6.17E-06	1.91E+04	C	Not reported				
	Cu	1.40E-04	2.09E-06	0.10	7.05E-03	6.79E+04	C	0.02	0.14	600.00	C	Yes
	Cr	Not applicable						0.05	0.13	160.00	C	

C: changed (higher than 5% difference between initial and final value); DM: dissolved metal; FAC: fatty acid composition; U: unchanged (lower than 5% difference between initial and final value).

3.3.2.2 Stage 2-2

Secondly, the deterioration of palm biodiesel with different physical properties under CRDE operation was compared. Table 3.14 shows the comparison of fuel deterioration for palm biodiesel with different physical properties operated under similar engine operation conditions. Here, higher than 5% difference between the initial and final value for each property independently is considered changed while otherwise is considered unchanged.

Focusing on the biodiesel oxidation, TAN and water content, it is clear that the trends of changes are closely matched between the two fuels despite the differences in the physical properties. Precisely, the OS, dissolved metals concentration, conductivity value, hydrogen ion concentration and C18:3 fatty acid were observed to be changed. On the other hand, the rest of the properties such as the other fatty acids, viscosity value, peroxide value, FTIR spectrum (as shown in Fig. 3.16), DO concentration, TAN and water content were found to be unchanged.

Above all, the rate of change of the deteriorated properties are significantly different between both the fuels as exhibited in Table 3.15. This rate of change was determined by measuring the divisional value of the total change of each property over the total engine operation duration. Here, the rate of change for all the changed properties such as OS, dissolved metals concentration, conductivity

value, hydrogen ion concentration and C18:3 fatty acid were determined to be higher for the Vance Bioenergy fuel as compared to the Carotech fuel by 178%, 31-68%, 142%, 82% and 99%, respectively.

Since the first-stage investigation conclusively determined that the reduction in OS was attributed to the increase in dissolved metals concentration in the fuel, the higher OS reduction here for the fuel from Vance Bioenergy over the fuel from Carotech is suggested to be due to the higher increase in all the 4 dissolved metals in the former fuel than the latter. In addition, since the changes of the conductivity value, hydrogen ion concentration and C18:3 fatty acid have also been attributed to the dissolved metals concentration, these supports the observed higher changes in all the measured properties for the fuel from Vance Bioenergy over the fuel from Carotech.

The difference in the initial conductivity value between both fuels is suggested to have influenced the rate of dissolved metals concentration change. This is because in the study by Meenakshi et al. [109] which investigated the effect of different initial conductivity value of biodiesel on the copper's corrosion rate under rotating cage investigation according to ASTM G184, the authors reported higher metal mass loss with higher biodiesel's initial conductivity value. It is observed that the fuel from Vance Bioenergy has 57% higher initial conductivity value than the fuel from Carotech as shown in Table 3.14. The correlation between the initial

conductivity value and the rate of dissolved metals concentration agrees to the reported relationship.

Hence, it is conclusively determined that palm-based biodiesel is expected to undergo changes in terms of the OS, dissolved metals concentration, conductivity value, hydrogen ion concentration and C18:3 fatty acid under CRDE operation. Conversely, the rest of the properties such as the other fatty acids, viscosity value, peroxide value, FTIR spectrum, DO concentration, TAN and water content would remain unchanged. Above all, the biodiesel's initial conductivity value would influence the rate of change in the biodiesel's OS, dissolved metals concentration, hydrogen ion concentration and C18:3 fatty acid under CRDE operation.

Finally, it was found that the palm-based biodiesel from Carotech with 8 h of OS was not oxidized as it still retained 95% of its initial OS after engine operation. Furthermore, the TAN and water content remained closed to their initial values after CRDE operation under the CEC-98-08 SLTC. These findings affirms the results obtained in the first-stage investigation of the unoxidized biodiesel as well as the unchanged TAN and water content under CRDE operation.

Table 3.14 Comparison of biodiesel deterioration with different initial physical properties.

Properties		Vance Bioenergy				Diff. (%)	Change	Carotech				Diff. (%)	Change	Similarity
		Initial		Final				Initial		Final				
		Mean	SD	Mean	SD			Mean	SD	Mean	SD			
Biodiesel oxidation														
Oxidation stability (h)		10.60	0.10	9.45	0.11	10.78	C	7.955	0.05834	7.544	0.05095	5.17	C	Yes
DM (ppm)	Al	2.93E-04	2.25E-05	0.37	0.01	1.26E+05	C	1.82E-04	1.76E-05	0.22	0.05	1.19E+05	C	Yes
	Fe	3.38E-04	9.19E-06	0.15	7.40E-03	4.27E+04	C	1.46E-04	1.81E-05	0.11	0.03	1.24E+05	C	Yes
	Zn	6.20E-04	4.20E-06	0.12	6.17-E06	1.91E+04	C	2.82E-05	2.13E-06	0.09	0.02	3.24E+05	C	Yes
	Cu	1.40E-04	2.09E-06	0.10	7.05E-03	6.79E+04	C	9.95E-05	1.04E-05	0.06	1.00E-02	5.77E+04	C	Yes
Conductivity (pS/m)		127.30	1.75	500.66	1.91	293.30	C	80.91	1.89	235.79	2.25	191.43	C	Yes
Hydrogen ion (mol/l)		3.18E-05	3.95E-06	6.92E-05	8.46E-06	117.45	C	3.16E-05	2.89E-06	6.72E-05	7.56E-06	112.44	C	Yes
FAC (%)	C12:0	0.20	0.01	0.20	0.01	0.01	U	0.18	0.02	0.18	0.02	0.02	U	Yes
	C14:0	1.09	0.02	1.09	0.03	0.05	U	1.09	0.03	1.09	0.04	0.05	U	Yes
	C16:0	41.78	0.87	41.77	0.73	0.02	U	41.84	0.94	41.85	1.78	0.92	U	Yes
	C18:0	4.86	0.26	4.85	0.25	0.21	U	5.21	0.31	5.21	0.45	0.23	U	Yes
	C18:1	41.21	0.27	41.18	0.30	0.07	U	39.78	0.35	39.74	0.09	0.16	U	Yes
	C18:2	10.34	0.84	10.32	0.65	0.19	U	11.21	0.91	11.20	0.26	0.54	U	Yes
	C18:3	0.55	0.08	0.51	0.09	7.27	C	0.37	0.22	0.35	0.51	5.41	C	Yes
Viscosity (mm^2/s)		4.54	0.01	4.53	0.02	0.22	U	4.56	0.01	4.57	0.01	0.22	U	Yes
Peroxide value (meq)		15.91	0.04	15.91	0.05	0.01	U	14.21	0.07	14.22	0.08	0.06	U	Yes
DO (ppm)		7.95	0.08	7.98	0.09	0.31	U	7.96	0.09	7.97	0.12	0.07	U	Yes
Total acid number														
TAN (mgKOH/g)		0.28	5.35E-03	0.28	7.56E-03	0.00	U	0.15	0.02	0.15	0.02	0.01	U	Yes
Water content														
Water content (%)		0.02	8.35E-04	0.02	7.56E-04	0.63	U	0.01	5.35E-04	0.01	6.25E-04	0.09	U	Yes

C: changed (higher than 5% difference between initial and final value); DM: dissolved metal; DO: dissolved oxygen; FAC: fatty acid composition; TAN: total acid number; U: unchanged (lower than 5% difference between initial and final value).

Table 3.15 Comparison on the rate of change for biodiesel properties under CRDE operation.

Properties rate of change		**Vance Bioenergy**	**Carotech**
Oxidation stability	(h/min)	9.52E-03	3.43E-03
Dissolved aluminum	(ppm/min)	2.97E-03	1.80E-03
Dissolved iron	(ppm/min)	1.32E-03	9.15E-04
Dissolved zinc	(ppm/min)	9.99E-04	7.62E-04
Dissolved copper	(ppm/min)	8.03E-04	4.78E-04
Conductivity	(pS/m/min)	3.12	1.29
Hydrogen ion	(mol/l)	3.11E+00	1.71E+00
C18:3	(%/min)	3.33E-04	1.67E-04

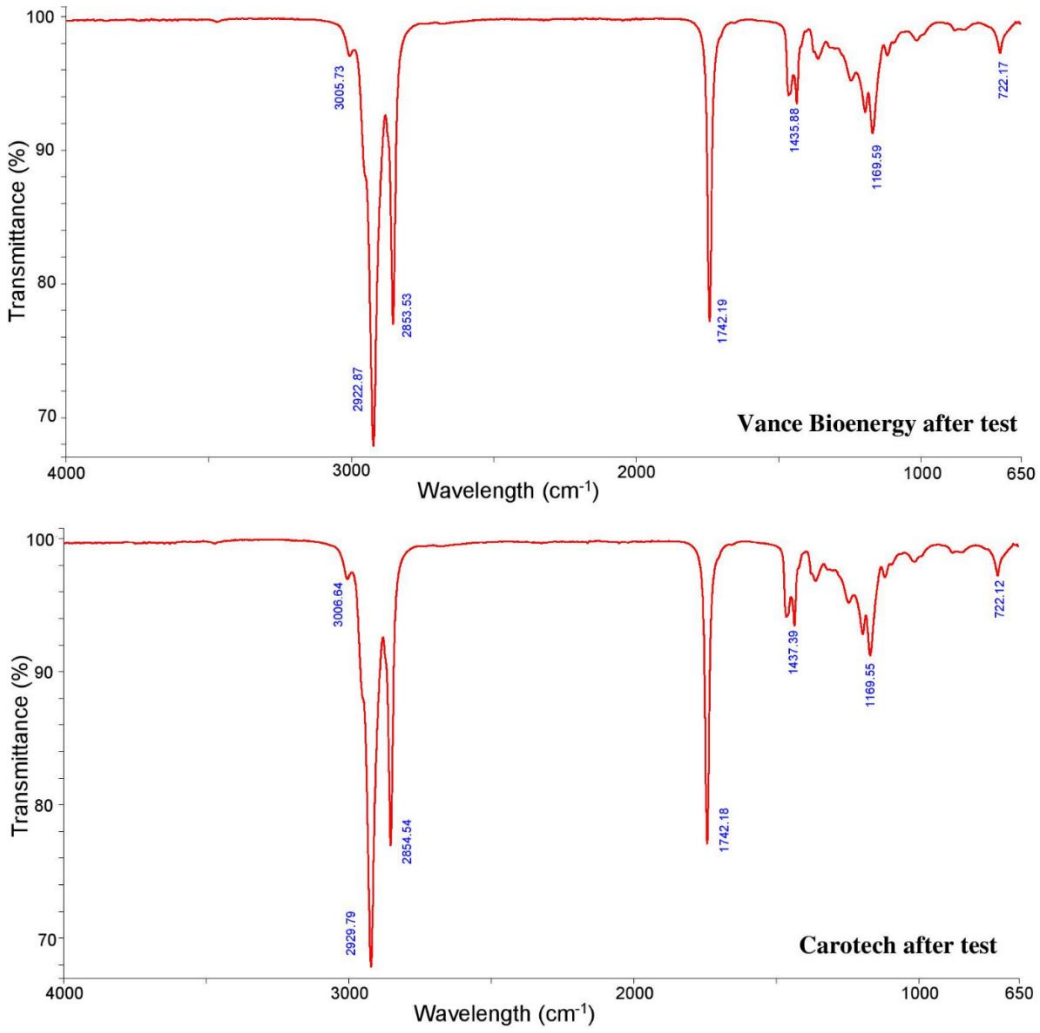

Fig. 3.16 FTIR spectrums of Vance Bioenergy and Carotech biodiesel fuel after CRDE operation under CEC F-98-08 SLTC.

3.3.2.3 Stage 2-3

The deterioration of palm biodiesel under different duration of CRDE operation under the same CEC F-98-08 SLTC was ascertained in the third comparison. Table 3.16 shows the comparison between the biodiesel deterioration under 1 full tank of operation and the biodiesel deterioration under 5 days of operation with 1 full tank each day.

After 5 days of operation, the final OS was observed to retain 96% of the initial OS. Furthermore, the presence of biodiesel oxidation products were not detected from the FTIR spectrum of the biodiesel after 5 days of operation as shown in Fig. 3.17. These findings demonstrate that the biodiesel did not oxidize even under 5 days of CRDE operation.

Additionally, the biodiesel's OS after 5 days of engine operation was found to retain 6% higher OS than the biodiesel after 1 full tank of CRDE operation. Since the OS reduction is suggested to be influenced by the increase in dissolved metals as described in the first-stage investigation, comparisons were conducted between the concentrations of dissolved metals in both the fuels after engine operation. Here, lower dissolved metals concentration was found in the fuel after 5 days of operation in comparison to the 1 full tank of operation. As such, this explains the higher OS of the former fuel in comparison to the latter.

Table 3.16 Comparison of palm biodiesel deterioration under 1 full tank operation to under 5 full tanks of operation.

Properties		Initial		1 full tank		5 full tanks	
		Mean	**SD**	**Mean**	**SD**	**Mean**	**SD**
Biodiesel oxidation							
Oxidation stability (h)		10.60	0.10	9.45	0.11	10.15	0.12
DM (ppm)	Al	2.93E-04	2.25E-05	0.37	0.01	0.17	0.05
	Fe	3.38E-04	9.19E-06	0.15	7.40E-03	0.06	8.98E-03
	Zn	6.20E-04	4.20E-06	0.12	6.17E-06	0.05	7.51E-06
	Cu	1.40E-04	2.09E-06	0.10	7.05E-03	0.04	8.09E-03
Conductivity	(pS/m)	127.30	1.75	500.66	1.91	295.10	2.99
Hydrogen ion	(mol/l)	3.18E-05	3.95E-06	6.92E-05	8.46E-06	4.11E-05	8.46E-06
FAC (%)	C12:0	0.20	0.01	0.20	0.01	0.20	0.01
	C14:0	1.09	0.02	1.09	0.03	1.09	0.04
	C16:0	41.78	0.87	41.77	0.73	41.77	0.89
	C18:0	4.86	0.26	4.85	0.25	4.86	0.31
	C18:1	41.21	0.27	41.18	0.30	41.21	0.30
	C18:2	10.34	0.84	10.32	0.65	10.32	0.74
	C18:3	0.55	0.08	0.51	0.09	0.52	0.10
Viscosity	(mm^2/s)	4.54	0.01	4.53	0.02	4.52	0.03
Peroxide value	(meq)	15.91	0.04	15.91	0.05	15.90	0.03
DO	(ppm)	7.95	0.08	7.98	0.09	7.96	0.08
Total acid number							
TAN	(mgKOH/g)	0.28	5.35E-03	0.28	7.56E-03	0.28	7.56E-03
Water content							
Water content	(%)	0.02	8.35E-04	0.02	7.56E-04	0.02	7.07E-04

DM: dissolved metal; DO: dissolved oxygen; FAC: fatty acid composition; TAN: total acid number.

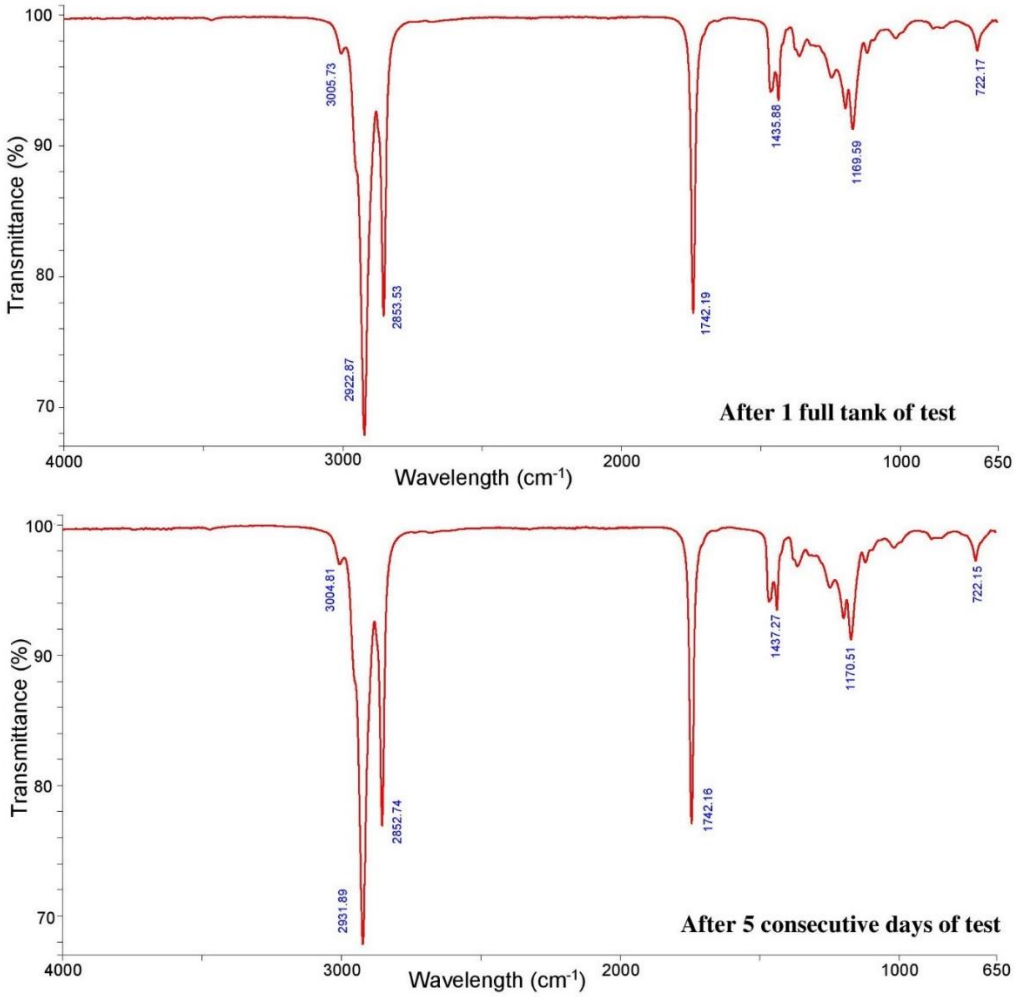

Fig. 3.17 FTIR spectrums of 1 full tank operation and 5 consecutive days of CRDE operation.

However, higher dissolved metals in the fuel is typically anticipated under longer engine operation. Corresponding to this, the concentration of dissolved metals was gauged instead of the total dissolved metals present in the fuel. The quantity of the fuel during the fuel sampling process would affect the dissolved metal concentration. During the fuel sampling after the 5 days of operation, an estimated 31.8 l of fuel was present. In comparison, only 6 l of fuel was present after 1 full tank of operation. This difference in the remaining fuel quantity reflected on the lower dissolved metals concentration under 5 days of CRDE operation in comparison to 1 full tank of CRDE operation.

Thus, it is conclusively determined that the deterioration level of biodiesel under CRDE operation is much higher under 1 full tank of operation in comparison to 5 days operation with 1 full tank each day. This outcome was heavily influenced by the lower dissolved metals concentration in the collected biodiesel samples due to the higher remaining fuel quantity under the much longer CRDE operation duration. Notably, the biodiesel was found unoxidized despite 5 days of CRDE operation with 1 full tank each day.

3.3.2.4 Stage 2-4

Here, the deterioration of biodiesel under CRDE operation was compared to the deterioration of biodiesel under metal immersion investigation according to ASTM G31 standard method as summarized in Table 3.17. The comparisons focussed on the TAN and water content changes under both the circumstances. Comparison in terms of biodiesel oxidation condition was however not possible since this property is not commonly reported for metal immersion studies. The study which evaluated the compatibility of copper with biodiesel was utilized here due to the great extent of incompatibility shown between copper and biodiesel. The unavailability of information reported in existing elastomer compatibility studies prevented a further comparison under elastomer immersion.

Table 3.17 Research specifications of the immersion study from literature [71].

Research specifications	
Fuel	B100
Feedstock	Palm
Immersion temperature (°C)	80
Immersion duration (h)	1200
Evaluated metal	copper
Immersion condition	Continuously stirred using magnetic stirrer @ 250 rev/min

Based on the results displayed in Table 3.18, it is observed that the TAN increased by 400% under metal immersion while the TAN remained close to its initial value under CRDE operation. Similar outcome was also observed for the water content whereby the water content increased by 826% under metal immersion while the water content remained close to its initial value under CRDE operation.

It is essential to stress here that the TAN and water content in biodiesel are indeed among the major factors promoting FDM degradation. Therefore, taking into account that these two properties did not increase under CRDE operation, the contradictory findings from the immersion studies indicated that current immersion test is not capable of elucidating the actual compatibility present between FDM and biodiesel. Hence, a more appropriate method is required to evaluate the actual compatibility of FDM with biodiesel in the FDS of a real-life CRDE which should take into account the deterioration of biodiesel under CRDE operation.

Table 3.18 Comparison of fuel deterioration under CRDE operation and immersion investigation.

Properties	Under CRDE operation					Under metal immersion			
	Initial		Final		Difference (%)	Initial	Final	Difference (%)	Similarity
	Mean	SD	Mean	SD					
Total acid number (mgKOH/g)	0.28	5.35E-03	0.28	7.56E-03	0.45	0.36	1.80	400	No
Water content (%)	0.02	8.35E-04	0.02	7.56E-04	0.63	0.04	0.41	826	No

3.3.3 Third stage-characterization of biodiesel's conductivity value

The influence of fuel temperature, dissolved metal, oxidized biodiesel and duration of fuel heating on the conductivity value of the biodiesel was ascertained independently here based on the results from the first-stage investigation. These are mainly chosen as they are the essential elements of CRDE operation. As shown in Fig. 3.18, the biodiesel's conductivity value was observed to increase with increasing biodiesel temperature, dissolved copper concentration, concentration of oxidized biodiesel and also the duration of fuel heating.

For the investigation to appraise the influence of biodiesel temperature, a maximum increase of 451% in conductivity value was measured between 25 and 100 °C. Typically, the increase in a solution's temperature will cause a decrease in its viscosity which nevertheless increases the mobility of the ions in the solution [198]. Since the conductivity of a solution is very dependent on the mobility of the ions, an increase in the solution's temperature will lead to the increase in the conductivity value. This explains the higher biodiesel's conductivity value observed with increasing fuel temperature.

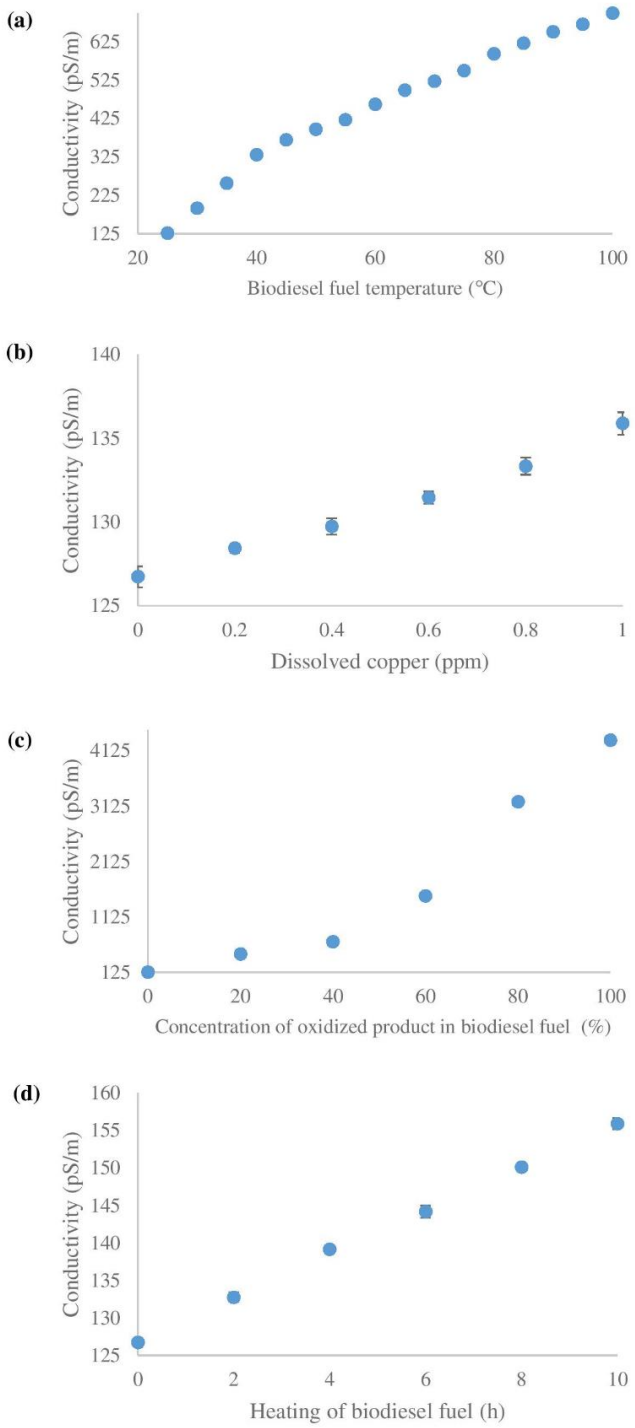

Fig. 3.18 Changes of conductivity value with respect to (a) fuel temperature, (b) dissolved copper, (c) oxidized biodiesel and (d) fuel heating duration.

In terms of the effect of dissolved copper concentration, a maximum increase of 133% in conductivity value was measured between 0 and 1 ppm of dissolved copper. Usually, the increase in the number of ions in the solution due to contaminants such as material leaching also causes the increase in conductivity value [198]. As such, the addition of the dissolved copper here which replicated the effects of dissolved metal has certainly raised the conductivity value. This is mainly attributed to the dissolved copper which increases the number of ions in the biodiesel.

As for the influence of oxidized biodiesel, fully oxidized biodiesel was found to have 34 times higher conductivity value than unoxidized biodiesel. On the other hand, a maximum increase of 91% in conductivity value was measured between 0 and 10 h of heating. Due to the increase in conductivity value of the oxidized and heated biodiesels, hydrogen ion analysis was conducted only for the 100% oxidized biodiesel and biodiesel which was heated for 10 h. This additional test was performed to determine the concentration of hydrogen ion in these samples because an increase in the number of ions due to molecular dissociation from the solution itself could also have resulted in an increase in the conductivity value [198]. From the tests, significant increases in hydrogen ion concentrations of 890% and 111% were measured for 100% oxidized biodiesel and for the biodiesel after 10 h of heating, respectively, when compared to that of the initial biodiesel sample. This significant increase demonstrates the dissociation of hydrogen ions from the biodiesel samples. As such, the increase in the number of ions due to

molecular dissociation is suggested as the reason for the increased conductivity value observed.

In summary, the conductivity of biodiesel is conclusively determined as a feasible indicator of the effects of parameters such as fuel temperature, presence of dissolved metal, oxidation state of biodiesel and biodiesel heating duration. Since all these four parameters cause biodiesel deterioration under CRDE operation, the biodiesel conductivity value can be used to indicate biodiesel deterioration level under actual CRDE operation. This is mainly attributed to the resulting increase of ions in biodiesel due to molecular dissociation and material leaching.

3.4 Summary

By determining the biodiesel deterioration under engine operation in the first-stage investigation, it is clear that the utilized biodiesel did not oxidize while, the TAN and the water content were unaffected at the end of the tests. These findings were supported by the outcomes of the second-stage investigations which highlighted that the deterioration of B20 under generator diesel engine set, deterioration of palm biodiesel with different physical properties and the deterioration of biodiesel under 5 consecutive days of CRDE operation matched the trend of changes obtained from the first-stage investigation. Above all, the inadequacy of existing immersion test in evaluating the compatibility of FDM with biodiesel in the FDS of a real-life CRDE was demonstrated.

The combined outcomes of the first and second-stage investigations suggested that a more suitable method of testing which incorporates the deterioration level of biodiesel under real CRDE operation is needed to assess the actual compatibility present between FDM and biodiesel in the FDS of a physical CRDE system. Hence, the characteristics of biodiesel's conductivity value were evaluated in the third-stage investigation since this property was demonstrated to be related to fuel deterioration level under actual engine operation. It can be concluded that conductivity of biodiesel is a property which can be measured as an indicator of biodiesel deterioration under CRDE operation. With regard to the above, the influence of biodiesel's conductivity value towards the FDM degradation would be investigated next.

CHAPTER 4-COMPATIBILITY OF FUEL DELIVERY METAL AND ELASTOMER IN PALM BIODIESEL

This chapter presents the details of investigations carried out as outlined in Fig. 4.1. The observed compatibility of FDM with biodiesel under physical CRDE after the conducted investigations are described and discussed accordingly here.

4.1 Background

The investigations in this chapter were carried out corresponding to the outcomes obtained from Chapter 3 which distinctly illustrated that the FDM degradation acceleration factors such as oxidized biodiesel was not present while the TAN and water content were found to be unaffected under CRDE operation. Instead, two other biodiesel properties such as the DO concentration and conductivity value were reported to be changed during and after CRDE operation, respectively. In addition, these two properties were reported to have influenced the biodiesel deterioration process. Critically, the influences of these two biodiesel properties on both metal corrosion and elastomer degradation are yet to be reported to date.

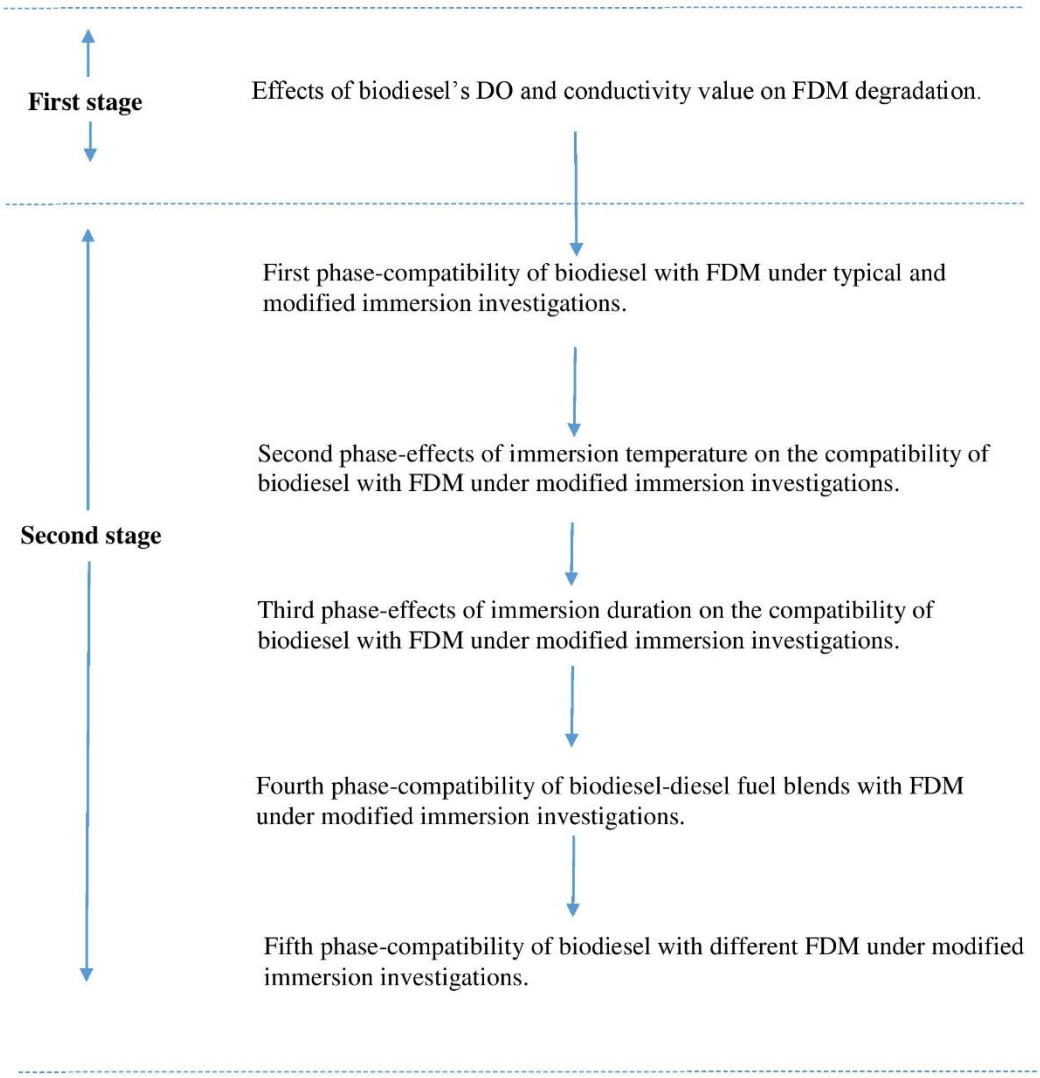

Fig. 4.1 Overview of investigations in Chapter 4.

In response to the above, a two-stage investigation was carried out here to ascertain the compatibility of FDM with biodiesel in the FDS of a real-life CRDE as shown in Fig. 4.1. For the first stage, the effects of biodiesel's DO concentration and conductivity value on FDM degradation were examined independently. These investigations were conducted using copper and NBR according to ASTM G31 and ASTM D471, respectively, at 25 °C for 120 h. Copper and NBR were evaluated here due to their greater incompatibility with biodiesel than other FDM [85, 125].

The second-stage investigations were conducted corresponding to the outcomes obtained from the first-stage investigations which clearly displayed the adverse effects of biodiesel's DO and conductivity properties on FDM degradation. Since the findings in the first-stage investigations were obtained under typical immersion investigations which did not resemble the actual conditions in the diesel engine's FDS, modified immersion investigations which resemble the biodiesel deterioration as reported in Chapter 3 section 3.3.1 were carried out here. In order to replicate the biodiesel deterioration under CRDE operation, the biodiesel's conductivity value was specifically employed here corresponding to the findings obtained in section 3.3.3. The continuous increase in biodiesel's conductivity value under CRDE operation until the re-fuelling process which resulted in the resetting of the conductivity value was precisely simulated here by adding fuel renewal interval in the existing typical immersion standard methods.

Concerning the fuel renewal duration, it is described under the methodology section 4.2.5

The incorporation of fuel renewal in immersion investigations has been conducted in several studies [83, 199]. However, the major difference between these studies and the present one is the aim of the fuel renewal incorporation. The studies in literature typically aimed to minimize the bulk solution composition changes and oxygen depletion, and to replenish the ionic contaminants through the incorporation of fuel renewal. In contrast, the incorporation of fuel renewal here is aimed to replicate the biodiesel deterioration under CRDE operation. This approach employed here is essential for determining the FDM degradation under real-life CRDE operation.

4.2 Material and methods

The material and methods involved throughout the conducted investigations of determining the compatibility of FDM with biodiesel are presented here.

4.2.1 Evaluated metal specimens

Aluminium, copper, galvanized steel and stainless steel coupons of 0.02 m in diameter by 0.002 m in thickness were evaluated in the present study due to their popularity as fuel delivery components' high pressure pump, fuel seal, fuel line and fuel rail materials, respectively. A hole of 0.002 m in diameter was drilled near the edge for hanging the coupons using a silk string. The metal coupon has a surface area of 0.000760 m^2 determined using ASTM G31 standard method. The elemental composition of the evaluated metals determined through elemental analysis using FEI's Quanta 400F FESEM scanning electron microscope are shown in Table 4.1.

4.2.2 Evaluated elastomer specimens

NBR, FKM and silicone rubber in the form of O-ring were evaluated in the present study due to their popularity as fuel delivery components' sub-fuel hose, high-pressure fuel seal and low-pressure fuel seal materials, respectively. In addition, nylon plastic specimen in dog-bone shape [180] as shown in Fig. 4.2 was also evaluated in the present study due to their popularity as fuel hose

materials. The dimensions of the evaluated elastomer specimens are shown in Table 4.2. The evaluated NBR specimen has 45% of acrylonitrile content determined via FTIR spectroscopy analysis [200, 201] and Kjeldhal method [202] while, the evaluated FKM specimen has 59% of fluorine content determined through energy dispersive X-ray spectroscopy analysis.

Table 4.1 Elemental composition of metal specimens.

No.	Elements	Weight (%)
	Aluminium	
1.	Aluminium	99.59
2.	Iron	0.28
3.	Silicon	0.10
4.	Zinc	0.03
	Copper	
1.	Copper	89.05
2.	Carbon	10.42
3.	Oxygen	0.43
4.	Silicon	0.10
	Galvanized steel	
1.	Zinc	99.08
2.	Iron	0.74
3.	Carbon	0.08
4.	Silicon	0.10
	Stainless steel	
1.	Iron	67.56
2.	Chromium	17.68
3.	Nickel	12.98
4.	Manganese	1.18
5.	Silicon	0.52
6.	Carbon	0.08

Table 4.2 Dimensions of elastomer specimens.

Specimen	External diameter (m)	Internal diameter (m)	Thickness (m)	Surface area (m^2)
Nitrile rubber	0.032580	0.03032	0.003140	0.000246
Fluoroelastomer	0.030990	0.02852	0.001870	0.000246
Silicone rubber	0.028020	0.02502	0.001620	0.000265
Nylon		Refer to **Fig. 4.2**		0.005814

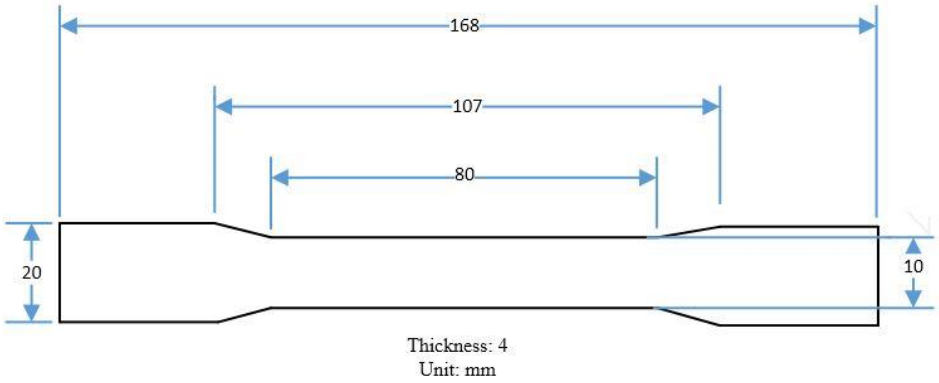

Fig. 4.2 Dimensions of nylon dog-bone specimen.

4.2.3 Test fuel

Palm biodiesel without additives from Vance Bioenergy, Singapore with specifications as shown in Table 4.3 was used here. The same batch of fuel was used throughout the investigation to eliminate batch to batch variations. As shown in Table 4.4, the fuel quantity for immersion investigations were measured and utilized according to the SAE J1747: 2013 [203] standard method in which requires a minimum surface area to fuel ratio of 0.2 cm^2/ml.

Table 4.3 Palm biodiesel fuel specifications.

Tests		**Methods**	**Specification**	**Results**
Ester content	(%)	EN 14103	96.5 minimum	98.30
Density @ 15 °C	(kg/m^3)	ISO 12185	860-900	874.00
Kinematic viscosity @ 40 °C	(mm^2/s)	ISO 3104	3.50-5.00	4.54
Water content	(%)	ISO 12937	0.05 maximum	0.02
Copper strip corrosion, 3 h @ 50 °C	(Rating)	ISO 2160	Class I	1a
Oxidation stability @ 110 °C	(h)	EN 14112	6.0 minimum	10.50
Total acid number	(mg KOH/g)	EN 14104	0.50 maximum	0.28

Table 4.4 Fuel quantity for each specimen.

	Fuel quantity (ml)	
Specimen	**Minimum**	**Utilized**
Metal coupons (Al, Cu, GS and SS)	38	38
Elastomer O-rings (NBR, FKM and silicone rubber)	15	15
Nylon dumbbell shaped	117	480

4.2.4 First-stage investigation

The effects of biodiesel's DO concentration and conductivity value on FDM degradation were examined independently here. To manipulate the biodiesel's conductivity value, the fuel was heated for 10 h continuously at 100 °C in a dark and closed condition. This sample was named Treated 1.

For manipulating the concentration of DO, the biodiesel was heated at 100 °C accompanied with nitrogen blanketing prior to the investigation to prevent absorption of oxygen into the fuel. This sample was named Treated 2. The laboratory setup to manipulate the concentration of DO in biodiesel as well as to measure the DO concentration simultaneously is shown in Fig. 4.3 [204]. The differences in physical properties between the untreated, Treated 1 and Treated 2 biodiesels in terms of OS, TAN, water content, DO concentration and conductivity value are presented in Table 4.5.

Once the fuels were successfully treated as described above, investigations were conducted using copper and NBR according to ASTM G31 and ASTM D471, respectively, at 25 °C for 120 h. The conducted analytical tests to determine the biodiesel properties changes under immersion investigation included the conductivity value, DO concentration, water content, TAN and OS. In terms of measuring the FDM degradation, the corrosion rate was determined for copper while the volume and tensile strength changes were determined for NBR.

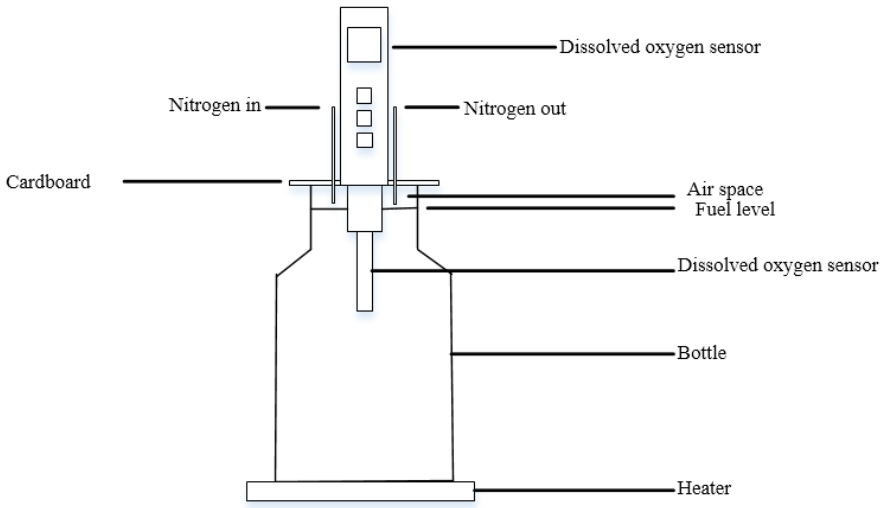

Fig. 4.3 Laboratory setup to manipulate and measure biodiesel fuel's dissolved oxygen concentration.

Table 4.5 Comparison of biodiesel fuels' initial physical properties.

Properties		Untreated		Treated 1		Treated 2	
		Mean	**SD**	**Mean**	**SD**	**Mean**	**SD**
Oxidation stability	(h)	10.60	0.10	10.58	0.12	10.59	0.15
TAN	(mgKOH/g)	0.28	5.35E-03	0.28	7.56E-03	0.28	5.35E-03
Water content	(%)	0.02	8.35E-04	0.02	9.30E-04	0.02	8.35E-04
Dissolved oxygen	(ppm)	7.95	0.08	7.99	0.10	0.3	5.35E-02
Conductivity	(pS/m)	127.30	1.75	155.88	1.54	127.15	1.56

TAN: total acid number

4.2.5 Second-stage investigations

In this stage, modified immersion investigations which incorporated fuel renewal in the existing standard methods as described in ASTM G31and ASTM D471 for metal and elastomer specimens, respectively, were carried out. To determine the fuel renewal duration, the time taken for the biodiesel immersed with copper and NBR independently, at 100 °C to reach 500 pS/m of conductivity value was measured. The 500 pS/m conductivity value was specifically used here by referring to the maximum biodiesel's deterioration reported under 1 full tank of CRDE operation in Chapter 3 section 3.3.1.1.8. Corresponding to the above, a fuel renewal interval duration of 108 and 192 h for metal and elastomer, respectively, were determined. The fuel renewal refers the replacement of the existing fuel sample with fresh fuel sample while retaining the specimen. Five phases of experiments were carried out here as outlined in Table 4.6. For comparison purposes, typical immersion investigations were conducted for the first phase with the exclusion of fuel renewal.

Table 4.6 Details of second-stage investigations.

Phase	Aim	Fuel	Material	Temperature (°C)	Duration (h)	Material analysis	Fuel analysis
First	Modified immersion and typical immersion	B100	Cu	100	540	CR and SM. EC for modified immersion sample only.	FTIR, TAN, water content and conductivty.
		B100	NBR	100	960	VC, TSC, hardness change and SM. EC for modified immersion sample only.	
Second	Influence of temperature on modified immersion	B100	Cu	25	540	CR, SM and EC.	
		B100	NBR	25	960	VC, TSC, hardness change, SM and EC.	
Third	Influence of duration on modified immersion	B100	Cu	100	108, 216, 324 & 432	CR and SM.	
		B100	NBR	100	192, 384, 576 & 768	VC, TSC and SM.	
Fourth	Biodiesel concentration on modified immersion	B0, B20, B50	Cu	100	540	CR and SM.	
		B0, B20, B50	NBR	100	960	VC, TSC and SM.	
Fifth	Influence of modified immersion on different types of materials	B100	SS, GS and Al.	100	540	CR and SM.	
		B100	FKM, nylon and silicone rubber.	100	960	VC, TSC and SM.	

CR: corrosion rate; EC: elemental composition; FTIR: Fourier transform infrared spectroscopy; SM: surface morphology; TAN: total acid number; TSC: tensile strength change; VC: volume change.

4.2.6 Metal corrosion investigation procedure and analysis

The metal corrosion investigation here was conducted according to the ASTM G1:2011 [205] and ASTM G31:2012 [134] standard methods. An additional specimen for each condition here was analysed as duplicate. The corrosion rate was then calculated based on the average mass loss measured from the duplicate specimens using the equation from ASTM G1 [206] as described in Appendix C.

4.2.7 Elastomer degradation investigation procedure and analysis

The elastomer degradation investigation here was conducted according to ASTM D471: 2012 [137]. The samples were characterized by measuring the volume, tensile strength and hardness changes. The calculated results from three specimens were averaged in determining the volume change as per described in ASTM D471. For the tensile strength determination, the tensile strength of the samples prior and after the immersion were measured at a strain rate of 500 mm/min according to ASTM D412:2013 [207]. Llyod Instruments' LR50K plus tensile strength tester was utilized for this analysis. In terms of the hardness change determination, the hardness value of the samples prior and after the immersion were measured according to ASTM D2240:2010 [208]. An Airforce's 560-10A digital Shore A hardness meter was utilized for this analysis. The sample calculation for volume, tensile strength and hardness changes are shown in Appendix D, Appendix E and Appendix F, respectively.

4.2.8 Surface morphology and elemental compositions material analysis

The surface morphology analysis using FEI's Quanta 400F FESEM scanning electron microscope (SEM) was conducted at 2000 and 500 times magnification to characterize the degradation behaviour of metal and elastomer specimens, respectively.

4.2.9 Analytical test

The fuel samples from the conducted immersion investigations were analysed using conductivity meter, DO meter, rancimat, TAN titrator, Karl-Fischer titrator, and FTIR spectrometer to examine the change in biodiesel's conductivity value, DO concentration, OS, TAN, water content and formation of oxidation products, respectively, as described in Table 4.7. All the samples were analysed within 72 h of collection and stored in dark room condition (25 °C) prior to the testing. The specifications of the utilized test equipment are as displayed in Table 4.8. Each analytical and material test here was conducted twice throughout the present study. For the graphs presented within the following results and discussion section, the error bars are based on standard errors to provide an estimated precision of the measured parameters. Within the tables, the error bars are based on standard deviations to show the dispersion of the measured parameters.

Table 4.7 Analytical tests conducted on biodiesel samples.

Analytical test	Standards	Equipment	Conditions
Conductivity	No information	Stanhope Seta's 997808-0 conductivity meter	Fuel sample of 30 ml in quantity was utilized here.
Dissolved oxygen	No information	Fisher Scientific's Traceable DO meter pen	This analysis was conducted at room temperature (~ 25 °C).
Oxidation stability	EN 14112:2003 [178]	Metrohm 743 Rancimat instrument	Samples of 7.5 g were analysed at a heating block temperature of 110 °C and a constant air flow of 10 l/h. The volatile compounds formed were collected in the conductivity cell with 60 ml of distilled water. The inflection point of the derivative curve of conductivity as a function of time was reported as the oxidation stability.
Total acid number	ASTM D664: 2011 [133]	Metrohm's 809 Titrando	Biodiesel samples of 10.0 g and standard titrant 0.01 M alcoholic KOH were used here.
Water content	ISO 12937:2000 [184]	Metrohm's 831 KF Coulometer	2.0 g of samples was utilized here.
Fourier infrared transform spectroscopy	No information	Perkin Elmer's Frontier model FTIR spectrometer	The functional groups in the FTIR spectrum were utilized for identifying the presence of secondary oxidation products here. Among the functional groups of concern here are aldehydes (C=O stretch at 1750-1625 cm^{-1}, C-H stretch off C=O at 2850 cm^{-1}, C-H stretch off C=O at 2750-2700 cm^{-1}), ketones (C=O stretch at 1750-1625 cm^{-1}) and carboxylic acid (C=O stretch at 1730-1650 cm^{-1}, hydrogen bonded O-H stretch at 3400-2400 cm^{-1}).

Table 4.8 Specifications of equipment for analytical and materials tests.

Test equipment specifications			
Conductivity meter	Manufacturer		Stanhope Seta
	Model		99708-0
	Range	(pS/m)	0-2000
Dissolved oxygen meter	Manufacturer		Fisher Scientific
	Model		Traceable DO meter pen
	Range	(mg/l)	0-20
	Resolution	(mg/l)	0.1
Rancimat	Manufacturer		Metrohm
	Model		743
	Temperature range	(°C)	50-220
	Conductivity range	(µS/m)	0-400
	Air flow range	(l/h)	7-25
Total acid number titrator	Manufacturer		Metrohm
	Model		809 Titrando (with 800 Dosino and 804 Ti Stand)
	Range	(mg/g)	0.05-250
Karl Fischer titrator	Manufacturer		Metrohm
	Model		831 KF Coulometer
	Range	(mg)	10 µg-200
	Precision	(µg)	± 3
Fourier transform infrared spectrometer	Manufacturer		Perkin Elmer
	Model		Frontier
	Wavelength range	(nm)	680-4800
	Software		Spectrum
Mass balance	Manufacturer		Sartorius BSA
	Model		BSA224S-CW
	Capability	(g)	220
	Readability	(g)	0.0001
	Repeatability	(g)	0.0001
Tensile strength tester	Manufacturer		Llyod Instruments
	Model		LR50K plus
	Crosshead speed range	(mm/min)	0.001-508
	Minimum load resolution	(N)	0.0001
Hardness meter	Manufacturer		Airforce
	Model		560-10A
	Shore		A
	Range	(HA)	0-100
Scanning electron microscope	Manufacturer		FEI
	Model		Quanta 400F FESEM
	Magnification range	(x)	40-250000
	Resolution	(nm)	Up to 3
Energy-dispersive X-ray	Manufacturer		Oxford Instruments
	Model		INCA 400 with X-Max Detector
	Active area size	(mm^2)	20

4.3 Results & discussion

The compatibility of FDM with biodiesel can be ascertained by evaluating the degradation underwent by the tested materials. Here, the effects of biodiesel's DO concentration and conductivity value towards FDM degradation were primarily investigated. Through this, essential information on the effects of biodiesel's DO concentration, as well as biodiesel's conductivity value towards FDM degradation can be conclusively determined. This was then accompanied with the investigations into the compatibility of FDM with biodiesel under modified immersion in which incorporated fuel renewal, aimed to replicate the fuel deterioration under real-life diesel engine operation. Through this, the actual compatibility of FDM with biodiesel in the FDS of a real-life diesel engine can be conclusively determined. The results obtained under both the stages are presented here.

4.3.1 First stage-effects of biodiesel's DO and conductivity value on FDM degradation

As shown in Table 4.9, the corrosion rate of copper was determined to be higher by 9% due to the exposure of Treated 1 biodiesel as compared to untreated biodiesel. Similarly, the volume swell and tensile strength reduction of NBR was determined to be higher by 13% and 20%, respectively, due to the exposure of Treated 1 biodiesel as compared to untreated biodiesel. With regard to these measurements, the exposure to Treated 1 biodiesel has caused greater adverse effect on both copper and NBR degradation as compared to untreated biodiesel.

The Treated 1 biodiesel was observed to inherit 22% higher conductivity value as compared to untreated biodiesel as shown in Table 4.5. Other properties such as OS, TAN, water content and DO concentration were closely matched between both the fuels. Hence, the greater biodiesel's conductivity value in Treated 1 biodiesel as compared to untreated biodiesel is suggested here to have significantly influenced the level of copper and NBR degradation.

Typically, the greater free ions present in biodiesel with higher conductivity value could have accelerated the ions exchange process during metal corrosion and elastomer degradation. Metal corrosion is an oxidation process of metal which occurs due to the natural phenomena of metal returning to its stable state. Likewise, elastomer degradation is a type of elastomer oxidation process which occurs due to the alteration of elastomer's chemical structure caused by the addition or removal of crosslinks. As such, since both the metal corrosion and elastomer degradation involves ion exchange, the presence of more free ions in biodiesel with higher conductivity value is suggested to have adversely influenced the FDM degradation.

Table 4.9 Comparisons of untreated and treated biodiesel fuels on copper and NBR degradation.

			Untreated biodiesel		**Treated 1 biodiesel**		**Differences**	**Treated 2 biodiesel**		**Differences**
			Mean	**SD**	**SD**	**Mean**	**wuB (%)**	**Mean**	**SD**	**wuB (%)**
Cu	Corrosion rate	(mm/yr)	1.75E-03	1.07E-07	1.91E-03	1.39E-07	+9.23	1.61E-04	8.76E-08	-90.77
NBR	Volume change	(%)	4.36	0.61	5.01	0.71	+13.04	3.18	0.42	-26.97
	Tensile strength change	(%)	6.80	0.03	8.14	0.03	+19.56	5.40	0.03	-20.60

wuB: with untreated biodiesel.

The outcome above also agrees with the findings reported by Anisha et al. [114] in which the authors investigated the effects of biodiesel's conductivity value on carbon steel's corrosion rate. The authors in the present study manipulated the biodiesel's conductivity value by adding sodium chloride which resulted in an increase in the biodiesel's conductivity value by 168% as compared to the untreated biodiesel. Based on this, the authors reported increased corrosion rate by 76% for carbon steel exposed to the biodiesel with sodium chloride as compared to the untreated biodiesel.

Furthermore, the influence of biodiesel's conductivity value on FDM degradation also agrees with several existing studies by taking into account the influence of temperature, dissolved metal and oxidized biodiesel on biodiesel's conductivity value as reported in Chapter 3 section 3.3.3. These existing studies which evaluated the effects of temperature [72, 97], oxidation condition [35, 70] and immersion duration [101, 117] indirectly evaluated the effects of biodiesel's conductivity value on FDM degradation. The effects of immersion duration can be associated to the leached metals/elastomers in biodiesel resulting in the increase in the conductivity value.

Critically, however, there are few studies from literature which reported otherwise. For example, in the study by Aquino et al. [118], the authors reported lower metal corrosion at higher fuel temperature under immersion investigation.

In another study, Fazal et al. [117] reported reduced metal corrosion after 1200 h of continuous increase in metal corrosion. These contradictory findings can nevertheless be explained from the results of the effects of biodiesel's DO concentration on the FDM degradation investigations.

As displayed in Table 4.9, the corrosion rate of copper was found to be lowered by 91% due to the exposure of Treated 2 biodiesel as compared to untreated biodiesel. Similarly, the volume swell and tensile strength reduction of NBR were lower by 27% and 21%, respectively, due to the exposure of Treated 2 biodiesel as compared to untreated biodiesel. These findings demonstrated that the exposure to Treated 2 biodiesel as compared to untreated biodiesel has resulted in lower adverse effects on FDM degradation. Concerning the above findings, the Treated 2 biodiesel is observed to inherit 96% lower concentration of DO as compared to untreated biodiesel as shown in Table 4.5. The other properties such as OS, TAN, water content and conductivity value are closely matched between both the fuels. Thus, the lower DO concentration in Treated 2 biodiesel as compared to untreated biodiesel has reduced the adverse effects of biodiesel exposure on FDM degradation.

Since the metal corrosion and elastomer degradation have been highlighted earlier as the oxidation process of metal and elastomer, respectively, oxygen is therefore an essential element in the degradation of material. This agrees with the

observation that lower concentration of DO in biodiesel has significantly lowered both the metal corrosion and elastomer degradation.

With regard to the above, the lower metal corrosion reported in the study by Aquino et al. [118] could be attributed to the lower concentration of DO in biodiesel despite the higher conductivity value as a result of higher fuel temperature. In terms of the reduction in corrosion rate after a continuous increase as reported by Fazal et al. [117], this could be possibly be linked to the presence of oxygen in dissolved form in the fuel. Since the sample was sealed, the DO could have eventually been used up. This therefore could have resulted in the reduction in corrosion rate after a continuous rise. From the discussion above, further investigations were carried out to determine the compatibility present between biodiesel and FDM in the FDS of a real-life diesel engine, of which the results are presented in section 4.3.2.

4.3.2 Second stage-compatibility of FDM with biodiesel under modified immersion

The results of the five phases of investigations to ascertain the compatibility present between biodiesel and FDM under diesel engine operating condition are presented and discussed as follows.

4.3.2.1 First phase-influence of modified and typical immersion on the compatibility of FDM with biodiesel

As shown in Table 4.10, the corrosion rate of copper due to exposure of biodiesel was found to be 13 times higher under typical immersion condition as compared to under modified immersion condition. Referring to Fig. 4.4, the grinding lines on the copper coupons prior to the investigation are clearly visible at 2000 times magnification. Upon 540 h of exposure, the surface of copper after exposure to biodiesel under modified immersion did not undergo any significant change since the grinding lines are still clearly visible as before. However, the surface of the copper coupon exposed to biodiesel under typical immersion changed significantly. Higher corrosion attack is suggested to have significantly degraded the copper surface under typical immersion condition as compared to modified immersion condition.

For elastomer degradation, as shown in Table 4.10, the volume, tensile strength and hardness changes for NBR exposed to biodiesel were determined to be higher

by 73%, 69% and 85%, respectively, under typical immersion condition as compared to modified immersion condition. From Fig. 4.5, more pits and cracks are present on the surfaces of NBR exposed to biodiesel under typical immersion condition as compared to modified immersion condition, at 500 times magnifications. This pit formation/microstructural changes could be attributed to the macromolecule chain scission/crosslinking due to permeation of polar oxygen groups into the elastomer. Hence, higher NBR degradation due to biodiesel exposure was found under typical immersion condition as compared to modified immersion conditions.

4.3.2.1.1 Deterioration of biodiesel under modified and typical immersion investigation

As shown in Fig. 4.6, the FTIR spectrums of biodiesel fuels after typical immersion condition with the exposure of copper and NBR, independently, underwent changes as compared to the FTIR spectrum of the as-received biodiesel. The main difference/feature that was newly detected from the spectrums was located at 3460 cm^{-1}. This peak corresponds to the oxygen bearing compound (C-OH) [209]. The presence of this compound reveals that these biodiesel fuels have oxidized. Contrarily, no new peaks were found for the FTIR spectrums of biodiesel fuels after modified immersion with the exposure of copper and NBR, independently. Additionally, these FTIR spectrums remained similar to the as-received biodiesel's FTIR spectrum. These findings indicate that

the biodiesel fuels due to the exposure of copper and NBR under modified immersion, independently, have not oxidized.

In addition to the FTIR analysis, the TAN, water content and conductivity value after the immersion investigations are as shown in Table 4.11. Here, the as-received biodiesel's TAN of 0.28 mg KOH/g falls within the permitted limit of 0.5 mg KOH/g given by ASTM standard. However, upon copper and NBR exposure to biodiesel under typical immersion investigations, independently, the TAN increased to 3.40 and 2.35 mg KOH/g, respectively. These significant increases indicate that under typical immersion conditions, the biodiesel has been degraded due to copper and NBR exposure. The degradation of biodiesel could be attributed to the oxidation of its unsaturated components in the presence of metal surface leading to the formation of acids, ketones, aldehydes [210]. In contrast, for the biodiesel sample exposed to copper and NBR under independent modified immersion investigations, the TAN remained close to its initial value of 0.28 mg KOH/g.

In terms of the water content, 12.5 and 8.5 times higher water content were measured for the biodiesel samples exposed to copper and NBR, respectively, after typical immersion investigations as compared to the initial values. This increase proved the hygroscopic nature of biodiesel which is capable of absorbing moisture from the atmosphere. Conversely, the water content of the biodiesel

sample exposed to copper and NBR under independent modified immersion conditions remained close to its initial value of 0.02%.

As for the conductivity, 22 and 17 times higher conductivity values were determined for the biodiesel samples exposed to copper and NBR after typical immersion condition, respectively, as compared to the initial values. By referring to Chapter 3 section 3.3.3, the presence of biodiesel oxidation products such as aldehydes, ketones, carboxylic acid and short-chain acid results in significant rise in biodiesel conductivity. Hence, the biodiesel samples here are suggested to have oxidized. Contrastingly, 4 and 2 times higher conductivity values were found for biodiesel samples exposed to copper and NBR under modified immersion, respectively, as compared to the initial conductivity values.

Based on the above findings, the biodiesel fuels exposed to copper and NBR independently were oxidized under typical immersion investigation. However, the biodiesel fuels exposed to copper and NBR under independent modified immersion investigation were not oxidized.

4.3.2.1.2 Compatibility of FDM with biodiesel under engine operation condition

The biodiesel samples exposed to copper and NBR under typical immersion were oxidized during the conducted investigation. This significantly influenced the high corrosion rate of copper and high degradation level of NBR. On the other hand, the biodiesel samples exposed to copper and NBR under modified immersion were found to be unoxidized. Therefore, significantly low corrosion rate of copper and low degradation of NBR were measured under modified immersion condition.

The obtained outcome of high FDM degradation under oxidized biodiesel agrees with the study by Haseeb et al. [35] which investigated the effects of oxidized and unoxidized biodiesel on copper corrosion. Here, the authors reported 59% higher corrosion rate for copper immersed in oxidized biodiesel than in un-oxidized biodiesel for 840 h of immersion at 60 °C. Besides the formation of oxidized biodiesel, the increase in water content under typical immersion investigation could have also accelerated the corrosion rate. Furthermore, the presence of water particularly at high temperatures can form different types of acids by reacting with esters which are more corrosive in nature [69, 211]. This could have as well increased the level of FDM degradation under typical immersion condition.

To date, the majority of the studies have evaluated the compatibility present between biodiesel and FDM without taking into account the real-life diesel engine operation condition. The manipulations carried out in these studies especially on the immersion temperature, immersion duration, and concentration of biodiesel in biodiesel-diesel fuel blends, despite being informative, could not be used to define the compatibility present between biodiesel and FDM under real-life diesel engine operation. For this reason, through the conducted modified immersion investigation here which was designed to resemble biodiesel deterioration under CRDE operation, the biodiesel's compatibility under physical diesel engine operation has been more thoroughly investigated. Based on the findings obtained, acceptable to good compatibility is found to be present between biodiesel and FDM under real-life diesel engine operation.

Table 4.10 Comparisons of modified and typical immersion investigations on copper and NBR degradation.

			Typical immersion		Modified immersion		Diff. between modified
			Mean	SD	Mean	SD	to typical (%)
Cu	Corrosion rate	(mm/yr)	1.20E-02	1.64E-07	9.29E-04	1.39E-07	-92.25
NBR	Volume change	(%)	39.66	2.42	10.79	0.55	-72.80
	Tensile strength change	(%)	-51.76	0.05	-16.02	0.03	-69.05
	Hardness change	(%)	-13.67	0.52	-2.00	0.50	-85.37

Table 4.11 Comparisons of biodiesel fuels deterioration under typical and modified immersion investigations for copper and NBR degradations.

		Copper corrosion						NBR degradation					
		Typical immersion		DTIV	Modified immersion		DTIV	Typical immersion		DTIV	Modified immersion		DTIV
Properties		Mean	SD	(%)	Mean	SD	(%)	Mean	SD	(%)	Mean	SD	(%)
TAN	(mgKOH/g)	3.40	1.06E-02	1115.62	0.28	5.18E-03	1.34	2.35	9.26E-03	739.29	0.28	1.25E-02	0.45
WC	(%)	0.25	5.18E-03	1131.25	0.02	8.35E-04	0.63	0.17	5.18E-03	768.75	0.02	8.86E-04	1.25
CON	(pS/m)	2800.80	1.03	2100.15	500.77	1.98	293.37	2209.87	1.21	1635.95	290.59	1.13	128.27

CON: conductivity; DTIV: differences to initial value; TAN: total acid number; WC: water content.

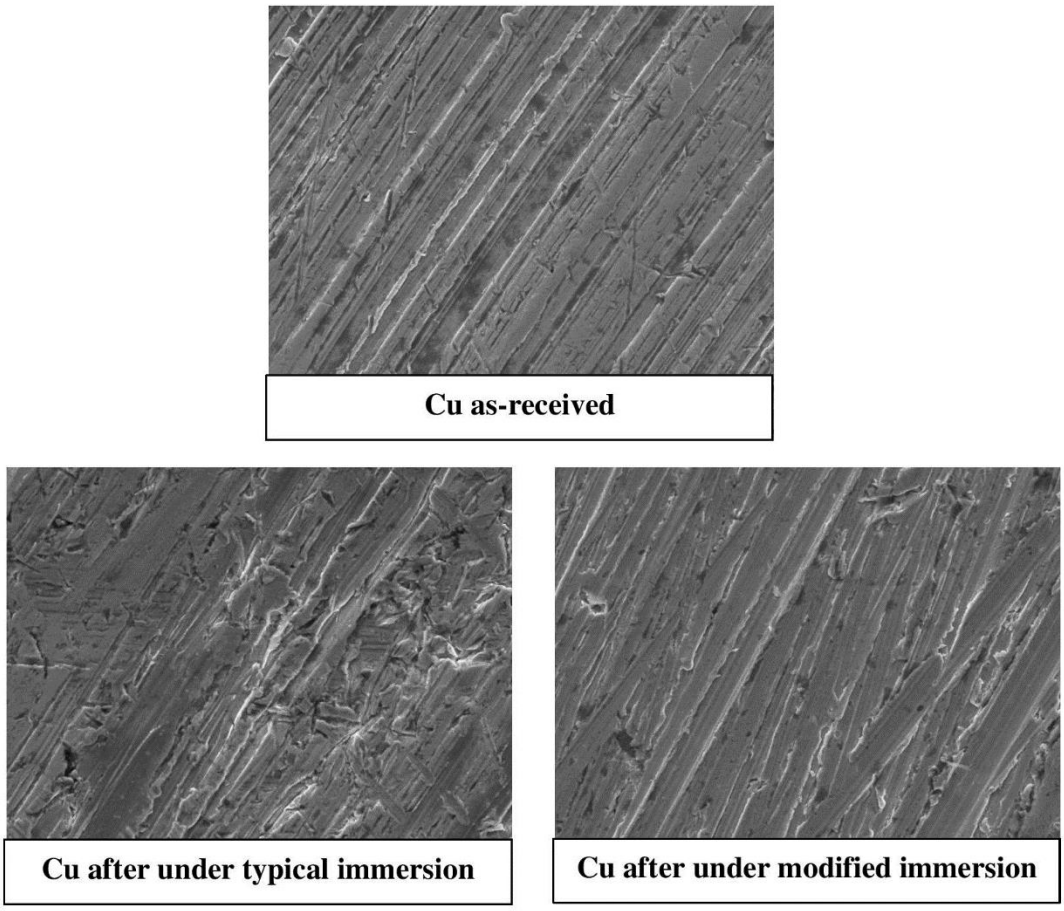

Fig. 4.4 SEM micrographs of copper after under typical and modified immersion investigations.

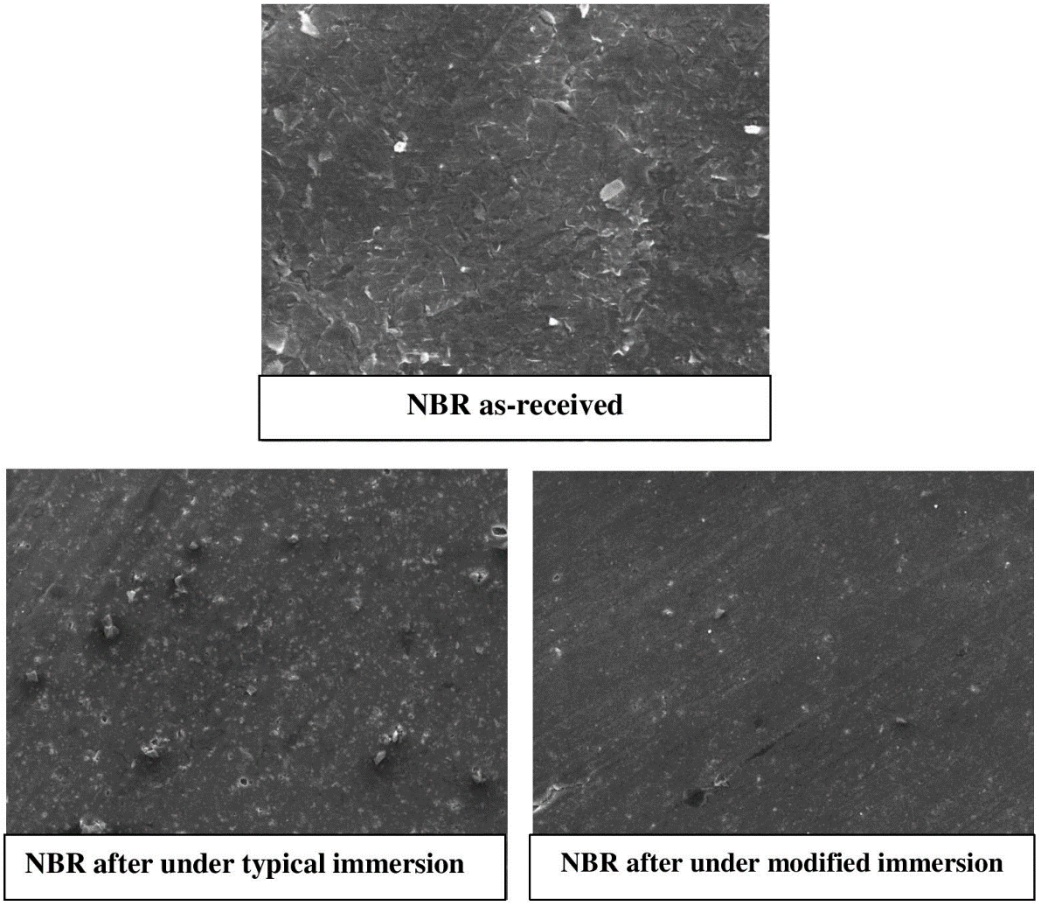

Fig. 4.5 SEM micrographs of NBR after under typical and modified immersion investigations.

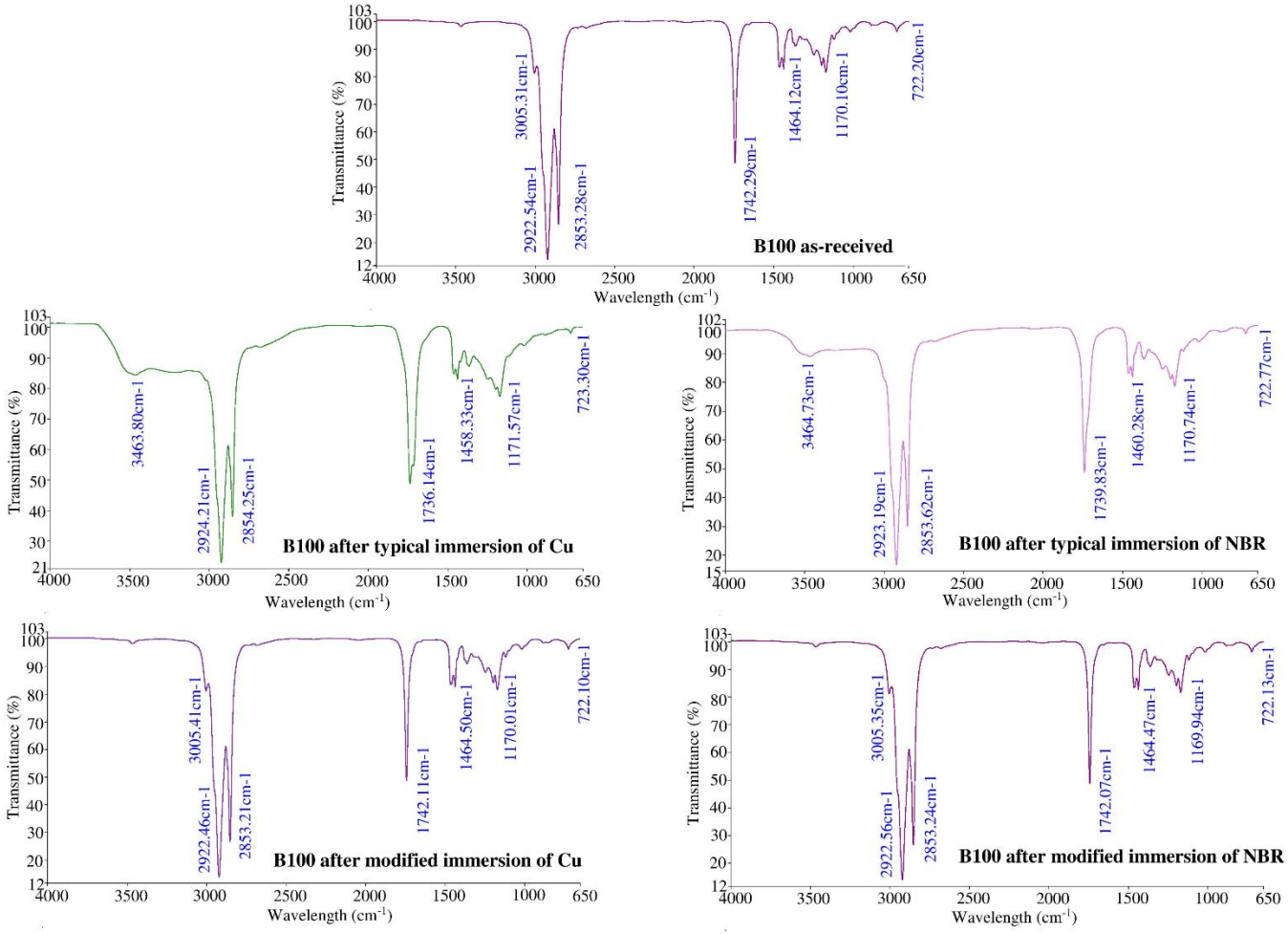

Fig. 4.6 Initial and final biodiesel fuel's FTIR spectrum under typical and modified immersion investigations.

4.3.2.2 Second phase-influence of temperature on the compatibility of FDM with biodiesel under modified immersion

As shown in Table 4.12, the corrosion rate of copper due to the exposure of biodiesel under modified immersion was found to be higher by 62% at 25 °C as compared to at 100 °C. The greater corrosion attack at 25 °C as compared to that at 100 °C was also evident from the obtained SEM micrographs obtained at 2000 times magnification as shown in Fig. 4.7. For the elemental composition analysis as shown in Fig. 4.8 (a), 5.7 and 2.2 times higher oxygen content was found on the copper coupon immersed at 25 and 100 °C, respectively, as compared to the as-received copper coupon. At these two temperatures, the biodiesel has 8 and 0.3 ppm of DO, as well as 126 and 700 pS/m of conductivity value at 25 and 100 °C, respectively. As such, the higher corrosion attack at 25 °C as compared to at 100 °C here is likely attributed to the effects of DO concentration instead of the conductivity value.

In terms of elastomer degradation, as shown in Table 4.12, the degradation of NBR due to biodiesel exposure under modified immersion is found to be higher by 8% and 10% for the volume and tensile strength changes, respectively, at 25 °C as compared to at 100 °C. From the SEM analysis, the NBR sample exposed to biodiesel at 25 °C changed significantly as pits are clearly visible on the surface as shown in Fig. 4.9. Meanwhile, the sample exposed to biodiesel at 100 °C did not undergo any significant change as compared to the as-received sample. For the elemental composition analysis as shown in Fig. 4.8 (b), 20% and 14% higher

oxygen content was found on the NBR sample immersed at 25 and 100 °C, respectively, as compared to the as-received sample. The outcome here of higher NBR degradation at 25 °C as compared to at 100 °C supports the adverse effect of biodiesel's DO concentration on NBR degradation.

4.3.2.2.1 Effects of immersion temperature on FDM degradation upon biodiesel exposure

The higher FDM degradation due to biodiesel exposure under modified immersion at 25 °C as compared to 100 °C was suggested to have occurred due to the greater DO concentration in biodiesel at 25 °C as compared to 100 °C. This outcome and suggestion however contradicts several existing studies. For example, Haseeb et al. [97] reported 6 times higher NBR degradation exposed to biodiesel in the form of volume change at 100 °C as compared to room temperature (~ 25 °C) for 500 h of immersion. In a different study, Haseeb et al. [35] reported higher copper corrosion rate by 37% at 60 °C as compared to room temperature (~ 25 °C) exposed to palm biodiesel for 2840 h. The authors suggested that the condensation or dissolution of oxygen from the atmosphere into the fuel is higher at 60 °C as compared to room temperature. By referring to Chapter 3 section 3.3.1.1.6, an inverse correlation is present between biodiesel temperature and the DO concentration in biodiesel determined by measuring the concentration of DO in biodiesel with respect to biodiesel temperature. This agrees with the outcome obtained from the present study which is essential in establishing the compatibility present between biodiesel and FDM at low fuel

temperature especially at fuel storage condition of 20-25 °C. Since the DO concentration has been suggested as the factor influencing the outcome above, emphasis should be placed towards reducing the DO concentration in biodiesel in mitigating the effects of biodiesel exposure on FDM degradation during fuel storage.

Table 4.12 Comparisons of fuel temperature effects on copper and NBR degradation under modified immersion investigations.

			25 °C		100 °C		Differences between 25 °C to 100 °C (%)
			Mean	**SD**	**Mean**	**SD**	
Cu	Corrosion rate	(mm/yr)	1.51E-3	6.19E-08	9.29E-4	1.39E-07	+62.09
NBR	Volume change	(%)	11.66	0.50	10.79	0.55	+8.06
	Tensile strength change	(%)	-17.56	0.03	-16.02	0.03	+9.61

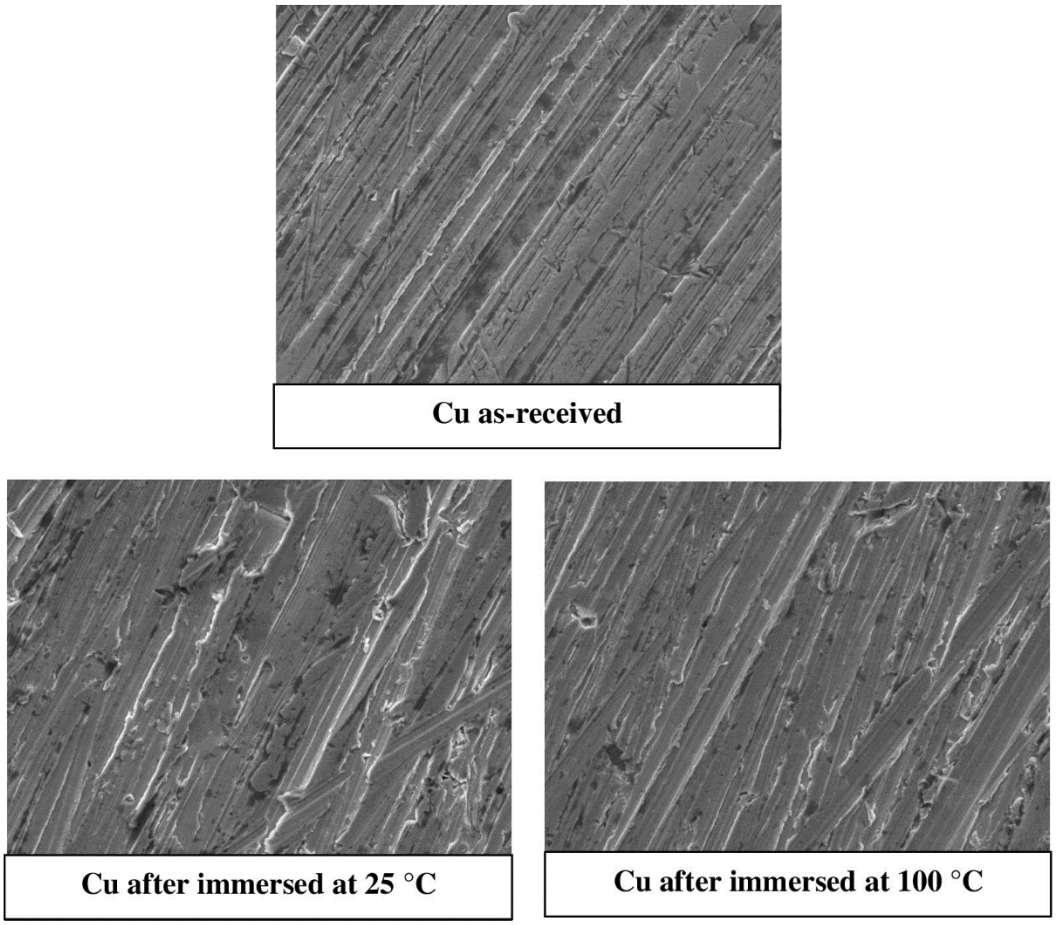

Fig. 4.7 SEM micrographs of copper after under modified immersion at 25 and 100 °C.

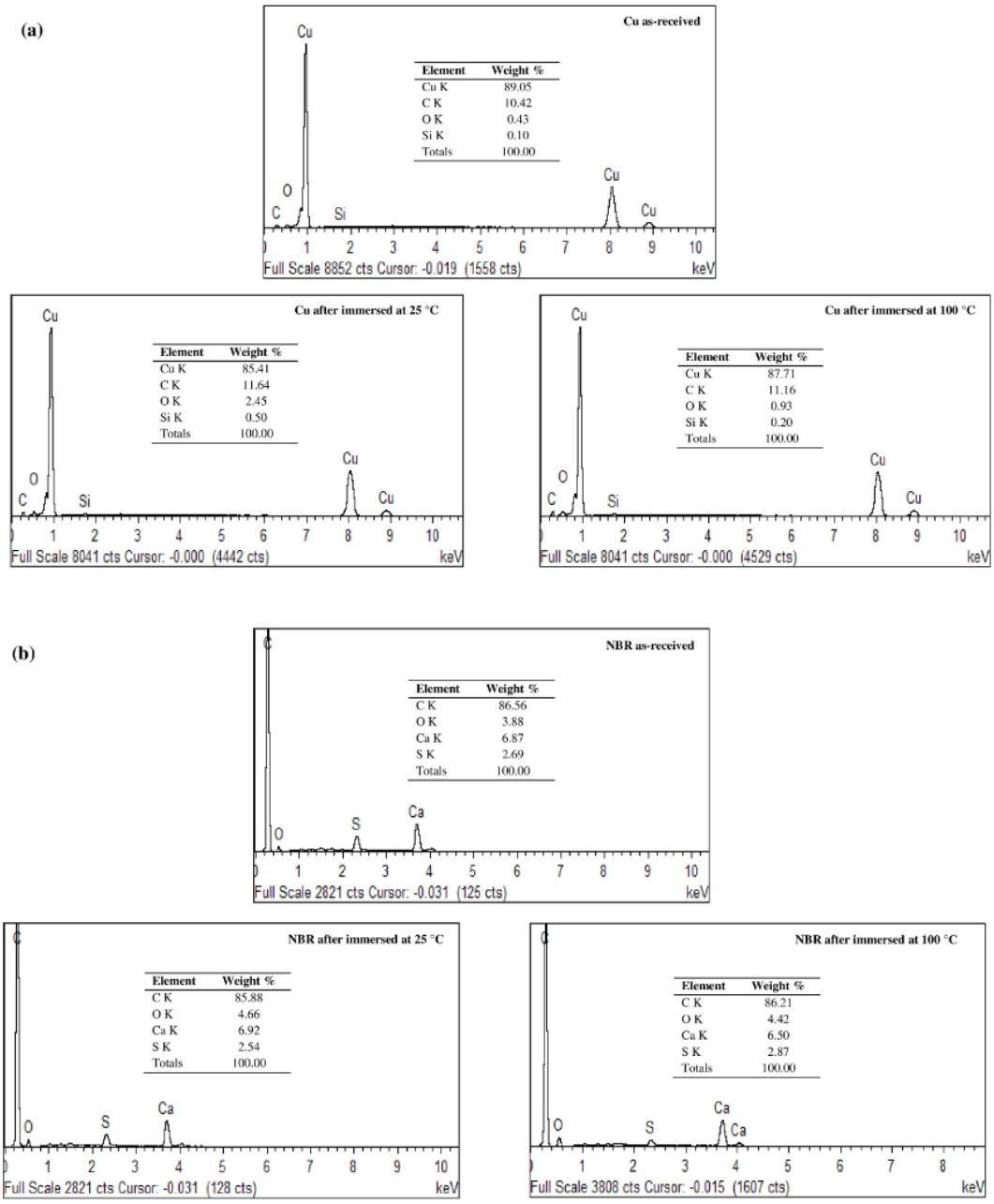

Fig. 4.8 Elemental composition of (a) copper and (b) NBR after under modified immersion at 25 and 100 °C.

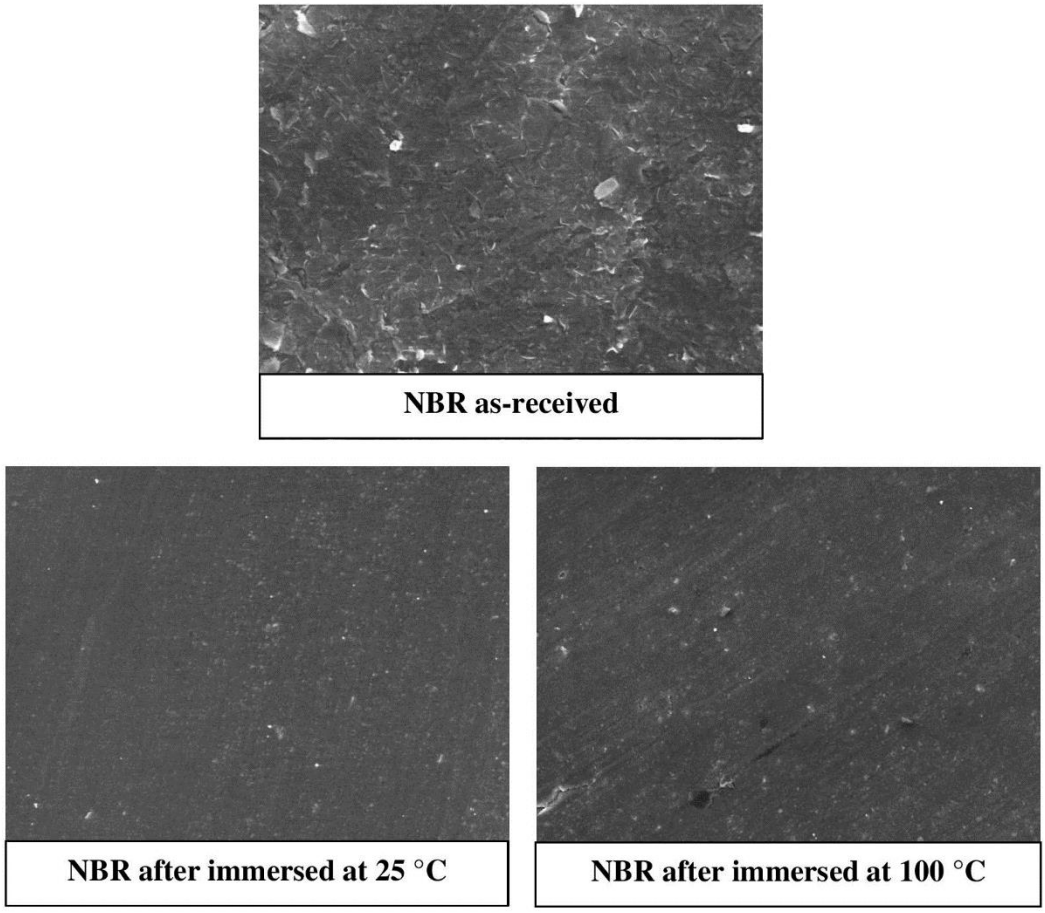

Fig. 4.9 SEM micrographs of NBR after under modified immersion at 25 and 100 °C.

4.3.2.3 Third phase-influence of immersion duration on the compatibility of FDM with biodiesel under modified immersion

As shown in Fig. 4.10 (a), the copper's corrosion rate was found to reduce with increasing immersion duration due to the exposure of biodiesel under modified immersion. The corrosion rate reduced by 3% after 540 h of immersion duration as compared to 108 h of immersion duration. The surface of the evaluated specimens also agreed with the trend above as it showed improvement with increasing immersion duration as shown in Fig. 4.11.

For the elastomer degradation, the NBR degradation in terms of volume and tensile strength changes were found to have increased with increasing immersion duration due to the exposure of biodiesel under the modified immersion as shown in Fig. 4.10 (b) and Fig. 4.10 (c). The volume and tensile strength changes increased by 48% and 12%, respectively, after 960 h of immersion duration as compared to 192 h of immersion duration. The trend above was also supported by the SEM analysis which showed greater NBR degradation with increasing immersion duration at 500 times magnifications as shown in Fig. 4.12. Although the NBR degradation increased with increasing immersion duration, the rate of NBR's volume and tensile strength changes actually reduced with increasing immersion duration by 70% and 77%, respectively, after 960 h of immersion duration as compared to 192 h of immersion duration.

4.3.2.3.1 Effects of immersion duration on FDM degradation upon biodiesel exposure

The reduced rate of FDM degradation due to biodiesel exposure with respect to immersion duration concurs with several existing studies. Fazal et al. [117] reported a reduced rate of copper corrosion by 19% due to the exposure of biodiesel after 2880 h of immersion duration as compared to 1200 h of immersion duration. In another study, Haseeb et al. [97] reported a reduced rate of NBR's volume change by 25% after 500 h of immersion duration as compared to 250 h of immersion duration due to the exposure of palm biodiesel at 26 °C. These findings demonstrate that the materials degradation due to biodiesel exposure becomes less severe after longer immersion time.

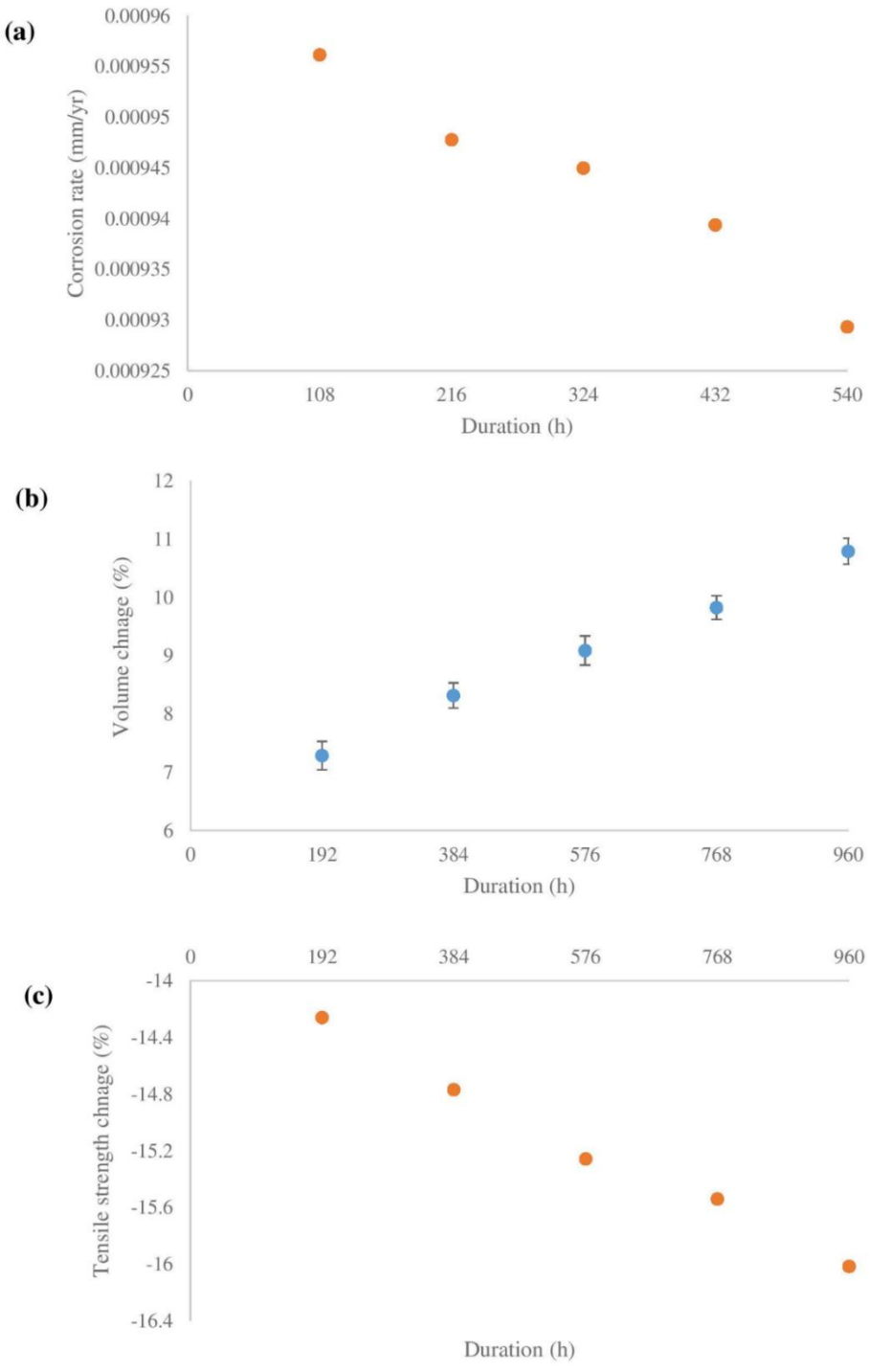

Fig. 4.10 Changes of (a) copper's corrosion rate, (b) NBR's volume change and (c) NBR's tensile strength change corresponding to the modified immersion investigations' duration.

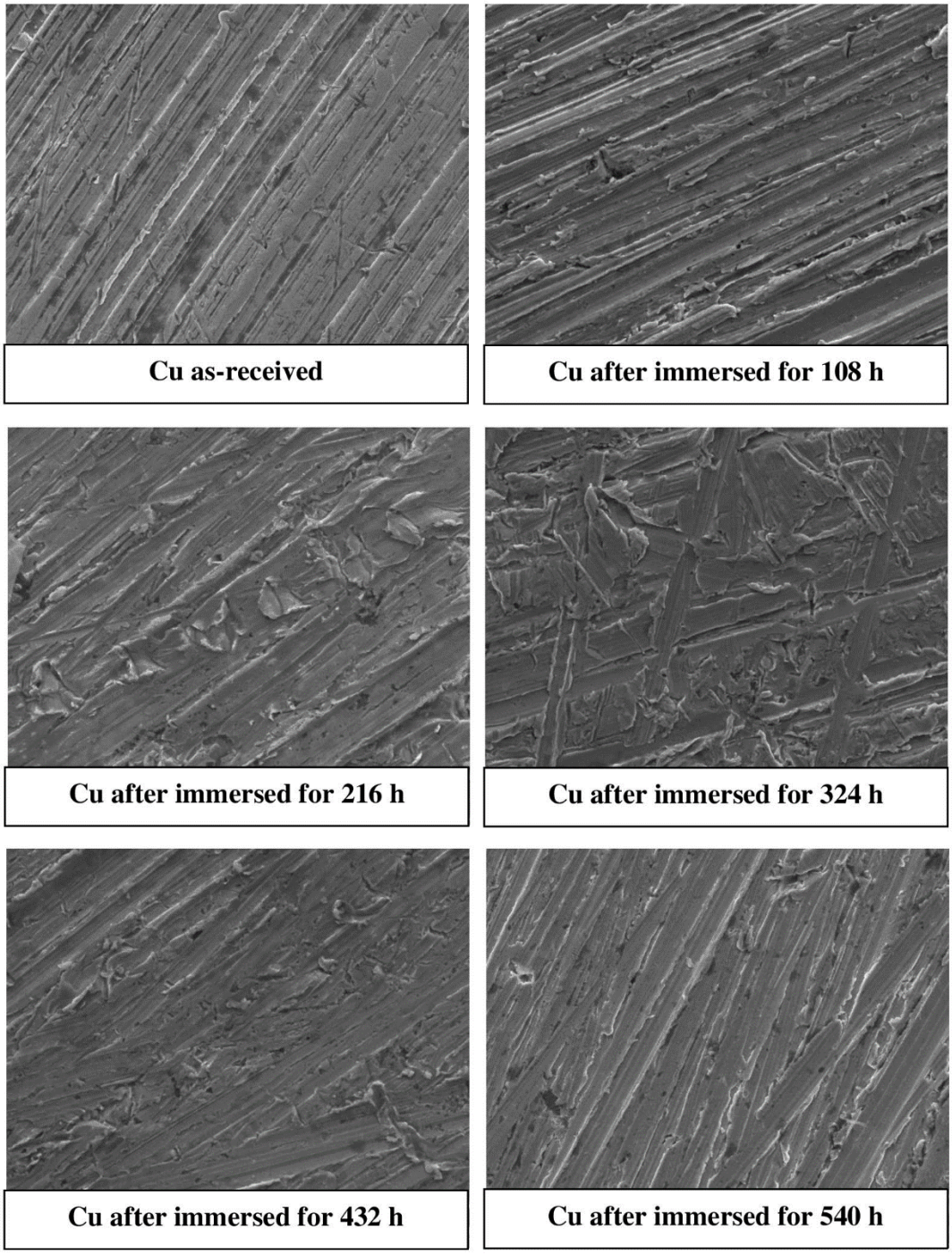

Fig. 4.11 SEM micrographs of copper corresponding to the modified immersion investigations' duration.

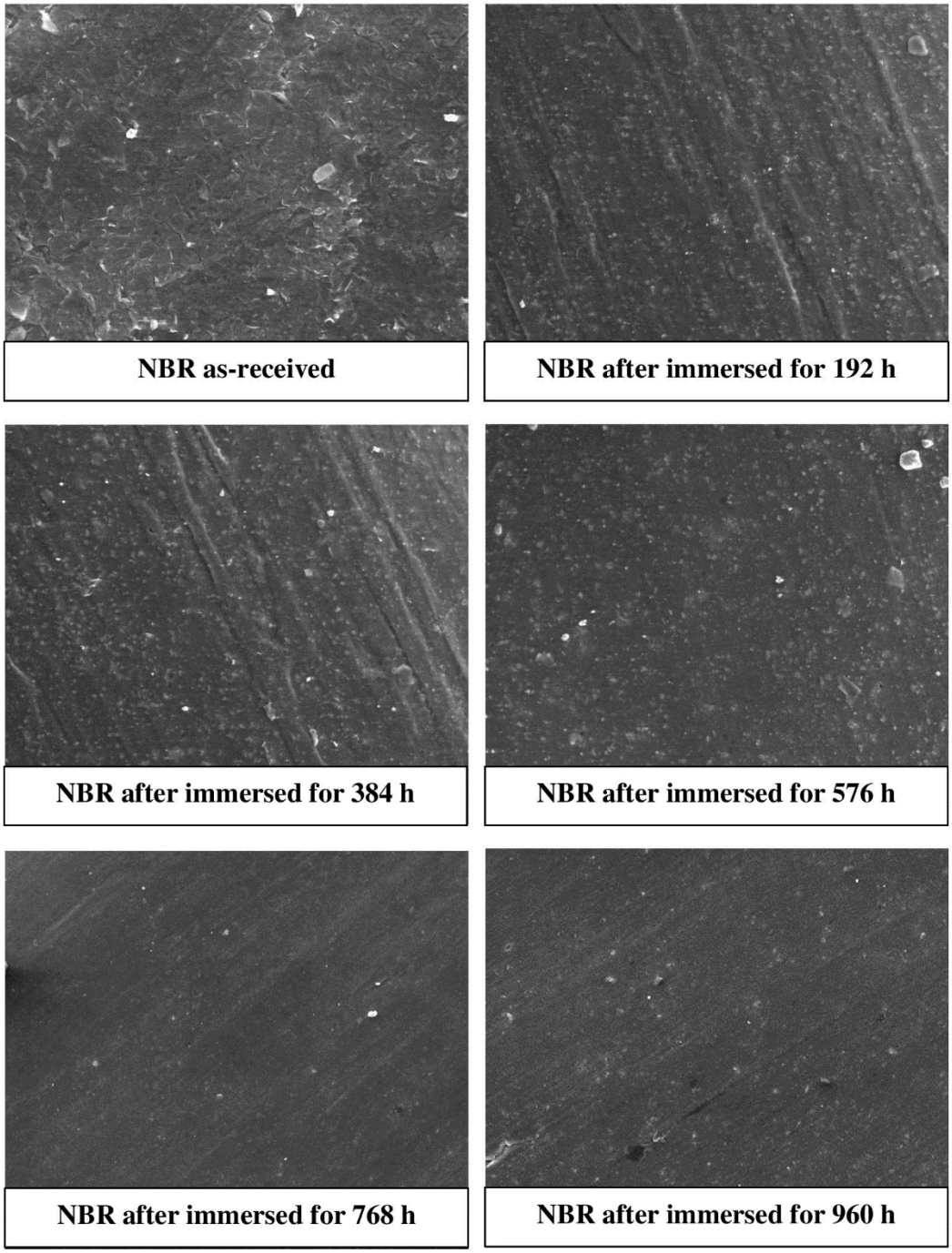

Fig. 4.12 SEM micrographs of NBR corresponding to the modified immersion investigations' duration.

4.3.2.4 Fourth phase-influence of biodiesel concentration in biodiesel-diesel fuel blends on the compatibility of FDM with biodiesel under modified immersion

As shown in Fig. 4.13 (a), the corrosion rate of copper coupons exposed to B0, B10, B20, B50 and B100 were found to have increased with an increasing concentration of biodiesel in biodiesel-diesel fuel blends under modified immersion. The corrosion rate was found higher by 10% due to the exposure of B100 as compared to B0. The increase in corrosion attack with increasing concentration of biodiesel in biodiesel-diesel fuel blends was also evident from the surface morphology of the evaluated copper coupons at 2000 times magnification as shown in Fig. 4.14.

For the elastomer degradation, as shown in Fig. 4.13 (b) and Fig. 4.13 (c), the NBR degradation in terms of both volume and tensile strength changes were found to have increased with increasing concentration of biodiesel in biodiesel-diesel fuel blends under modified immersion. A higher volume and tensile strength change by 34% and 33%, respectively, were found due to the exposure of B100 as compared to B0. This trend of increasing degradation corresponding to increasing concentration of biodiesel in biodiesel-diesel fuel blends was also evident from the surface morphology analysis conducted on the evaluated specimens at 500 times magnification as shown in Fig. 4.15.

4.3.2.4.1 Effects of biodiesel concentration in biodiesel-diesel fuel blends on FDM degradation

Although the increased copper corrosion and elastomer degradation corresponding to the increased concentration of biodiesel in biodiesel-diesel fuel blends agrees well with existing studies [35, 71, 72, 85, 107, 146], the determined maximum difference in the degradation level due to exposure of B0 and B100 differs significantly. A maximum difference of 163% [35, 71, 72, 85, 107, 146] and 500% [100, 101] of metal corrosion and elastomer degradation, respectively, were determined due to the exposure of B0 as compared to B100 from the existing studies while, only a maximum difference of 10% and 34% of metal corrosion and elastomer degradation, respectively, were determined in the present study. The significant difference is suggested to have occurred due to the experimental condition of incorporating fuel renewal in the immersion investigation designed to simulate diesel engine operating conditions. This demonstrates that the increase in biodiesel concentration in biodiesel-diesel fuel blends does not produce such severe effects on FDM as per reported in the literatures. Therefore, the prohibition placed on the use of biodiesel concentration beyond B20 should be re-assessed.

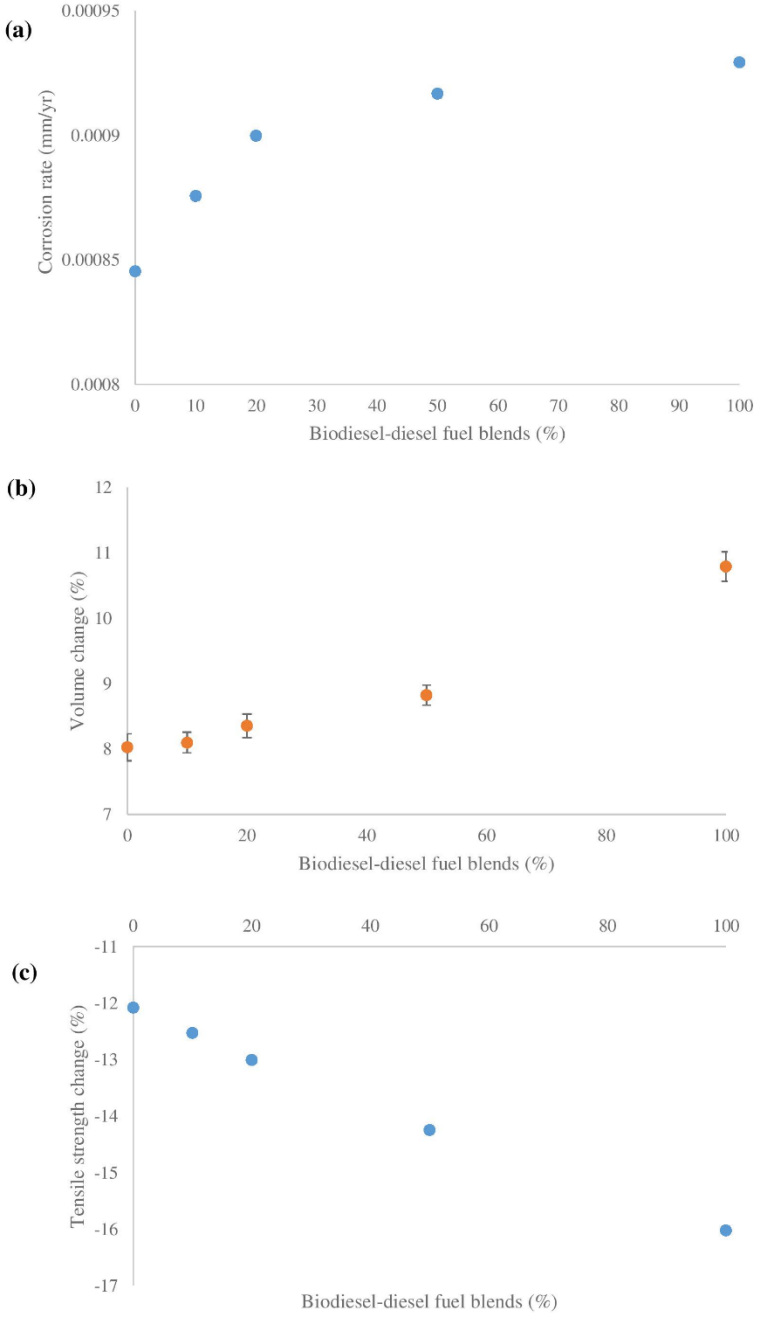

Fig. 4.13 Changes of (a) copper's corrosion rate, (b) NBR's volume change and (c) NBR's tensile strength change corresponding to the concentrations of biodiesel-diesel fuel blends under modified immersion investigations.

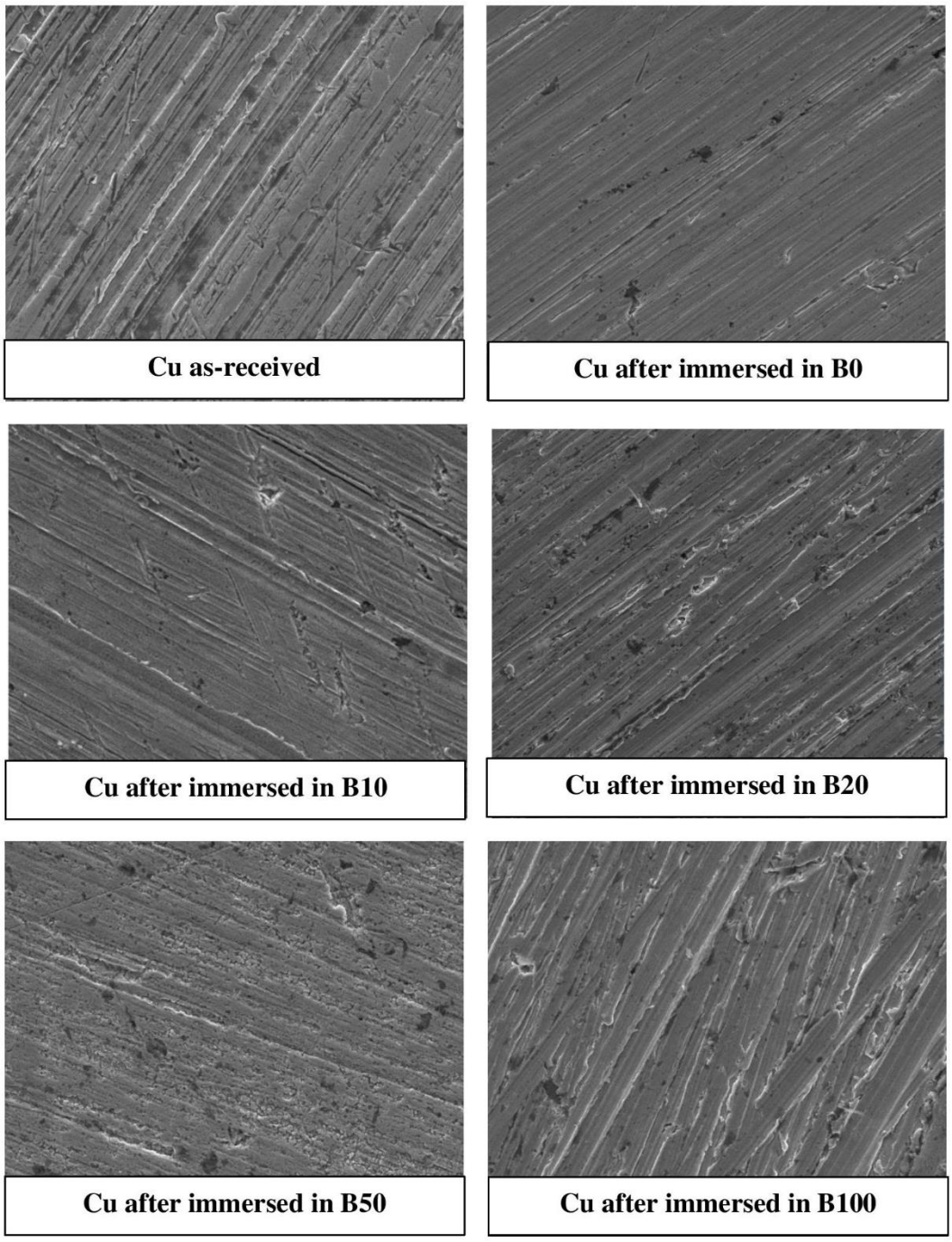

Fig. 4.14 SEM micrographs of copper after exposed to B0, B10, B20, B50 and B100 under modified immersion investigations.

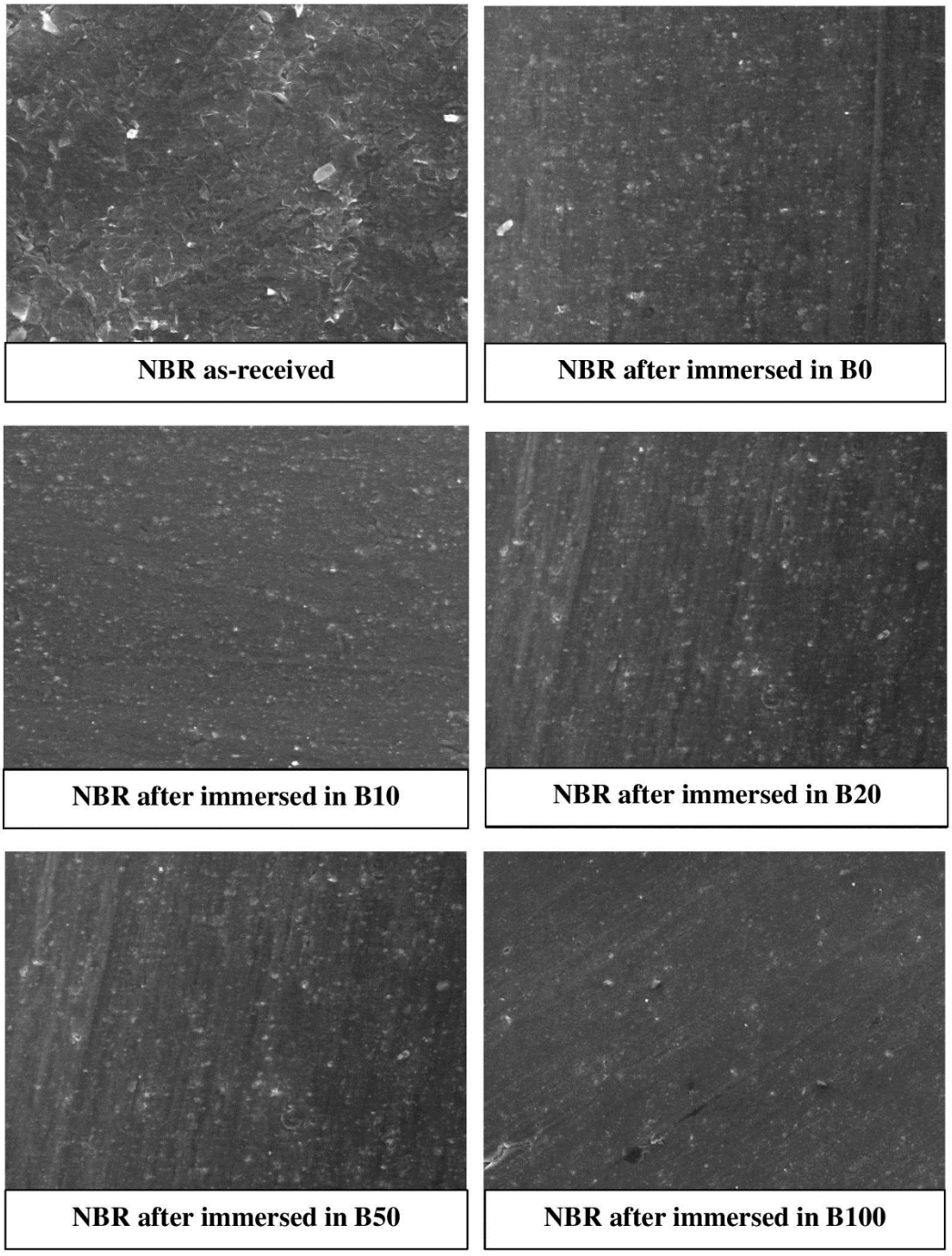

Fig. 4.15 SEM micrographs of NBR after exposed to B0, B10, B20, B50 and B100 under modified immersion investigations.

4.3.2.5 Fifth phase-degradation of different FDM due to biodiesel exposure under modified immersion

As shown in Fig. 4.16 (a), the corrosion rate of copper is the highest followed by galvanized steel, aluminium, and finally stainless steel (copper > galvanized steel > aluminium > stainless steel) due to the biodiesel exposure under modified immersion. Comparing to copper, 33%, 74% and 80% lower corrosion rates were determined for galvanized steel, aluminium and stainless steel, respectively. Referring to Fig. 4.17, the surface morphology of the as-received metal coupons are clearly visible for all 4 metals at 2000 times magnification. Upon 540 h of exposure, the surface morphology of aluminium and stainless steel did not undergo any significant changes. However, the copper coupon has undergone changes as explained earlier in section 4.3.2.1 while peeling has taken place for the galvanized steel coupon. Thus, copper is subjected to the highest corrosion attack, followed by galvanized steel, aluminium and stainless steel.

For the elastomer degradation, as shown in Fig. 4.16 (b) and Fig. 4.16 (c), it is observed that NBR underwent the greatest change in terms of both volume and tensile strength, respectively, followed by silicone rubber, FKM and nylon (NBR > silicone rubber > FKM > nylon) due to the exposure of biodiesel under modified immersion investigations. Comparing to NBR, 26%, 78% and 106% lower volume changes were determined for silicone rubber, FKM and nylon, respectively. In addition, 28%, 82% and 94% lower tensile strength changes were determined for silicone rubber, FKM and nylon, respectively, as compared to

NBR. Fig. 4.18 shows the comparative SEM micrographs of NBR, nylon, FKM and silicone rubber prior and after the immersion investigation. Based on the SEM micrographs as well as the changes in terms of both volume and tensile strength, it is evident that NBR has undergone the most significant degradation followed by silicone rubber, FKM and nylon.

4.3.2.5.1 Compatibility of different FDM with biodiesel

The trend of highest corrosion attack for copper followed by galvanized steel, aluminium and stainless steel corroborates the findings of several existing studies [71, 119, 139, 140]. This trend could be attributed to the higher reactivity of copper with biodiesel in comparison to the other metals. The metal arrangement in galvanic series which shows that copper is the least noble metal followed by galvanized steel, aluminium and finally stainless steel supports the observed correlation.

For elastomers, the trend of highest degradation for NBR followed by silicone rubber, FKM and nylon agrees with several existing studies [97, 100, 101]. This trend can be explained based on the differences in polarity between the elastomer and fuel as per suggested by Hu et al. [100]. The authors suggested that there is a correlation between the polarity difference of fuel and elastomer towards elastomer swelling. For example, NBR demonstrates weak polarity since –CN polarity group is present in its molecule. Since diesel is non-polar, large polarity

differences between NBR and diesel results in less swelling. In contrast, since biodiesel is weakly polar, the lesser polarity differences between biodiesel and NBR results in high swelling. In terms of FKM, the large polarity differences between biodiesel and FKM results in less swelling.

Hence, close attention should be given towards the adversely affected materials especially during materials selection process for FDS. However, since biodiesel is being adopted for usage in existing diesel engines to date, emphasis should be placed on mitigating the adverse effects of biodiesel exposure on FDM degradation by treating the biodiesel, instead of replacing the materials. As such, recommendations are made to further improve the compatibility present between biodiesel and FDM in section 4.3.3 despite the acceptable to good compatibility which has been determined to be present between biodiesel and FDM under diesel engine operating conditions.

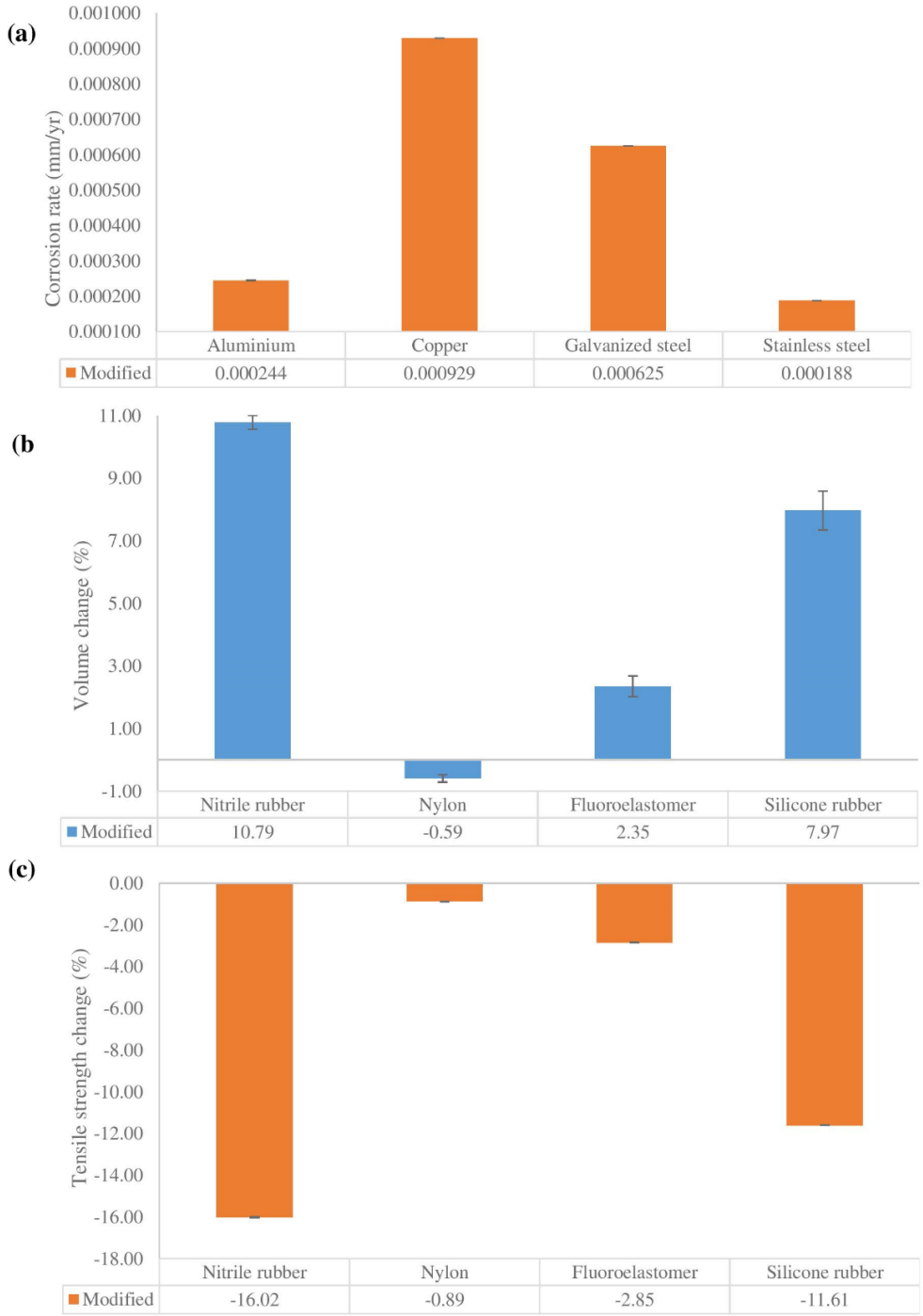

Fig. 4.16 (a) Corrosion rate of metals, (b) volume change of elastomers and (c) tensile strength change of elastomers after under modified immersion investigations.

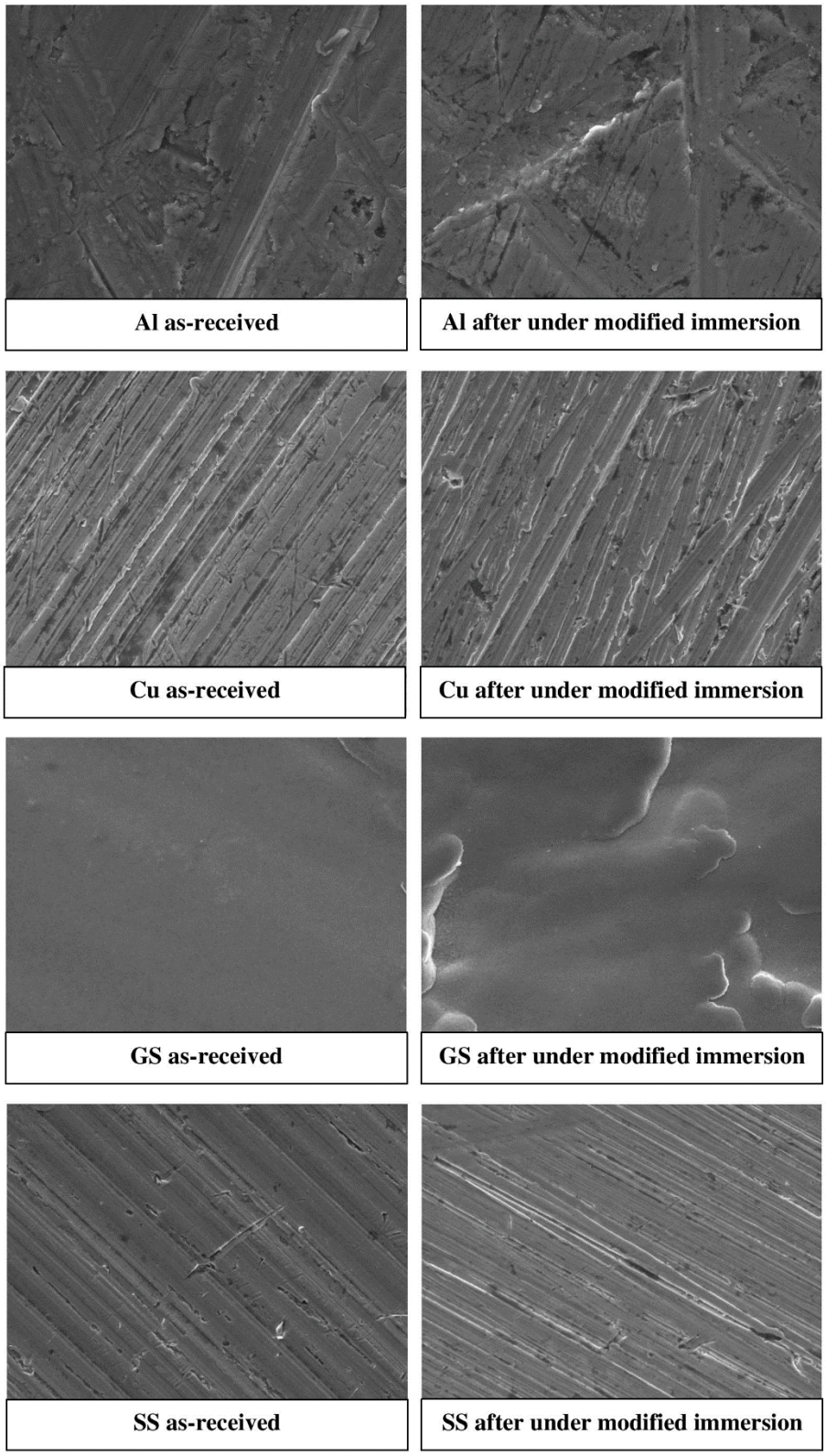

Fig. 4.17 SEM micrographs of metals after under modified immersion.

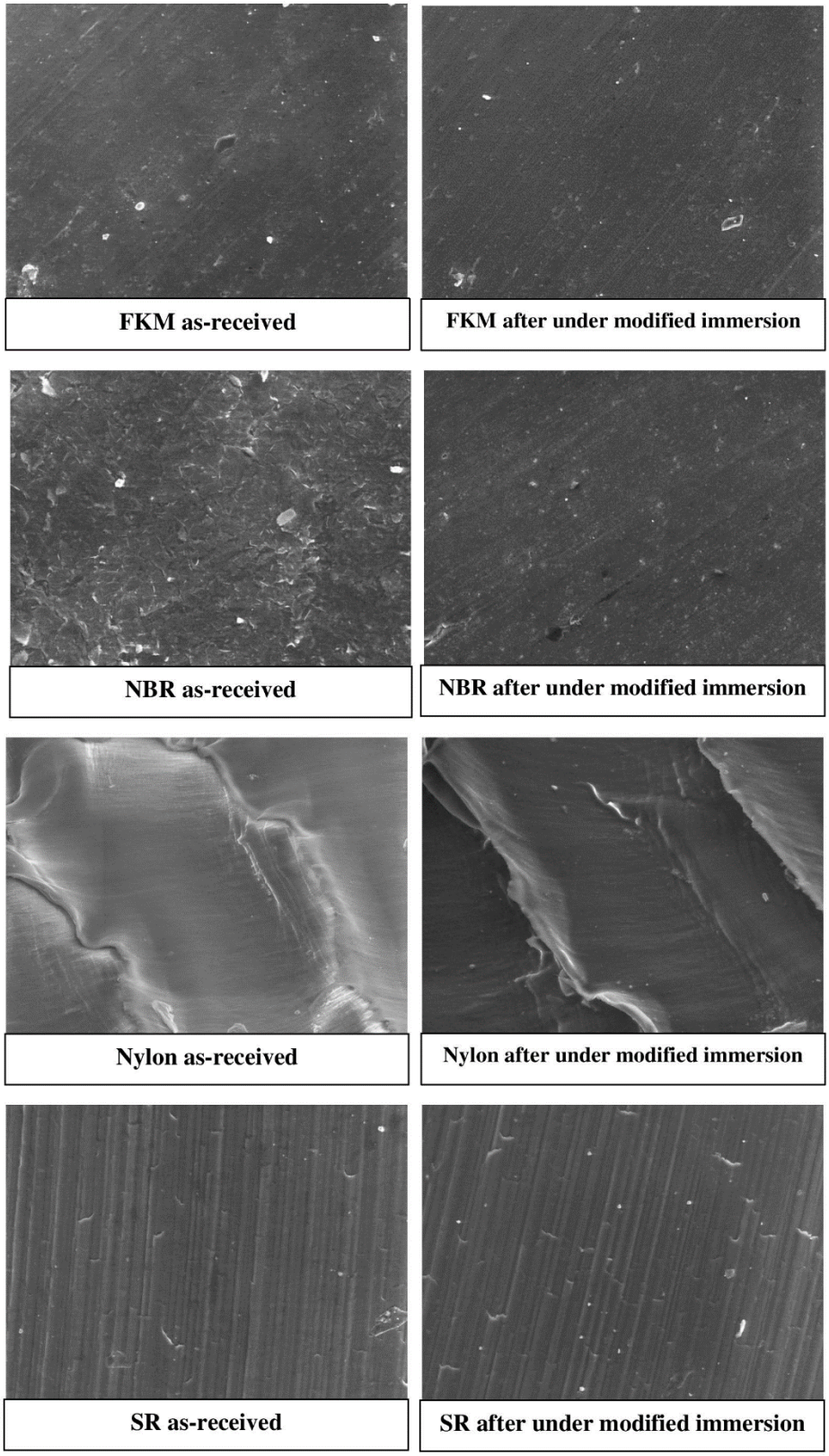

Fig. 4.18 SEM micrographs of elastomers after under modified immersion.

4.3.3 Recommendations for mitigating the effects of biodiesel exposure on FDM degradation

Corresponding to the outcomes obtained, the degradation of FDM due to biodiesel exposure has been classified into three separate regions as shown in Fig. 4.19. The data presented in Fig. 4.19 is reiterated from the results presented in Chapter 3 section 3.3.3. Based on it, in region 1 which is at the typical fuel storage temperature of 25 °C and below, the oxidation process is heavily influenced by the presence of DO in the biodiesel. On the other hand, in region 3 which is at the typical fuel engine-operating temperature of 100 °C and above, the oxidation process is heavily influenced by the biodiesel's conductivity value. In region 2 which lies between the fuel temperatures of 25 and 100 °C, the oxidation process is influenced by both the conductivity value and DO concentration.

Hence, the adverse effects of biodiesel on FDM should always be viewed from the perspectives of these three regions. This is suggested by taking into account all three biodiesel, metal and elastomer oxidation together. Since the degradation of FDM due to exposure of biodiesel is majorly and partially influenced by the DO concentration in region 1 and region 2, respectively, eliminating the DO in biodiesel by heating followed with nitrogen blanketing prior to storing the fuel after production could curb the problem at these regions. As for the partial and major adverse effects of biodiesel conductivity's on FDM degradation in region 2 and region 3, respectively, its effects were found to be minimal. Furthermore, by ensuring that no contaminants such as trace metals and catalyst residues are

present as well as by the addition of additives, the conductivity value could be reduced leading to a reduction in FDM degradation.

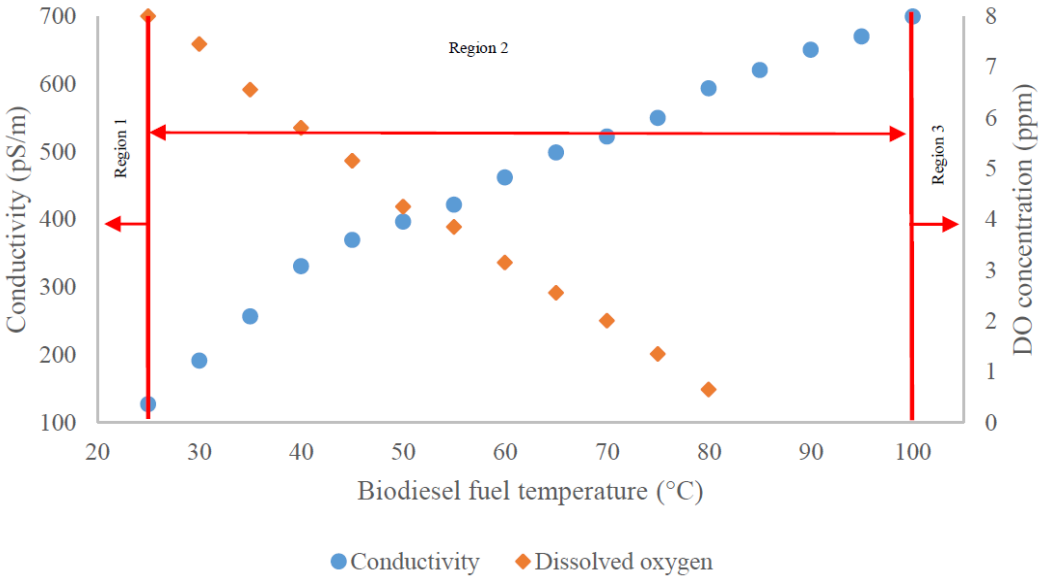

Fig. 4.19 Changes of biodiesel fuel's conductivity value and dissolved oxygen concentration corresponding to fuel temperature.

4.4 Summary

Based on the first-stage investigations, both the biodiesel's DO and conductivity properties were found to adversely affect FDM degradation independently. Hence, the compatibility of FDM with biodiesel under CRDE operation were subsequently investigated under modified immersion through five phases of investigations in the second stage. Based on the results obtained, acceptable to good compatibility is found to be present between FDM and biodiesel under a real-life CRDE operation. The reason for this lies in the observed trend of lower FDM degradation due to biodiesel exposure under modified immersion which was designed to replicate the biodiesel deterioration under CRDE operation. Finally, recommendations are made to further improve the compatibility present between biodiesel and FDM under 3 separate regions according to the fuel temperature.

CHAPTER 5-CONCLUSIONS AND RECOMMENDATIONS FOR FURTHER WORK

The present study aimed to assess the actual compatibility present between FDM and biodiesel in the FDS under real-life CRDE operation in an effort to determine whether the current use of biodiesel to power diesel engine could be further expanded beyond B20. The main findings of the present study are firstly presented followed by recommendations for further work.

5.1 Conclusions

An evaluation of the existing studies indicated that they are inadequate to comprehensively appraise the actual compatibility present between biodiesel and FDM under real-life diesel engine operation. This is because the standard methods employed in determining the compatibility present between biodiesel and FDM do not replicate the conditions of a typical diesel engine such as the varying fuel pressure/temperature and the presence of various materials in the FDS. Furthermore, there is also a lack of investigation on the actual elastomers elemental composition fitted in diesel engine although the elastomers' resistance towards fuel attack is highly dependent on it. For this reason, a multi-faceted experimental work was chiefly carried out here to elucidate the compatibility present between FDM and biodiesel in the FDS of a real-life CRDE. The outcomes are divided into 2 distinct parts as described below:

Part 1-Deterioration of palm biodiesel under CRDE operation.

- After running under WHSC, CEC F-98-08 and in-house developed SLTCs' independently, the palm biodiesel samples were not oxidized while its TAN and water content were unchanged since they were within a maximum of 0.446% and 0.625% of their initial values, respectively. The obtained outcomes suggests the elimination of the concerns placed on the influence of formed oxidation products, increase in TAN and water content as a consequence of CRDE operation towards FDM degradation. On the other hand, the biodiesel's DO concentration and conductivity value were not only found to have changed during and after engine operation by -93% and 293%, respectively, but were also found to have influenced the biodiesel deterioration under engine operation.

- The trends of fuel deterioration of B100 under common rail type diesel engine and B20 under unit pump type diesel engine in terms of OS, fatty acid composition and dissolved metals concentration were found to be similar. This shows that the trend of biodiesel deterioration as a consequence of diesel engine operation is similar irrespective of neat or blended form with diesel as well as under different types of fuel injection system.

- For two palm biodiesel fuels (Vance Bioenergy and Carotech) with different physical properties operated under CRDE by utilizing CEC F-98-

08 SLTC, the changes in terms of biodiesel oxidation condition, TAN and water content were similar, but the rate of change for OS, dissolved metals concentration, conductivity value, hydrogen ion concentration and C18:3 fatty acid were different by 178%, 31-68%, 142%, 82% and 99%, respectively. These differences were suggested to have been influenced by the fuel's initial conductivity value in which higher initial conductivity value resulted in a greater rate of change. It was observed that the fuel from Vance Bioenergy had 57% higher initial conductivity value as compared to the fuel from Carotech.

- Palm biodiesel samples collected after 5 days of operation with 1 full tank per day were found to have higher OS by 6% as compared to the samples collected after 1 full tank operation under CEC F-98-08 SLTC. The lower dissolved metals concentration in the former sample as compared to the latter sample by 118%, 150%, 140% and 150% for aluminium, iron, zinc and copper, respectively, mainly due to its higher remaining fuel quantity at the end of the test are suggested to have influenced this outcome. The biodiesel was not oxidized while both the TAN and water content were unaffected since they were within 0.446% and 0.625% to their initial values despite 5 days of CRDE operation.

- The TAN and water content of palm biodiesel were found to have increased by 400% and 826%, respectively, under metal immersion investigation while both properties remained close to their initial values by within 0.446% and 0.625%, respectively, after under CRDE operation. Taking into account the adverse effects of TAN and water content towards FDM degradation, the creditability of immersion studies in exhibiting the actual compatibility between biodiesel and FDM is questioned. As such, a more appropriate method which takes into account biodiesel deterioration consequent to diesel engine operation is suggested here for evaluating the actual compatibility of FDM with biodiesel in the FDS of a real-life diesel engine.

- Corresponding to the correlation of biodiesel's conductivity value to the parameters which cause fuel deterioration under CRDE operation such as fuel temperature, dissolved metal, oxidation state of biodiesel and heating duration, the conductivity property was found as a feasible indicator of biodiesel deterioration under engine operation.

Part 2-Compatibility of fuel delivery metals and elastomers with palm biodiesel.

- Both palm biodiesel's conductivity value and DO concentration were found to adversely affect copper corrosion and NBR degradation independently. For a 22% increase in conductivity value, the copper

corrosion rate and NBR volume change increased by 9% and 13%, respectively. Conversely, for a 96% reduction in the DO concentration, the copper corrosion rate and NBR volume swelling reduced by 91% and 27%, respectively. Since these properties were affected under CRDE operation, the findings stressed the importance of determining the compatibility between biodiesel and FDM under real-life diesel engine operation.

- Copper corrosion and NBR volume change were found to be lowered by up to 92% and 73%, respectively, under modified immersion which resembles typical diesel engine operation as compared to typical immersion condition. This shows that acceptable to good compatibility is present between FDM and biodiesel under engine operating condition. The oxidation of biodiesel under typical immersion as compared to the modified immersion during the investigation has significantly influenced the degradation level of FDM.

- For the effects of immersion temperature under modified immersion, the copper corrosion and NBR volume change underwent higher degradation by 62% and 8%, respectively, due to exposure at 25 °C as compared to 100 °C. The higher concentration of DO in biodiesel at 25 °C than at 100 °C was suggested as a cause for this result. These findings are indicative that higher FDM degradation is expected during fuel storage than

conditions under typical engine operation due to biodiesel exposure. As such, emphasis should be placed towards mitigating the adverse effects of biodiesel towards FDM under fuel storage condition especially by reducing or eliminating the DO present in biodiesel.

- Under modified immersion, the rate of copper corrosion and NBR volume change reduced by 3% and 70% between 108 to 540 and 192 to 960 h of immersion duration, respectively, due to biodiesel exposure. Based on this, the materials degradation due to biodiesel exposure becomes less severe after longer exposure duration.

- The degradation level of FDM with increasing biodiesel concentration was found to be incremental and not significant under modified immersion investigation, contrary to the findings reported in literature. Between B0 and B100, a maximum increase of copper corrosion and NBR degradation by 10% and 34%, respectively, was determined under modified immersion, as compared to 163% and 500%, respectively, as reported in literature.

- The highest corrosion rate of copper followed by galvanized steel, aluminium and stainless steel, as well as the greatest elastomer degradation of NBR followed by silicone rubber, FKM and nylon due to biodiesel exposure, agrees with the findings reported in literature.

As outlined above, fundamental understanding of the actual compatibility of biodiesel with FDM in the FDS of a real-life CRDE was obtained. With regard to this, good compatibility is found to be present between metal and biodiesel under typical diesel engine operation since only a maximum lifespan reduction of 1.5 years is predicted for these metals exposed to biodiesel as compared to diesel for a typical component lifespan of 15 years. For the elastomers, acceptable compatibility is found based on the 11% volume change determined under typical diesel engine operation which conforms to the tolerance level of elastomer degradation as stated by the elastomer manufacturers. These findings firmly contradicts the existing findings. As such, the original knowledge derived from the present study is not only expected to aid in the adoption of higher concentration biodiesel-diesel fuel blend beyond B20 to power diesel engine, but also strongly suggests re-assessment of the prohibition placed on the use of biodiesel greater than 20 vol% in diesel to power diesel engine.

5.2 Recommendations for further work

In the process of progressing from the present nationwide B7 implementation in Malaysia to a much higher biodiesel-diesel fuel blend concentration, future investigations are suggested as described below.

Firstly, the deterioration of biodiesel operated under newer generation CRDE especially those equipped with much higher fuel injection pressure of up to 2000 bar can be investigated. This would assess the range of applicability of the results obtained in the present study to include more extreme diesel engine operation conditions.

Secondly, the impacts of biodiesel conductivity value and DO concentration on FDM degradation for other biodiesel fuels such as soy, rapeseed and coconut are suggested as a focus of future investigation. Such a study would provide valuable data for comparison between different biodiesels.

Thirdly, the compatibility of biodiesel with elastomers of different elemental composition for instance higher/lower fluorine or acrylonitrile content can be determined by comparing the differences in the elemental composition present between those elastomers and the evaluated elastomers in the present study.

Fourthly, field trials on new vehicles equipped with CRDE focusing on FDM degradation can be conducted. This would appraise the applicability of the results from the modified laboratory immersion studies in representing the FDM degradation under real-life CRDE operation.

Lastly, the compatibility present between diesel exposed FDM and biodiesel under modified laboratory immersion tests can be investigated. Through this, important data on the degradation of FDM on used vehicle which was operated using diesel prior to using biodiesel-diesel fuel blend can be obtained.

REFERENCES

[1] How much energy is consumed in the world by each sector ?, United States Energy Information Administration (2014). http://www.eia.gov/tools/faqs/faq.cfm?id=447&t=1 [accessed in September 2014].

[2] J. Sheehan, V. Camobreco, J. Duffield, M. Graboski, H. Shapouri, An overview of biodiesel and petroleum diesel life cycles, National Renewable Energy Laboratory Report No: NREL/TP-580-24772, United States Department of Agriculture and United States Department of Energy (1998) 60p. http://www.nrel.gov/docs/legosti/fy98/24772.pdf [accessed in September 2014].

[3] Addressing Air Emissons from the Petroleum Refinery Sector, United States Environmental Protection Agency (2011) 52p. http://www3.epa.gov/apti/video/10182011Webinar/101811webinar.pdf [accessed in January 2012].

[4] International Agency for Research on Cancer: Diesel engine exhaust carcinogenic, World Health Organisation (2012) p.1. https://www.iarc.fr/en/media-centre/pr/2012/pdfs/pr213_E.pdf [accessed in August 2012].

[5] E. Crabbe, C. Nolasco-Hipolito, G. Kobayashi, K. Sonomoto, A. Ishizaki, Biodiesel production from crude palm oil and evaluation of butanol extraction and fuel properties, Process Biochemistry, 37 (2001) 65-71.

[6] American Society of the International Association for Testing and Materials. Standard Specification for Biodiesel Fuel Blend Stock (B100) for Middle Distillate Fuels, ASTM D6751-15c (2015).

[7] American Society of the International Association for Testing and Materials. Standard Specification for Diesel Fuel Oil, Biodiesel Blend (B6-B20), ASTM D7467-15c (2015).

[8] B. Flach, K. Bendz, R. Krautgartner, S. Lieberz, EU Biofuels Annual 2013, GAIN Report No: NL3034, USDA Foreign Agricultural Service-Global Agricultural Information Network, The Hague, Netherlands (2013) p.19. http://gain.fas.usda.gov/Recent%20GAIN%20Publications/Biofuels%20Annual_The%20Hague_EU-27_8-13-2013.pdf [accessed in January 2016].

[9] B. Flach, S. Lieberz, M. Rondon, B. Williams, C. Teiken, EU Biofuels Annual 2015, GAIN Report No: NL5028, USDA Foreign Agricultural Service-Global Agricultural Information Network, The Hague, Netherlands (2015) p.21. http://gain.fas.usda.gov/Recent%20GAIN%20Publications/Biofuels%20Annual_The%20Hague_EU-28_7-15-2015.pdf [accessed in January 2016].

[10] S. Barros, Brazil–Biofuels Annual–Annual Report 2013, GAIN Report No: BR13005, USDA Foreign Agricultural Service-Global Agricultural Information Network, Sao Paulo, Brazil (2013) p.20. http://gain.fas.usda.gov/Recent%20GAIN%20Publications/Biofuels%20Annual_Sao%20Paulo%20ATO_Brazil_9-12-2013.pdf [accessed in January 2016].

[11] S. Barros, Brazil–Biofuels Annual–Annual Report 2015, GAIN Report No: BR15006, USDA Foreign Agricultural Service-Global Agricultural Information Network, Sao Paulo, Brazil (2015) p.23. http://gain.fas.usda.gov/Recent%20GAIN%20Publications/Biofuels%20Annual_Sao%20Paulo%20ATO_Brazil_8-4-2015.pdf [accessed in January 2016].

[12] A.G. Wahab, Malaysia Biofuels Annual Report 2013, GAIN Report No: MY3007, USDA Foreign Agricultural Service-Global Agricultural Information Network, Kuala Lumpur, Malaysia (2013) p.4. http://gain.fas.usda.gov/Recent%20GAIN%20Publications/Biofuels%20Annual_Kuala%20Lumpur_Malaysia_7-9-2013.pdf [accessed in January 2016].

[13] A.G. Wahab, Malaysia Biofuels Annual Report 2015, GAIN Report No: MY5012, USDA Foreign Agricultural Service-Global Agricultural Information Network, Kuala Lumpur, Malaysia (2015) p.4. http://gain.fas.usda.gov/Recent%20GAIN%20Publications/Biofuels%20Annual_Kuala%20Lumpur_Malaysia_9-9-2015.pdf [accessed in January 2016].

[14] R. Farrell, Australia Biofuels Annual, GAIN Report No: AS1516, USDA Foreign Agricultural Service-Global Agricultural Information Network, Canberra, Australia (2015) p.18. http://gain.fas.usda.gov/Recent%20GAIN%20Publications/Biofuels%20Annual_Canberra_Australia_8-3-2015.pdf [accessed in January 2016].

[15] Monthly Biodiesel Production Report, United States Energy Information Administration (2015). http://www.eia.gov/biofuels/biodiesel/production/ [accessed in January 2016].

[16] G. Knothe, J.H. Van Gerpen, J. Krahl, The biodiesel handbook, 1st edition AOCS Press, 2005.

[17] J.H. Ng, H.K. Ng, S. Gan, Advances in biodiesel fuel for application in compression ignition engines, Clean Technologies and Environmental Policy, 12 (2010) 459-493.

[18] A.S.M.A. Haseeb, M.A. Fazal, M.I. Jahirul, H.H. Masjuki, Compatibility of automotive materials in biodiesel: A review, Fuel, 90 (2011) 922-931.

[19] R.O. Dunn, Effect of oxidation under accelerated conditions on fuel properties of methyl soyate (biodiesel), Journal of the American Oil Chemists' Society, 79 (2002) 915-920.

[20] A. Demirbas, Biodiesel-A realistic fuel alternative for diesel engines, 1st edition Springer, 2008.

[21] H.L. Fang, T.L. Alleman, R.L. McCormick, Quantification of biodiesel content in fuels and lubricants by FTIR and NMR spectroscopy: SAE Technical Paper No. 2006-01-3301, 2006.

[22] A. Agarwal, Experimental investigations of the effect of biodiesel utilization on lubricating oil tribology in diesel engines, Proceedings of the Institution of

Mechanical Engineers, Part D: Journal of Automobile Engineering, 219 (2005) 703-713.

[23] H.L. Fang, S.D. Whitacre, E.S. Yamaguchi, M. Boons, Biodiesel impact on wear protection of engine oils: SAE Technical Paper No. 2007-01-4141, 2007.

[24] M. Andreae, H. Fang, K. Bhandary, Biodiesel and fuel dilution of engine oil: SAE Technical Paper No. 2007-01-4036, 2007.

[25] A. Murugesan, C. Umarani, R. Subramanian, N. Nedunchezhian, Bio-diesel as an alternative fuel for diesel engines—A review, Renewable and Sustainable Energy Reviews, 13 (2009) 653-662.

[26] Biodiesel blends, Biofuels Association of Australia (2016). http://biofuelsassociation.com.au/biofuels/biodiesel/oems-and-approved-blends/ [accessed in January 2016].

[27] Biodiesel in Australia, Biofuels Association of Australia (2013). http://www.biofuelsassociation.com.au/biodiesel-in-australia [accessed in January 2014].

[28] J. Lane, Biofuels Mandates Around the World: 2016, Biofuels Digest (2016). http://www.biofuelsdigest.com/bdigest/2016/01/03/biofuels-mandates-around-the-world-2016/ [accessed in January 2016].

[29] Biodiesel Blends, United States Department of Energy - Energy Efficiency and Renewable Energy (2016).

http://www.afdc.energy.gov/fuels/biodiesel_blends.html [accessed in January 2016].

[30] H. Zainal, B7 biodiesel to be launched to replace B5 at petrol stations from Nov 1, Thestar, (2014). http://www.thestar.com.my/news/nation/2014/10/29/b7-biodiesel-to-be-launched-lower-emission-fuel-to-replace-b5-at-petrol-stations-from-nov-1/ [accessed in January 2016].

[31] I. Farhana, Malaysia to implement B10 biodiesel mandate by October, Thestar (2015). http://www.thestar.com.my/business/business-news/2015/06/08/malaysia-to-implement-b10-biodiesel-mandate-by-october/ [accessed in January 2016].

[32] K. Yamane, K. Kawasaki, K. Sone, T. Hara, T. Prakoso, Oxidation stability of biodiesel and its effects on diesel combustion and emission characteristics, International Journal of Engine Research, 8 (2007) 307-319.

[33] A. Sarin, R. Arora, N.P. Singh, M. Sharma, R.K. Malhotra, Influence of metal contaminants on oxidation stability of Jatropha biodiesel, Energy, 34 (2009) 1271-1275.

[34] R.L. McCormick, M. Ratcliff, L. Moens, R. Lawrence, Several factors affecting the stability of biodiesel in standard accelerated tests, Fuel Processing Technology, 88 (2007) 651-657.

[35] A.S.M.A. Haseeb, H.H. Masjuki, L.J. Ann, M.A. Fazal, Corrosion characteristics of copper and leaded bronze in palm biodiesel, Fuel Processing Technology, 91 (2010) 329-334.

[36] K. Wadumesthrige, N. Johnson, M. Winston-Galant, H. Tang, K.S. Ng, S.O. Salley, Deterioration of B20 from compression ignition engine operation: SAE Technical Paper No. 2010-01-2120, 2010.

[37] R. Dinkov, G. Hristov, D. Stratiev, V. Boynova Aldayri, Effect of commercially available antioxidants over biodiesel/diesel blends stability, Fuel, 88 (2009) 732-737.

[38] R.O. Dunn, Effect of antioxidants on the oxidative stability of methyl soyate (biodiesel), Fuel Processing Technology, 86 (2005) 1071-1085.

[39] A. Sarin, R. Arora, N.P. Singh, R. Sarin, R.K. Malhotra, M. Sharma, A.A. Khan, Synergistic effect of metal deactivator and antioxidant on oxidation stability of metal contaminated Jatropha biodiesel, Energy, 35 (2010) 2333-2337.

[40] Y.C. Liang, C.Y. May, C.S. Foon, M.A. Ngan, C.C. Hock, Y. Basiron, The effect of natural and synthetic antioxidants on the oxidative stability of palm diesel, Fuel, 85 (2006) 867-870.

[41] I. Miyata, Y. Takei, K. Tsurutani, M. Okada, Effects of bio-fuels on vehicle performance: degradation mechanism analysis of bio-fuels: SAE Technical Paper No. 2004-01-3031, 2004.

[42] B. Kowalski, Evaluation of activities of antioxidants in rapeseed oil matrix by pressure differential scanning calorimetry, Thermochimica acta, 213 (1993) 135-146.

[43] B. Kowalski, Evaluation of the stability of some antioxidants for fat-based foods, Thermochimica acta, 177 (1991) 9-14.

[44] B. Kowalski, Thermal-oxidative decomposition of edible oils and fats. DSC studies, Thermochimica acta, 184 (1991) 49-57.

[45] J. Paligová, L. Joríková, J.n. Cvengroš, Study of FAME stability, Energy & Fuels, 22 (2008) 1991-1996.

[46] G. Karavalakis, D. Hilari, L. Givalou, D. Karonis, S. Stournas, Storage stability and ageing effect of biodiesel blends treated with different antioxidants, Energy, 36 (2011) 369-374.

[47] G. Karavalakis, S. Stournas, Impact of antioxidant additives on the oxidation stability of diesel/biodiesel blends, Energy & Fuels, 24 (2010) 3682-3686.

[48] E.S. Almeida, F.M. Portela, R.M.F. Sousa, D. Daniel, M.G.H. Terrones, E.M. Richter, R.A.A. Muñoz, Behaviour of the antioxidant tert-butylhydroquinone on the storage stability and corrosive character of biodiesel, Fuel, 90 (2011) 3480-3484.

[49] B.Y. Lamba, G. Joshi, A.K. Tiwari, D.S. Rawat, S. Mallick, Effect of antioxidants on physico-chemical properties of EURO-III HSD (high speed diesel) and Jatropha biodiesel blends, Energy, 60 (2013) 222-229.

[50] M. Lapuerta, J. Rodríguez-Fernández, Á. Ramos, B. Álvarez, Effect of the test temperature and anti-oxidant addition on the oxidation stability of commercial biodiesel fuels, Fuel, 93 (2012) 391-396.

[51] G. Joshi, B.Y. Lamba, D.S. Rawat, S. Mallick, K.S.R. Murthy, Evaluation of additive effects on oxidation stability of Jatropha curcas biodiesel blends with conventional diesel sold at retail outlets, Industrial & Engineering Chemistry Research, 52 (2013) 7586-7592.

[52] M.A.S. Rios, F.F.P. Santos, F.J.N. Maia, S.E. Mazzetto, Evaluation of antioxidants on the thermo-oxidative stability of soybean biodiesel, Journal of Thermal Analysis and Calorimetry, 112 (2012) 921-927.

[53] D.S. Rawat, G. Joshi, B.Y. Lamba, A.K. Tiwari, S. Mallick, Impact of additives on storage stability of Karanja (Pongamia Pinnata) biodiesel blends with conventional diesel sold at retail outlets, Fuel, 120 (2014) 30-37.

[54] T.T. Kivevele, M.M. Mbarawa, A. Bereczky, T. Laza, J. Madarasz, Impact of antioxidant additives on the oxidation stability of biodiesel produced from Croton Megalocarpus oil, Fuel Processing Technology, 92 (2011) 1244-1248.

[55] M. Serrano, M. Martínez, J. Aracil, Long term storage stability of biodiesel: Influence of feedstock, commercial additives and purification step, Fuel Processing Technology, 116 (2013) 135-141.

[56] M. Serrano, A. Bouaid, M. Martínez, J. Aracil, Oxidation stability of biodiesel from different feedstocks: Influence of commercial additives and purification step, Fuel, 113 (2013) 50-58.

[57] S.S. Pantoja, L.R.V. da Conceição, C.E.F. da Costa, J.R. Zamian, G.N. da Rocha Filho, Oxidative stability of biodiesels produced from vegetable oils having different degrees of unsaturation, Energy Conversion and Management, 74 (2013) 293-298.

[58] E.C.R. Maia, D. Borsato, I. Moreira, K.R. Spacino, P.R.P. Rodrigues, A.L. Gallina, Study of the biodiesel B100 oxidative stability in mixture with antioxidants, Fuel Processing Technology, 92 (2011) 1750-1755.

[59] R. Guzman, H. Tang, S. Salley, K.Y.S. Ng, Synergistic effects of antioxidants on the oxidative stability of soybean oil-and poultry fat-based biodiesel, Journal of the American Oil Chemists' Society, 86 (2009) 459-467.

[60] W.W. Focke, I.v.d. Westhuizen, A.B.L. Grobler, K.T. Nshoane, J.K. Reddy, A.S. Luyt, The effect of synthetic antioxidants on the oxidative stability of biodiesel, Fuel, 94 (2012) 227-233.

[61] S. Schober, M. Mittelbach, The impact of antioxidants on biodiesel oxidation stability, European Journal of Lipid Science and Technology, 106 (2004) 382-389.

[62] S.S. Damasceno, N.A. Santos, I.M.G. Santos, A.L. Souza, A.G. Souza, N. Queiroz, Caffeic and ferulic acids: An investigation of the effect of antioxidants on the stability of soybean biodiesel during storage, Fuel, 107 (2013) 641-646.

[63] N.A. Santos, S.S. Damasceno, P.H. de Araújo, V.C. Marques, R. Rosenhaim, V.J. Fernandes Jr, N. Queiroz, I.M. Santos, A.S. Maia, A.G. Souza, Caffeic acid: an efficient antioxidant for soybean biodiesel contaminated with metals, Energy & Fuels, 25 (2011) 4190-4194.

[64] A.K. Domingos, E.B. Saad, W.W. Vechiatto, H.M. Wilhelm, L.P. Ramos, The influence of BHA, BHT and TBHQ on the oxidation stability of soybean oil ethyl esters (biodiesel), Journal of the Brazilian Chemical Society, 18 (2007) 416-423.

[65] M. Chakraborty, D.C. Baruah, Investigation of oxidation stability of Terminalia belerica biodiesel and its blends with petrodiesel, Fuel Processing Technology, 98 (2012) 51-58.

[66] J. Xin, H. Imahara, S. Saka, Kinetics on the oxidation of biodiesel stabilized with antioxidant, Fuel, 88 (2009) 282-286.

[67] H. Tang, A. Wang, S.O. Salley, K.S. Ng, The effect of natural and synthetic antioxidants on the oxidative stability of biodiesel, Journal of the American Oil Chemists' Society, 85 (2008) 373-382.

[68] P. Wanasundara, F. Shahidi, Antioxidants: Science, technology, and applications, Bailey's Industrial Oil and Fat Products, 6th edition Wiley-Interscience, 2005.

[69] E.W. Thomas, R.E. Fuller, K. Terauchi, Fluoroelastomer compatibility with biodiesel fuels: SAE Technical Paper No. 2007-01-4061, 2007.

[70] R.L. McCormick, B. Terry, Impact of biodiesel blends on fuel system component durability: SAE Technical Paper No. 2006-01-3279, 2006.

[71] M.A. Fazal, A.S.M.A. Haseeb, H.H. Masjuki, Comparative corrosive characteristics of petroleum diesel and palm biodiesel for automotive materials, Fuel Processing Technology, 91 (2010) 1308-1315.

[72] M. Fazal, A. Haseeb, H. Masjuki, Effect of temperature on the corrosion behavior of mild steel upon exposure to palm biodiesel, Energy, 36 (2011) 3328-3334.

[73] J. Bacha, J. Freel, A. Gibbs, L. Gibbs, G. Hemighaus, K. Hoekman, J. Horn, M. Ingham, L. Jossens, Diesel fuels technical review, Chevron Corporation (2007) 161p. http://www.chevron.com/documents/pdf/DieselFuelTechReview.pdf [accessed in January 2012].

[74] H. Aatola, M. Larmi, T. Sarjovaara, S. Mikkonen, Hydrotreated vegetable oil (HVO) as a renewable diesel fuel: trade-off between NOx, particulate emission, and fuel consumption of a heavy duty engine: SAE Technical Paper No. 2008-01-2500, 2008.

[75] F.D. Gunstone, The chemistry of oils and fats: sources, composition, properties, and uses, 1st edition Blackwell, 2004.

[76] H. Yamagata, The science and technology of materials in automotive engines, Elsevier, 2005.

[77] W. Crouse, D. Anglin, Automotive mechanics, 10th edition Mc-Graw Hill, 1993.

[78] VP44 endurance test with E diesel, Internal Report No: 00/47/3156, Robert Bosch Corporation (2001).

[79] K. Sorate, P. Bhale, Impact of biodiesel on fuel system materials durability, Journal of Scientific & Industrial Research, 72 (2013) 48-57.

[80] S. Kaul, R.C. Saxena, A. Kumar, M.S. Negi, A.K. Bhatnagar, H.B. Goyal, A.K. Gupta, Corrosion behavior of biodiesel from seed oils of Indian origin on diesel engine parts, Fuel Processing Technology, 88 (2007) 303-307.

[81] D.P. Geller, T.T. Adams, J.W. Goodrum, J. Pendergrass, Storage stability of poultry fat and diesel fuel mixtures: specific gravity and viscosity, Fuel, 87 (2008) 92-102.

[82] M. Sgroi, G. Bollito, G. Saracco, S. Specchia, BIOFEAT: biodiesel fuel processor for a vehicle fuel cell auxiliary power unit: study of the feed system, Journal of Power Sources, 149 (2005) 8-14.

[83] T. Tsuchiya, H. Shiotani, S. Goto, G. Sugiyama, A. Maeda, Japanese standards for diesel fuel containing 5% FAME: Investigation of acid generation in FAME blended diesel fuels and its impact on corrosion: SAE Technical Paper No. 2006-01-3303, 2006.

[84] M. Fazal, A. Haseeb, H. Masjuki, Comparative corrosive characteristics of petroleum diesel and palm biodiesel for automotive materials, Fuel Processing Technology, 91 (2010) 1308-1315.

[85] M.A. Fazal, A.S.M.A. Haseeb, H.H. Masjuki, Degradation of automotive materials in palm biodiesel, Energy, 40 (2012) 76-83.

[86] J. Hancsók, M. Bubálik, M. Törő, J. Baladincz, Synthesis of fuel additives on vegetable oil basis at laboratory scale, European Journal of Lipid Science and Technology, 108 (2006) 644-651.

[87] J. Hancsók, M. Bubálik, Á. Beck, J. Baladincz, Development of multifunctional additives based on vegetable oils for high quality diesel and biodiesel, Chemical Engineering Research and Design, 86 (2008) 793-799.

[88] M.A. Fazal, A.S.M.A. Haseeb, H.H. Masjuki, Effect of different corrosion inhibitors on the corrosion of cast iron in palm biodiesel, Fuel Processing Technology, 92 (2011) 2154-2159.

[89] M. Kalam, H. Masjuki, Biodiesel from palmoil—an analysis of its properties and potential, Biomass and Bioenergy, 23 (2002) 471-479.

[90] D.R. Petrash, Oilfield corrosion inhibitors and their effects on elastomeric seals: NACE Technical Paper No. 24016, 2002.

[91] A. Sarin, R. Arora, N.P. Singh, R. Sarin, M. Sharma, R.K. Malhotra, Effect of metal contaminants and Aantioxidants on the oxidation stability of the methyl ester of Pongamia, Journal of the American Oil Chemists' Society, 87 (2009) 567-572.

[92] A. Sarin, R. Arora, N.P. Singh, R. Sarin, R.K. Malhotra, Oxidation stability of palm methyl ester: effect of metal contaminants and antioxidants, Energy & Fuels 24 (2010) 2652-2656.

[93] G. Knothe, Some aspects of biodiesel oxidative stability, Fuel Processing Technology, 88 (2007) 669-677.

[94] E.T. Denisov, I.B. Afanas' ev, Oxidation and antioxidants in organic chemistry and biology, CRC press, 2005.

[95] B.R. Clark, A. Wang, S.O. Salley, K.S. Ng, Catalytic effects of transition metals on the oxidative stability of various biodiesels: Proceeedings of the AIChE Annual Meeting, 2007.

[96] M. Canakci, A. Monyem, J. Van Gerpen, Accelerated oxidation processes in biodiesel, Transactions-American Society of Agricultural Engineers, 42 (1999) 1565-1572.

[97] A.S.M.A. Haseeb, H.H. Masjuki, C.T. Siang, M.A. Fazal, Compatibility of elastomers in palm biodiesel, Renewable Energy, 35 (2010) 2356-2361.

[98] X. Zhang, L. Li, Z. Wu, Z. Hu, Material Compatibilities of Biodiesels with Elastomers, Metals and Plastics in a Diesel Engine: SAE Technical Paper No. 2009-01-2799, 2009.

[99] G.B. Bessee, J.P. Fey, Compatibility of elastomers and metals in biodiesel fuel blends: SAE Technical Paper No. 971690, 1997.

[100] Z. Hu, Y. Zhou, J. Deng, Z. Wu, L. Li, Compatibility of biodiesels and their blends with typical rubbers and copperish metals: SAE Technical Paper No. 2010-01-0476, 2010.

[101] A.S.M.A. Haseeb, T.S. Jun, M.A. Fazal, H.H. Masjuki, Degradation of physical properties of different elastomers upon exposure to palm biodiesel, Energy, 36 (2011) 1814-1819.

[102] E.C. Zuleta, L. Baena, L.A. Rios, J.A. Calderón, The oxidative stability of biodiesel and its impact on the deterioration of metallic and polymeric materials: a review, Journal of the Brazilian Chemical Society, 23 (2012) 2159-2175.

[103] E.W. Thomas, Fluoroelastomer compatibility with bioalcohol fuels: SAE Technical Paper No. 2009-01-0994, 2009.

[104] Viton-Excelling in Modern Automotive Fuel Systems, DuPont Dow Elastomers (1999) 20p. http://www.biofuels.coop/archive/viton.pdf [accesseed in August 2011].

[105] V.L. Hofman, Biodiesel fuel, North Dakota State University Extension Service (2003) 4p. https://www.ag.ndsu.edu/pubs/ageng/machine/ae1240.pdf [accesseed in July 2012].

[106] B. Singh, J. Korstad, Y.C. Sharma, A critical review on corrosion of compression ignition (CI) engine parts by biodiesel and biodiesel blends and its inhibition, Renewable and Sustainable Energy Reviews, 16 (2012) 3401-3408.

[107] S. Norouzi, F. Eslami, M.L. Wyszynski, A. Tsolakis, Corrosion effects of RME in blends with ULSD on aluminium and copper, Fuel Processing Technology, 104 (2012) 204-210.

[108] M.A. Jakab, S.R. Westbrook, S.A. Hutzler, Testing for compatibility of steel with biodiesel, Southwest Research Institute Project No: 08.13070, Southwest Research Institute (2008) 16p. http://biodiesel.org/reports/20080407_gen385.pdf [accessed in November 2011].

[109] H. Meenakshi, Parameswaran, A. Anand, S.R. Krishnamurthy, A comparison of corrosion behavior of copper and its alloy in Pongamia pinnata oil at different conditions: Journal of Energy Article ID 932976, 2013.

[110] J. Kamiński, K. Kurzydłowski, Use of impedance spectroscopy to testing corrosion resistance of carbon steel and stainless steel in water-biodiesel configuration, Journal of Corrosion Measurement, 6 (2008) B35-B39.

[111] J.H. Van Gerpen, E.G. Hammond, L. Yu, A. Monyem, Determining the influence of contaminants on biodiesel properties: SAE Technical Paper No. 971685, 1997.

[112] H. Meenakshi, A. Anand, R. Shyamala, R. Saratha, Compatibility of biofuel/diesel blends on storage tank material, Chemical Science Transactions, (2013) S99-S104.

[113] H. Meenakshi, A. Anand, R. Shyamala, S. Mohanapriya, Use of used palm oil as biofuel and its corrosion behaviour on a few indutrial metals, International Journal of Current Research, 5 (2013) 1525-1528.

[114] A. Anisha, H. Meenakshi, R. Shyamala, R. Saratha, S. Papavinasam, Compatibility of metals in Jatropha oil: NACE Technical Paper No. 11140, 2011.

[115] P. Felizardo, P. Baptista, J.C. Menezes, M.J.N. Correia, Multivariate near infrared spectroscopy models for predicting methanol and water content in biodiesel, Analytica Chimica Acta, 595 (2007) 107-113.

[116] P. Shah, C. Wee, J.M. White, S. Sanford, G. Meier, Experimental determination and thermodynamic modeling of water content in biodiesel-diesel blends, Renewable Energy Group (2010) 35p. https://www.researchgate.net/publication/229047314_Experimental_Determinatio

n_and_Thermodynamic_Modeling_of_Water_Content_in_Biodiesel-Diesel_Blends [accessed in January 2013].

[117] M.A. Fazal, A.S.M.A. Haseeb, H.H. Masjuki, Corrosion mechanism of copper in palm biodiesel, Corrosion Science, 67 (2013) 50-59.

[118] I.P. Aquino, R.P.B. Hernandez, D.L. Chicoma, H.P.F. Pinto, I.V. Aoki, Influence of light, temperature and metallic ions on biodiesel degradation and corrosiveness to copper and brass, Fuel, 102 (2012) 795-807.

[119] A. Anisha, H. Meenakshi, R. Shyamala, Study on the impact of Jatropha Curcus biodiesel on selected metals, The Ecoscan, 1 (2011) 291-294.

[120] F.N. Linhares, H.L. Corrêa, C.N. Khalil, M.C. Amorim Moreira Leite, C.R. Guimarães Furtado, Study of the compatibility of nitrile rubber with Brazilian biodiesel, Energy, 49 (2013) 102-106.

[121] H.L. Fang, Spectroscopic study of biodiesel degradation pathways: SAE Technical Paper No. 2006-01-3300, 2006.

[122] G. Micallef, Elastomer selection for bio-fuel requires a systems approach, Sealing Technology, 2009 (2009) 7-10.

[123] M. Mittelbach, C. Remschmidt, Biodiesel: the comprehensive handbook, 2nd edition Martin Mittelbach, 2004.

[124] J.A. Waynick, Characterization of Biodiesel Oxidation and Oxidation Products: Technical Literature Review. Task 1 Results, National Renewable

Energy Laboratory Report No: NREL/TP-540-39096, United Sates Department of Energy (2005) 51p. http://www.nrel.gov/docs/fy06osti/39096.pdf [accessed in July 2011].

[125] W. Trakarnpruk, S. Porntangjitlikit, Palm oil biodiesel synthesized with potassium loaded calcined hydrotalcite and effect of biodiesel blend on elastomer properties, Renewable Energy, 33 (2008) 1558-1563.

[126] M. Crouse, The Effects of Non-Petroleum Based Fuels on Thermoset Elastomers: SAE Technical Paper No. 2002-01-0634, 2002.

[127] D. Hertz Jr, Fluorine-containing elastomers introduction, Seals Eastern Inc. (2007) 17p. http://www.sealseastern.com/PDF/FluoroAcsChapter.pdf [accessed in July 2011].

[128] American Society of the International Association for Testing and Materials. Standard Test Method for Corrosiveness to Copper from Petroleum Products by Copper Strip Test, ASTM D130-12 (2012).

[129] R.L. McCormick, L. Ha, H.L. Fang, 100,000-Mile evaluation of transit buses operated on biodiesel blends (B20): SAE Technical Paper No. 2006-01-3253, 2006.

[130] C. Mazzoleni, H.D. Kuhns, H. Moosmüller, J. Witt, N.J. Nussbaum, M.C. Oliver Chang, G. Parthasarathy, S.K.K. Nathagoundenpalayam, G. Nikolich, J.G. Watson, A case study of real-world tailpipe emissions for school buses using a 20% biodiesel blend, Science of the total environment, 385 (2007) 146-159.

[131] U. Rashid, F. Anwar, G. Knothe, Evaluation of biodiesel obtained from cottonseed oil, Fuel Processing Technology, 90 (2009) 1157-1163.

[132] S. Clark, L. Wagner, M. Schrock, P. Piennaar, Methyl and ethyl soybean esters as renewable fuels for diesel engines, Journal of the American Oil Chemists Society, 61 (1984) 1632-1638.

[133] American Society of the International Association for Testing and Materials. Standard Test Method for Acid Number of Petroleum Products by Potentiometric Titration, ASTM D664-11 (2011).

[134] American Society of the International Association for Testing and Materials. Standard Guide for Laboratory Immersion Corrosion Testing of Metals, ASTM G31-12a (2012).

[135] American Society of the International Association for Testing and Materials. Standard Practice for Evaluating and Qualifying Oil Field and Refiney Corrosion Inhibitors Using Rotating Cage, ASTM G184-12 (2012).

[136] American Society of the International Association for Testing and Materials. Standard Test Method for Conducting Potentiodynamic Polarization Resistance Measurements, ASTM G59-97 (2014).

[137] American Society of the International Association for Testing and Materials. Standard Test Method for Rubber Property-Effect of Liquids, ASTM D471-12 (2012).

[138] K.V. Chew, A.S.M.A. Haseeb, H.H. Masjuki, M.A. Fazal, M. Gupta, Corrosion of magnesium and aluminum in palm biodiesel: A comparative evaluation, Energy, 57 (2013) 478-483.

[139] E. Hu, Y. Xu, X. Hu, L. Pan, S. Jiang, Corrosion behaviors of metals in biodiesel from rapeseed oil and methanol, Renewable Energy, 37 (2012) 371-378.

[140] H. Meenakshi, A. Anisha, R. Shyamala, R. Saratha, S. Papavinasam, Corrosivity of Pongamia pinnata biodiesel-diesel blends on a few industrial metals: NACE Technical Paper No. 11142, 2011.

[141] L. Díaz-Ballote, J. López-Sansores, L. Maldonado-López, L. Garfias-Mesias, Corrosion behavior of aluminum exposed to a biodiesel, Electrochemistry Communications, 11 (2009) 41-44.

[142] W. Wan Nik, S. Syahrullail, R. Rosliza, M. Rahman, M. Zulkifli, Corrosion behaviour of aluminium alloy in palm oil methyl ester (B100), Jurnal Teknologi, 58 (2012) 73-76.

[143] D.L. Cursaru, G. Brănoiu, I. Ramadan, F. Miculescu, Degradation of automotive materials upon exposure to sunflower biodiesel, Industrial Crops and Products, 54 (2014) 149-158.

[144] S. Malarvizhi, R. Shyamala, S. Papavinasam, Assessment of Microbiologically Influenced Corrosion of Metals in Biodiesel from Jatropha curcas: NACE Technical Paper No. 5772, 2015.

[145] S. Papavinasam, A. Anand, M. Paramesh, J. Krausher, J. Li, P. Liu, S. Mani, S. Krishnamurthy, Corrosion of Metals in Biofuels, ECS Transactions, 33 (2011) 1-19.

[146] M.M. Maru, M.M. Lucchese, C. Legnani, W.G. Quirino, A. Balbo, I.B. Aranha, L.T. Costa, C. Vilani, L.Á. de Sena, J.C. Damasceno, T. dos Santos Cruz, L.R. Lidízio, R. Ferreira e Silva, A. Jorio, C.A. Achete, Biodiesel compatibility with carbon steel and HDPE parts, Fuel Processing Technology, 90 (2009) 1175-1182.

[147] J. Liu, Y.K. Fang, Effect of Dissolved Oxygen on Corrosion of 20R Steel in Bio-diesel Reactor Raw Mixture [J], Corrosion & Protection, 10 (2009) 009.

[148] D. Cursaru, S. Mihai, Corrosion Behaviour of Automotive Materials in Biodiesel from Sunflower Oil, Revista De Chimie, 63 (2012) 945-948.

[149] D.M. Fernandes, R.H.O. Montes, E.S. Almeida, A.N. Nascimento, P.V. Oliveira, E.M. Richter, R.A.A. Muñoz, Storage stability and corrosive character of stabilised biodiesel exposed to carbon and galvanised steels, Fuel, 107 (2013) 609-614.

[150] W. Wang, P.E. Jenkins, Z. Ren, Heterogeneous corrosion behaviour of carbon steel in water contaminated biodiesel, Corrosion Science, 53 (2011) 845-849.

[151] D. Jin, X. Zhou, P. Wu, L. Jiang, H. Ge, Corrosion behavior of ASTM 1045 mild steel in palm biodiesel, Renewable Energy, 81 (2015) 457-463.

[152] G.I. Ononiwu, F.V. Adams, I.V. Joseph, Corrosion Behaviour of Mild Steel in Biodiesel Prepared from Ghee Butter, Proceedings of the World Congress on Engineering, (2015) 858-862.

[153] S. Li, J. Kealoha, L.H. Hihara, Corrosion of Low-Carbon Steel in Seawater/Biodiesel Mixtures–a Study Related to the Corrosion of Fuel Tanks in Ships: NACE Technical Paper No. 6095, 2015.

[154] Y.Y. Ku, T.W. Tang, K.W. Lin, S. Chan, The Impact upon Applicability of Metal Fuel Tank Using Different Biodiesel: SAE Technical Paper No. 2015-01-0521, 2015.

[155] M.A. Maleque, B. Ghazal, M.Y. Ali, M. Hayyan, A. Saleh, Corrosion of surface modified AISI 4340 steel in Jatropha biodiesel, Advanced Materials Research, 1115 (2015) 243-246.

[156] K.A. Sorate, P.V. Bhale, B.Z. Dhaolakiya, A material compatibility study of automotive elastomers with high FFA based biodiesel, Energy Procedia, 75 (2015) 105-110.

[157] L.M.A. Silva, E.G.A. Filho, A.J. Simpson, M.R. Monteiro, T. Venâncio, Comprehensive multiphase NMR spectroscopy: A new analytical method to study the effect of biodiesel blends on the structure of commercial rubbers, Fuel, 166 (2016) 436-445.

[158] R. Rudbahs, R. Smigins, Experimental research on biodiesel compatibility with fuel system elastomers, Proceedings of the 13th International Scientific Conference Engineering for Rural Development, (2014) 278-282.

[159] B. Flitney, Which elastomer seal materials are suitable for use in biofuels?, Sealing Technology, 2007 (2007) 8-11.

[160] J. Kerwin, Biofuels put seals to the test, Precision Polymer Engineering (2009) 4p. http://www.prepol.com/Adobe/Biofuels%20put%20seals%20to%20the%20test.pdf [accessed in July 2011].

[161] E. Frame, R.L. McCormick, Elastomer compatibility testing of renewable diesel fuels, National Renewable Energy Laboratory Report No: NREL/TP-540-38834, United States Department of Energy (2005) 21p. http://biodiesel.org/reports/20051101_gen-367.pdf [accessed in July 2011].

[162] T. Maxson, B. Logan, S. O'Brien, Performance in diesel and biodiesels of fluorosilicone rubber materials used for automotive quick connector fuel line orings and other sealing applications: SAE Technical Paper No. 2001-01-1124, 2001.

[163] L. Zhu, C.S. Cheung, W.G. Zhang, Z. Huang, Compatibility of different biodiesel composition with acrylonitrile butadiene rubber (NBR), Fuel, 158 (2015) 288-292.

[164] M. Coronado, G. Montero, B. Valdez, M. Stoytcheva, A. Eliezer, C. García, H. Campbell, A. Pérez, Degradation of nitrile rubber fuel hose by biodiesel use, Energy, 68 (2014) 364-369.

[165] S.M. Alves, V.S. Mello, J.S. Medeiros, Palm and soybean biodiesel compatibility with fuel system elastomers, Tribology International, 65 (2013) 74-80.

[166] S. Akhlaghi, M.S. Hedenqvist, M.T. Conde Braña, M. Bellander, U.W. Gedde, Deterioration of acrylonitrile butadiene rubber in rapeseed biodiesel, Polymer Degradation and Stability, 111 (2015) 211-222.

[167] M. Loo, J.B. Le Cam, A. Andriyana, E. Robin, J. Coulon, Effect of swelling on fatigue life of elastomers, Polymer Degradation and Stability, 124 (2016) 15-25.

[168] M.S. Loo, J.B. Le Cam, A. Andriyana, E. Robin, A.M. Afifi, Fatigue of swollen elastomers, International Journal of Fatigue, 74 (2015) 132-141.

[169] A. Chai, A. Andriyana, E. Verron, M. Johan, Mechanical characteristics of swollen elastomers under cyclic loading, Materials & Design, 44 (2013) 566-572.

[170] C.N.S. Ying, A. Andriyana, E. Verron, R. Ahmad, Diffusion of palm biodiesel in elastomers undergoing multiaxial large deformations, Defect and Diffusion Forum, 334 (2013) 77-82.

[171] D. Lamprecht, Elastomer Compatibility of Blends of Biodiesel and Fischer-Tropsch Diesel: SAE Technical Paper No. 2007-01-0029, 2007.

[172] P.S. Choudhury, P. Mallick, Effect of Biodiesel on the Tensile Properties of Nylon-6: SAE Technical Paper No. 2012-01-0752, 2012.

[173] E. Richaud, B. Flaconnèche, J. Verdu, Biodiesel permeability in polyethylene, Polymer Testing, 31 (2012) 1070-1076.

[174] S. Thangavelu, C. Piraiarasi, A. Ahmed, F. Ani, Compatibility of elastomers in biodiesel-diesel-bioethanol Blend (BDE), Advanced Materials Research, 1098 (2015) 51-57.

[175] United Nations Working Party on Pollution and Energy group. Global Technical Regulation-World Harmonized Stationary Cycle, WHSC. https://www.dieselnet.com/standards/cycles/whsc.php [accessed in July 2013].

[176] The Co-ordinating European Council for the Development of Performance Tests for Fuels, Lubricants and other Fluid. Direct Injection-Common Rail Diesel Engine Nozzle Coking Test, CEC F-98-08 (2008). http://www.cectests.org/disptestdoc1.asp [accessed in July 2013].

[177] Engine Manufacturer Association. 200 hour preliminary durability screening test to assess the potential impact of alternative fuels on diesel engine durability, EMA 200 (1982). https://biodiesel.org/reports/19960501_gen-237.pdf [accessed in January 2013].

[178] European Committee for Standardization. Fat and Oil Derivatives. Fatty Acid Methyl Esters (FAME). Determination of Oxidative Stability (Accelerated Oxidation Test), EN 14112: 2003 (2003).

[179] European Committee for Standardization. Fat and Oil Derivatives. Fatty Acid Methyl Esters (FAME). Determination of ester and linolenic acid methyl ester, EN 14103: 2003 (2003).

[180] T. Ogawa, S. Kajiya, A. Ohshima, A. Murase, Y. Suzuki, H. Hayashi, Analysis of the Deterioration of Nylon-66 Immersed in GTL Diesel Fuel Part 1. Analysis and Test of Nylon and GTL Diesel Fuel Before and After Immersion: SAE Technical Paper No. 2006-01-3326, 2006.

[181] Lubrizol Standard Test Procedure. Peroxide Value – AOCS Method, AATM 516-01 (2006).

[182] International Organization for Standardization. Petroleum products – Transparent and opaque liquids – Determination of kinematic viscosity and calculation of dynamic viscosity, ISO 3104:1994 (1994).

[183] American Society of the International Association for Testing and Materials. Standard Test Method for Multielement Determination of Used and Unused Lubricating Oils and Base Oils by Inductively Coupled Plasma Atomic Emission Spectrometry (ICP-AES), ASTM D5185-13 (2013).

[184] International Organization for Standardization. Petroleum products – Determination of water – Coulometric Karl Fisher titration method, ISO 12937:2000 (2000).

[185] G. Knothe, Dependence of biodiesel fuel properties on the structure of fatty acid alkyl esters, Fuel Processing Technology, 86 (2005) 1059-1070.

[186] G. Knothe, "Designer" Biodiesel: Optimizing Fatty Ester Composition to Improve Fuel Properties, Energy & Fuels, 22 (2008) 1358-1364.

[187] C. Scrimgeour, Chemistry of fatty acids, Bailey's Industrial Oil and Fat Products, 6th edition Wiley-Interscience, 2005.

[188] E.N. Frankel, Lipid oxidation, 1st edition The Oily Press, 1998.

[189] K. Schaich, Lipid oxidation: theoretical aspects, Bailey's Industrial Oil and Fat Products, 6th edition Wiley-Interscience, 2005.

[190] H. Shiotani, S. Goto, Studies of fuel properties and oxidation stability of biodiesel fuel: SAE Technical Paper No. 2007-01-0073, 2007.

[191] S. Jain, M. Sharma, Correlation development for effect of metal contaminants on the oxidation stability of Jatropha curcas biodiesel, Fuel, 90 (2011) 2045-2050.

[192] S. Tagliabue, A. Gasparoli, L.d. Bella, P. Bondioli, Influence of metal contamination on biodiesel thermo-oxidation stability, Rivista Italiana delle Sostanze Grasse, 82 (2005) 93-96.

[193] Z. Yang, B.P. Hollebone, Z. Wang, C. Yang, M. Landriault, Factors affecting oxidation stability of commercially available biodiesel products, Fuel Processing Technology, 106 (2013) 366-375.

[194] G. Knothe, R.O. Dunn, Dependence of oil stability index of fatty compounds on their structure and concentration and presence of metals, Journal of the American Oil Chemists' Society, 80 (2003) 1021-1026.

[195] G.S. Dodos, F. Zannikos, S. Stournas, Effect of metals in the oxidation stability and lubricity of biodiesel fuel: SAE Technical Paper No. 2009-01-1829, 2009.

[196] S. Jain, M.P. Sharma, Effect of metal contaminants and antioxidants on the storage stability of Jatropha curcas biodiesel, Fuel, 109 (2013) 379-383.

[197] S. Jain, M.P. Sharma, Effect of metal contents on oxidation stability of biodiesel/diesel blends, Fuel, 116 (2014) 14-18.

[198] J.J. Barron, C. Ashton, The effect of temperature on conductivity measurement, Reagecon Diagnostics Ltd (2005) 5p. http://www.reagecon.com/pdf/technicalpapers/Effect_of_Temperature_TSP-07_Issue3.pdf [accessed in February 2013].

[199] G. Mead, B. Jones, P. Steevens, M. Timanus, The Effects of E20 on metals used in automotive fuel system components, Fuel, 2 (2008) 22-2008.

[200] J.R. Parker, W.H. Waddell, Quantitative characterization of polymer structure by photoacoustic Fourier transform infrared spectroscopy, Journal of elastomers and plastics, 28 (1996) 140-160.

[201] S. Chakraborty, S. Bandyopadhyay, R. Ameta, R. Mukhopadhyay, A. Deuri, Application of FTIR in characterization of acrylonitrile-butadiene rubber (nitrile rubber), Polymer Testing, 26 (2007) 38-41.

[202] International Organization for Standardization. Rubber, raw natural, and rubber latex, natural – Determination of nitrogen content, ISO 1656:2014 (2014).

[203] Society of Automotive Engineers International. Recommended Methods for Conducting Corrosion Tests in Hydrocarbon Fuels or Their Surrogates and Their Mixtures with Oxygenated Additives, J1747, (2013).

[204] J. Sabau, I. Fofana, Y. Hadjadj, M. Brahami, Dissolved oxygen and moisture removal system for freely breathing transformers, IEEE Electrical Insulation Magazine, 26 (2010) 35-43.

[205] American Society of the International Association for Testing and Materials. Standard Practice for Preparing, Cleaning, and Evaluating Corrosion Test Specimens, ASTM G1-11 (2011).

[206] M.G. Fontana, Corrosion engineering, 3rd edition Tata McGraw-Hill Education, 2005.

[207] American Society of the International Association for Testing and Materials. Standard Test Method for Vulcanized Rubber and Thermoplastic Elastomers-Tension, ASTM D412-06a (2013).

[208] American Society of the International Association for Testing and Materials. Standard Test Method for Rubber Property-Durometer Hardness, ASTM D2240-05 (2010).

[209] N.A. Gomez, R. Abonia, H. Cadavid, I.H. Vargas, Chemical and spectroscopic characterization of a vegetable oil used as dielectric coolant in distribution transformers, Journal of the Brazilian Chemical Society, 22 (2011) 2292-2303.

[210] L. Niczke, F. Czechowski, I. Gawel, Oxidized rapeseed oil methyl ester as a bitumen flux: Structural changes in the ester during catalytic oxidation, Progress in organic coatings, 59 (2007) 304-311.

[211] J. Van Gerpen, D. Clements, G. Knothe, Biodiesel production technology, National Renewable Energy Laboratory Subcontractor Report No: NREL/SR-510-36244, United States Department of Energy (2004) 110p. http://www.nrel.gov/docs/fy04osti/36244.pdf [accessed in December 2015].

APPENDICES

APPENDIX A-EXPERIMENTAL SETUP

The addition of the cooling system which consist of a blower and duct to the existing engine test-bed facility as explained in Chapter 3 is the essential modification required for achieving the aims of the present study as shown in Fig. A and Fig. B. These were necessary to overcome the engine overheating issue experienced as a consequence of extended high speed-load engine operation duration as well as to maximize the heat rejection of the compressed air at the intercooler for obtaining maximum power output.

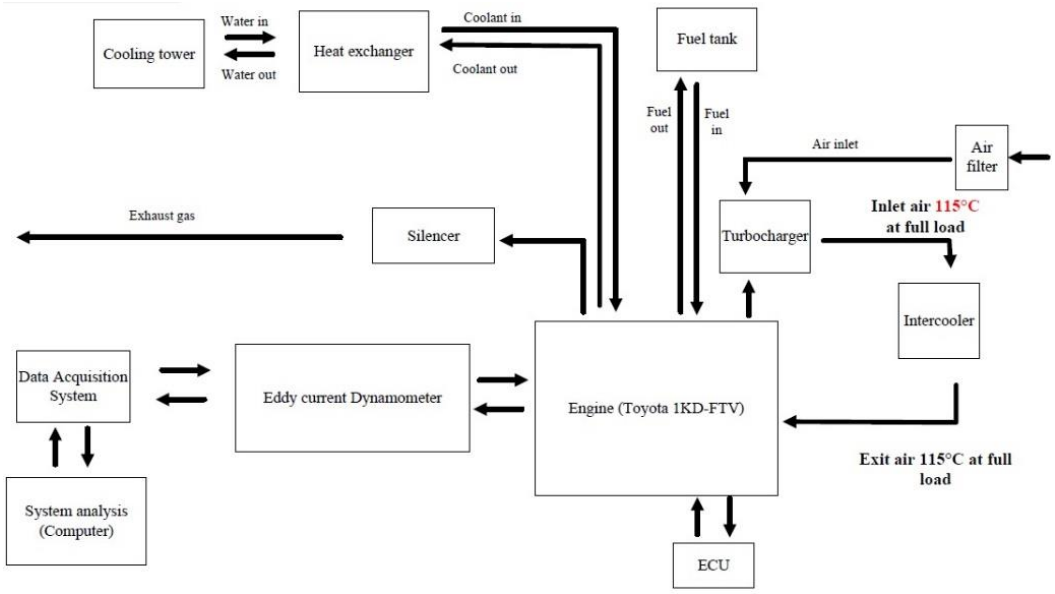

Fig. A Original layout of engine testing facility.

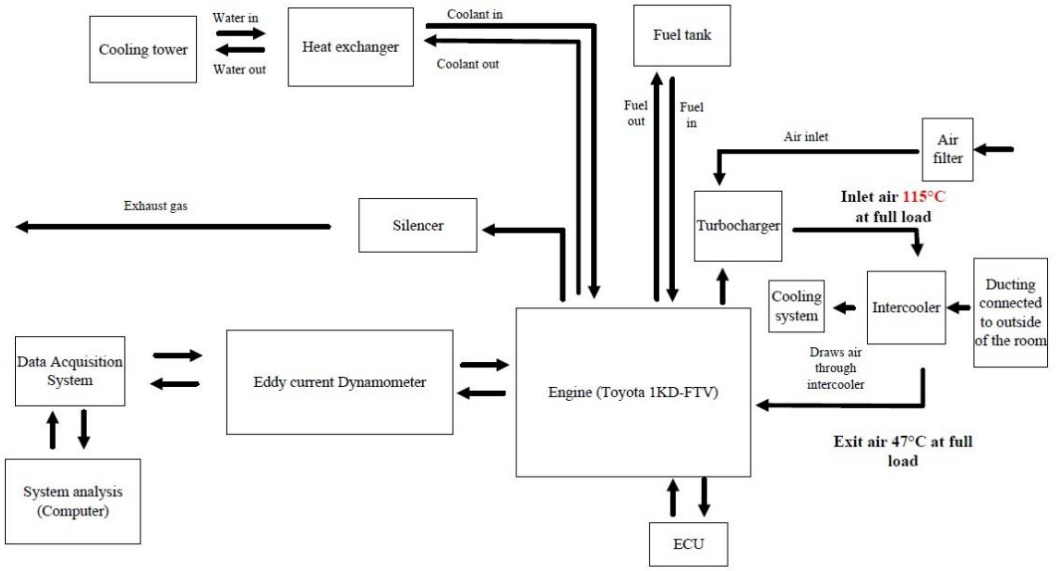

Fig. B Modified layout with the addition of cooling system to turbo-intercooler.

APPENDIX B-ENGINE OPERATION PROTOCOL

Checks prior to engine start-up

1. Check water level for cooling towers storage tank.
2. Check fuel level in the tank.
3. Check coolant level in the heat exchanger.
4. Check engine oil level.
5. Check the bolt and nut markings at the engine test-bed cell and ensure it is aligned.
6. Switch on the main isolator cooling tower control panel and power temperature controller.
7. Switch on the cooling, ventilation and blower systems.
8. Check dynamometer water pressure level.
9. Check any fuel, oil, coolant and water leakage along the lines, hoses and pipes.
10. Check shaft cover between engine-dyno is closed.

Engine start-up procedure

11. Switch on control cabinet isolator.
12. Power on universal power supply and computer.
13. Launch DaTAQ Pro (V2) program from the desktop icon.
14. Login into the system by entering the User ID and password.
15. Select test and key in test-run information.

16. Click start test.
17. Ensure dyno and throttle is set to 0 % in manual mode.
18. Click ignition followed by the crank.
19. Release the crank once the engine has started.

Fig. C Engine-dyno control room.

Experimental procedure and data logging

20. Control the dyno and throttle knob according to the desired engine speed and load respectively.
21. Stroke the F11 key to log the required data manually.

Shut down procedure

22. Ensure both dyno and throttle is set to 0 %.
23. Allow the engine to run at this condition for 2 minutes.
24. Click off the ignition to turn off the engine.
25. Switch off the computer followed with universal power supply and cabinet isolator.
26. Switch off cooling, ventilation and blower systems.
27. Switch on the main isolator cooling tower control panel and power temperature controller.

APPENDIX C-EXAMPLE CALCULATION OF METAL CORROSION RATE

Given: Constant, K= 8760

Time of exposure, T (h) = 960

Area, A (cm^2) = 7.606

Mass loss, W (g) = 0.006925

Density, D (g/cm^3) = 8.94

Calculate: Corrosion rate (mm/year) $= \frac{K \; x \; W}{A \; x \; T \; x \; D}$ *(Equation 3 from ASTM G31-72 (2004))*

$$= \frac{8760 \text{ x } 0.006925}{7.606 \text{ x } 960 \text{ x } 8.94}$$

$$= 0.000929$$

APPENDIX D-EXAMPLE CALCULATION OF ELASTOMER VOLUME CHANGE

Given: Initial mass of specimen in air, M_1 (g) = 1.1199

Initial mass of specimen in water, M_2 (g) = 1.075

Mass of specimen in air after immersion, M_3 (g) = 1.1987

Mass of specimen in water after immersion, M_4 (g) = 1.1490

Calculate: Change in volume, $\Delta V(\%) = \frac{(M_3 - M_4) - (M_1 - M_2)}{(M_1 - M_2)} \times 100$

(Equation 2 from ASTM D471-12a)

$$= \frac{(1.1987 - 1.1490) - (1.1199 - 1.075)}{(1.1199 - 1.075)} \times 100$$

$$= 10.8259$$

APPENDIX E-EXAMPLE CALCULATION OF ELASTOMER TENSILE STRENGTH CHANGE

Given: Original tensile strength before immersion, P_o(MPa) = 37.812

Tensile strength after immersion, P_i (MPa) = 35.240

Calculate: Change in tensile strength, $\Delta P\ (\%) = \frac{P_i - P_o}{P_o}$ x 100

(Equation 10 from ASTM D471-12a)

$$= \frac{37.812 - 35.240}{35.240} \text{ x } 100$$

$$= -6.804$$

APPENDIX F-EXAMPLE CALCULATION OF ELASTOMER HARDNESS CHANGE

Given: Original hardness before immersion, H_o(A) = 82.167

Hardness after immersion, H_i (A) = 68.500

Calculate: Hardness change, $\Delta H\ (A) = H_i - H_o$ *(Equation 11 from ASTM D471-12a)*

$$= 68.500 - 82.167$$

$$= -13.667$$

APPENDIX G-EXAMPLE CALCULATION OF PROPAGATION ERROR USING STANDARD DEVIATIONS

For subtraction

Given: Initial value, I = 88 ± 0.01

Final value, F = 80 ± 0.02

Calculate: Change between initial and final, $G = F - I$

First calculate: $G = F - I$

$= 80 - 88$

$= -8$

Second calculate: $\Delta G = ((\Delta F)^2 + (\Delta I)^2)^{1/2}$

$= ((0.02)^2 + (0.01)^2)^{1/2}$

$= 0.02236068$

For division

Given: $G = -8 \pm 0.02236068$

$I = 88 \pm 0.01$

Calculate: $H = \frac{G}{I}$

First calculate: $H = \frac{G}{I}$

$= -0.091$

Second calculate: $\Delta H = H((\frac{\Delta G}{G})^2 + (\frac{\Delta I}{I})^2)^{1/2}$

$= -0.091((\frac{0.02236068}{-8})^2 + (\frac{0.01}{88})^2)^{1/2}$

$= -0.00002797$